AD-A040 980 NAVAL WEAPONS CENTER CHINA LAKE CALIF F/G 4/2
PROJECT FOGGY CLOUD VI: DESIGN AND EVALUATION OF WARM-FOG DISPE--ETC(U)
MAY 77 R F REINKING, R S CLARK, W G FINNEGAN
UNCLASSIFIED NWC-TP-5824 NL

1 OF 2
AD A040980

AD A040980

NWC TP 5824

Project Foggy Cloud VI: Design and Evaluation of Warm-Fog Dispersal Techniques

by
R. F. Reinking
R. S. Clark
W. G. Finnegan
T. L. Wright
J. W. Carroz
R. W. Evert
L. A. Mathews
Research Department

DDC
RECEIVED
JUN 28 1977

MAY 1977

Approved for public release; distribution unlimited.

DDC FILE COPY

Naval Weapons Center
CHINA LAKE, CALIFORNIA 93555

Naval Weapons Center

AN ACTIVITY OF THE NAVAL MATERIAL COMMAND

R. G. Freeman, III, RAdm., USN ..... Commander

G. L. Hollingsworth ..... Technical Director

FOREWORD

This report describes the development and field testing of three warm-fog clearing systems. This work was authorized by Air Task A370-05F0/216C/IW3712-0000 issued by the Naval Air Systems Command.

Project Foggy Cloud VI was the sixth in a series of research and development programs conducted by the Earth and Planetary Sciences Division of the Research Department. The primary objective was to improve visibility when it was restricted by warm fog. Tests were conducted during the period 15 August through 4 November 1973.

Conclusions presented herein are subject to later review and change because of the continuing nature of the warm-fog program. Pierre St.-Amand and S. D. Elliott have reviewed this report for technical accuracy.

Released by
EDWIN B. ROYCE, *Head*
Research Department
7 October 1976

Under authority of
G. L. HOLLINGSWORTH
Technical Director

NWC Technical Publication 5824

Published by . . . . . Technical Information Department
Collation . . . . . Cover, 54 leaves
First printing . . . . . 275 unnumbered copies

UNCLASSIFIED

SECURITY CLASSIFICATION OF THIS PAGE *(When Data Entered)*

REPORT DOCUMENTATION PAGE

READ INSTRUCTIONS BEFORE COMPLETING FORM

1. REPORT NUMBER: NWC TP 5824	2. GOVT ACCESSION NO.
3. RECIPIENT'S CATALOG NUMBER	
4. TITLE *(and Subtitle)*: PROJECT FOGGY CLOUD VI: DESIGN AND EVALUATION OF WARM-FOG DISPERSAL TECHNIQUES	5. TYPE OF REPORT & PERIOD COVERED: A summary report 15 Aug-4 Nov 1973
	6. PERFORMING ORG. REPORT NUMBER
7. AUTHOR(s): R. F. Reinking, R. S, Clark, W. G. Finnegan, T. L. Wright, J. W. Carroz, R. W. Evert, and L. A. Mathews	8. CONTRACT OR GRANT NUMBER(s)
9. PERFORMING ORGANIZATION NAME AND ADDRESS: Naval Weapons Center, China Lake, CA 93555	10. PROGRAM ELEMENT, PROJECT, TASK AREA & WORK UNIT NUMBERS: A370-05F0/216C/IW3712-0000
11. CONTROLLING OFFICE NAME AND ADDRESS: Naval Weapons Center, China Lake, CA 93555	12. REPORT DATE: May 1977
	13. NUMBER OF PAGES: 106
14. MONITORING AGENCY NAME & ADDRESS *(if different from Controlling Office)*	15. SECURITY CLASS. *(of this report)*: UNCLASSIFIED
	15a. DECLASSIFICATION/DOWNGRADING SCHEDULE

16. DISTRIBUTION STATEMENT *(of this Report)*

Approved for public release; distribution unlimited.

17. DISTRIBUTION STATEMENT *(of the abstract entered in Block 20, if different from Report)*

D D C
RELEASED
JUN 28 1977
D

403 019

18. SUPPLEMENTARY NOTES

19. KEY WORDS *(Continue on reverse side if necessary and identify by block number)*

Fog dispersal
Evaporation suppression
Charged water droplets
Electrostatic induction charging system
Monomolecular film
Charged, hygroscopic bubbles

20. ABSTRACT *(Continue on reverse side if necessary and identify by block number)*

See back of form.

DD FORM 1 JAN 73 1473 EDITION OF 1 NOV 65 IS OBSOLETE
S/N 0102-014-6601

UNCLASSIFIED
SECURITY CLASSIFICATION OF THIS PAGE *(When Data Entered)*

(U) *Project Foggy Cloud VI: Design and Evaluation of Warm-Fog Dispersal Techniques* (U), by R. F. Reinking, R. S. Clark, W. G. Finnegan, T. L. Wright, J. W. Carroz, R. W. Evert, and L. A. Mathews. China Lake, Calif., Naval Weapons Center, May 1977. 106 pp. (NWC TP 5824, publication UNCLASSIFIED.)

(U) During the period 15 August to 4 November 1973, the Naval Weapons Center, working in collaboration with various activities listed herein, conducted a series of warm-fog modification experiments under Project Foggy Cloud VI. Electrostatically-charged droplets dispensed from aircraft to induce fog droplet coalescence and rainout, and electrostatically-charged bubbles dispensed from the surface to collect and precipitate fog droplets were techniques tested at the Arcata-Eureka Airport in northern California. The spreading and maintenance of monomolecular films on the water surface to suppress evaporation and inhibit fog formation was the basis for testing in the Panama Canal.

(U) Results from tests employing the airborne electrical charging system, while initially inconsistent, gave evidence of increasing positive effects as system modification was accomplished in the field.

(U) Charged bubble experiments, while theoretically sound, presented problems with regard to bubble production and buoyancy as well as targeting. With the airborne electrical charging system in a more advanced state of design and giving promise for a more immediate fog dispersal system, the charged bubble concept should be relegated to engineering improvement until the airborne system is finalized.

(U) Evaporation suppression tests conducted in Panama were extremely encouraging. Evidence showed a strong correlation between fog intensity and film coverage. In areas where the film remained intact during the nocturnal fog-formative hours, ceilings and visibilities generally held above that required for safe ship transits. In areas where the film became broken and patchy, ceilings were lowered and visibility was reduced to below that required for safe navigation.

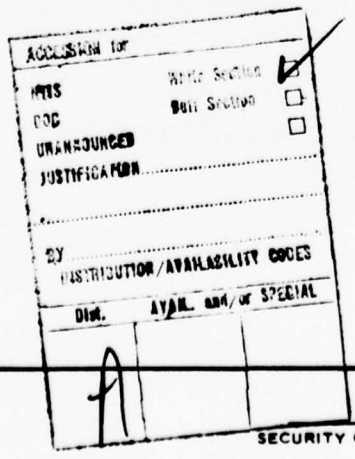

CONTENTS

Introduction 3

Background 4
Charged Droplet Tests 4
Charged Bubble Tests 5
Evaporation Suppression Tests 7

Project Objectives 9
Primary Objectives 9
Secondary Objectives 9

Field Test Sites and Test Conditions 10
The Arcata-Eureka Airport 10
Arcata Fogs 12
The Panama Canal 13
Panama Canal Fogs 14

Field Instrumentation 15

Phase I Systems and Testing 22
Equipment 22
Procedures 26
Test Results 28

Phase II Systems and Testing 35
Comparison of Charged Bubbles and Charged Droplets 35
Bubble Generator Design 41
Results--Electrical 45
Results--Bubble Production 45
Results--Fog Dispersal Tests 49
Results--Gas Consumption 54

Phase III Systems and Testing 54
Material and Equipment 54
Procedures 57
Data Acquisition 61
Results 67

Discussion 70
Phase I - Aerial Dispensing of Charged Water Droplets 70
Phase II - Charged, Hygroscopic Bubbles 70
Phase III - Evaporation Suppression Testing 70

References 71

Appendixes:
A. Details of Airborne Fog Dispersal Tests 73
B. Cloud Condensation Nuclei at the Arcata-Eureka Airport 91

Figures:
1. Arcata-Eureka Airport 10
2. Project Site and Instrumentation Locations 11
3. Limited Visibility Conditions at Arcata-Eureka Airport 12
4. Panama Canal and Canal Zone 14
5. Sketch of Primary Monitoring Site 15

Figures: (Contd.)

6. Photograph of Primary Monitoring Site 16
7. Equipment Arrangement at the "CB" Area 16
8. Sensing and Recording System 17
9. Laser Transmissometer 18
10. Videographs 19
11. Atmospheric Electric Field Measurement System 20
12. Spray System Schematic 22
13. Seeder Taking on Water Load 23
14. Plumbing Connecting Spray Boom at Fuselage 23
15. Section of Induction Grid and Nozzles 24
16. Electrostatic Induction Charging System Schematic 25
17. Power Supply for Induction Charging System 25
18. Radar Plot Showing "Dog Bone" Seeding Pattern 26
19. Racetrack Seeding Pattern 27
20. Laboratory Aircraft Flight Pattern 27
21. U-3 Aircraft Flight Pattern 28
22. Electrical Potentials Between Spray Booms and Grids 30
23. Clearing Over Runway Through Fog of ~ 300 ft. Depth 33
24. Estimate of Fog Water Collected and Precipitated 39
25. Small Wheel Bubble Generator 41
26. Large Wheel Bubble Generator 42
27. Large Wheel Bubble Generator and Fan Arrangement 43
28. Tray Design Bubble Generators 43
29. Bubble Generator Used on Project Foggy Cloud V 43
30. Sketch of Bubble Generating Device, Foggy Cloud VI 44
31. Bubble Generators in Operation at "CB" Area 46
32. Grid Used to Measure Bubble Size Distribution 46
33. Size Distribution of Charged and Uncharged Bubbles 47
34. Visibility Variations With Time, Test B(1) 50
35. Visibility Variations With Time, Test B(2) 52
36. Spray System in Standby Position 55
37. Spray System in Operating Position 56
38. Emulsion Spray From 0.8 GPM Nozzle 56
39. Map of Evaporation Suppression Experimental Area 57
40. Portion of Gaillard Cut - Partially Coated 59
41. Film Coating Operation on the Chagres River 59
42. Sample Observation Log 62
43. Early Morning Views of Canal Showing Film Coverage 63

Tables:

1. Fog and Stratus Characteristics 29
2. Summary of Operations 29
3. Performance of the Spray-Charging System 30
4. Test Results 31
5. Collected Water Required to Produce Neutral Bubble Buoyancy . . 38
6. Size Characteristics of Charged and Uncharged Bubbles 47
7. Estimates of Mass of Water Precipitated From Fog 48
8. Treatment and Observations - Test Period 64
9. Observations - Control Period 66
10. Comparative Indicated Canal Conditions (Test Period) 68
11. Comparative Indicated Canal Conditions (Control Period) 69

INTRODUCTION

Warm fog presents a navigation hazard for movement of airborne, seagoing, and land vehicles. Visual observation of any activity is also inhibited by fog. Fog control, which includes prevention, creation, stabilization, and dispersal, is therefore of interest to the Armed Forces and numerous civilian organizations. Emphasis is on fog dispersal, but much of the same technology applies to the other aspects of control.

The Naval Weapons Center, China Lake, California, has been conducting a laboratory and field program for improving visibility in warm fog. This work began on a limited basis in 1963. The Project Foggy Cloud series of studies was initiated in 1968 in response to a requirement for military aircraft operations in fog. During Foggy Cloud Projects I-V tests were conducted with hygroscopic fog seeding agents, sea water and tap water spray, helicopter downwash, aircraft vortices, electrostatically-charged droplets, and evaporation suppression agents. Successes under a limited range of fog conditions were demonstrated. Results of Projects I-V are reported in Naval Weapons Center Technical Publications.[1-5]

The Foggy Cloud VI tests represent a continued effort to disperse fog with charged particles, and to suppress fog formation and raise ceilings by means of evaporation suppression.

---

[1] Naval Weapons Center. *Project Foggy Cloud I*, by E. Alex Blomerth and others. China Lake, Calif., NWC, August 1970. 85 pp. (NWC TP 4929, publication UNCLASSIFIED.)

[2] Naval Weapons Center. *Project Foggy Cloud III, Phase I*, by Tommy L. Wright and others. China Lake, Calif., NWC, April 1972. 68 pp. (NWC TP 5297, publication UNCLASSIFIED.)

[3] Naval Weapons Center. *Project Foggy Cloud IV, Phase I*, by E. E. Hindman, II and others. China Lake, Calif., NWC, August 1973. 52 pp. (NWC TP 5413, publication UNCLASSIFIED.)

[4] Naval Weapons Center. *Project Foggy Cloud IV, Phase II*, by R. B. Loveland and others. China Lake, Calif., NWC, December 1972. 42 pp. (NWC TP 5338, publication UNCLASSIFIED.)

[5] Naval Weapons Center. *Project Foggy Cloud V*, by R. S. Clark and others. China Lake, Calif., NWC, December 1973. 92 pp. (NWC TP 5542, publication UNCLASSIFIED.)

BACKGROUND

CHARGED DROPLET TESTS

The possibility of using charged collectors of fog droplet (e.g., spray droplets or bubbles) to disperse fog has been shown to merit careful field investigation. Charged collectors induce dipoles in surrounding fog droplets, and thus attract and collect the droplets; clearing occurs as the droplets are gathered and precipitated. The driving process is one of electrically enhanced coalescence. The charged-collector technique is not only theoretically sound, but also promises advantages in cost, logistical, and ecological considerations above any other method that has proven useful to date.

Theory basic to fog dispersal with charged droplets and bubbles was developed during Foggy Cloud IV. This important background material is covered in Project Foggy Cloud IV, Phase II, NWC Technical Report[4]. Various instruments and techniques for charging and delivering droplets and bubbles in fog, and for evaluating the effectiveness of these methods, were placed under development. Foggy Cloud IV resulted in the conclusion that the use of charged droplets was very promising, and that a major effort should be made to develop this concept of fog dispersal.

During Foggy Cloud V, the first major field tests of both surface-dispensed charged droplets and aircraft-dispensed charged droplets were conducted.

The equipment for surface dispensing of charged droplets, designated as the electrogasdynamic (EGD) system, was developed by Gourdine Systems, Inc., Livingston, N.J., for the Federal Aviation Administration (FAA). The EGD system employs a matrix of spray guns installed along and around airport runways to shoot charged water droplets into a fog. These charged spray droplets form a space charge that induces an electric field from cloud to ground. The spray droplets also induce dipoles in and coalesce with fog droplets. The fog droplets thus gain a net charge, and are repelled from the space charge and forced to precipitate to the ground by the induced field. Results were that visibility improvement occurred during the treatment or treatment-lag period in six of eight test cases. Correlations with the treatments were inconsistent partly because of highly variable visibility conditions and an insufficient number of generators for field testing under wind conditions encountered during test periods[5]. Further testing was to be conducted by the FAA.

In three tests of Foggy Cloud V, aircraft-dispensed charged water was used as the fog dispersal agent. Electrogasdynamics, Inc., Hanover, N. J., was given a contract to build the airborne droplet-charging system. A long spray boom with approximately 175 nozzles was fitted to each wing of a B-26 aircraft. This system was capable of delivering

about 400 gallons of water per hour, in the form of droplets with diameters approximating 40 microns.

The spray was electrically charged by passing it through an induction charging grid. For charge-equilibrium purposes, the total charge for the spray system was divided equally between positive on one wing and negative on the other. The release of the positively and negatively charged particles was arranged so that mixing and neutralization were held to a level which did not significantly reduce performance. The anticipated total spray current of 1.2 milliamperes may have been achieved, but because of instrument problems it was not measured.

This first charged-water dispensing apparatus was insufficiently airworthy to permit a good evaluation of this technique, but a decided decrease in fog density was observed on one of the three tests. Thus improvement and further testing of the system were warranted.

CHARGED BUBBLE TESTS

In 1972, NWC theoretical studies of particle collection by charged bubbles were found to be in agreement with studies performed by others[6,7] and the potential for fog dispersal using charged bubbles was recognized. The design and testing of equipment to dispense charged bubbles from the surface was initiated during Foggy Cloud V.

The prototype charged-bubble generator used during that project evolved from the theoretical and experimental studies conducted with charged-water droplets at NWC. Initially, induction charging of water drops formed by vibrating hypodermic-needle nozzles was tried. The needles vibrating at rates of 500 to 1,500 Hz formed discrete drops. Charges sufficient to cause drop breakup upon exit from the high-field region in the vicinity of the induction ring were easily obtained. However, calculations showed that an unrealistically large number of needles would be required for fog clearing, so this system was set aside. This technique may be worth further investigation for other applications because of its capability for producing water droplets with very high charge per unit surface area.

The second approach attempted was contact-charging of plastic spheres. The charge that can be placed on a particle is proportional to its surface

---

[6]V. V. Smirnov and A. D. Solov'en. "Generation and Properties of Particles With Expanded Surfaces (Liquid Bubbles)," in Proceedings of the Institute of Experimental Meteorology, 1(33), pp. 3-23. Trudy Institut Eksperimental' noi Meteorologii. Moscow, 1972.

[7]Y. S. Sedunov. "Laboratory Experiment on the Cloud Droplet Spectrum Formation and Its Modification," presented at the Third Conference on Weather Modification, Rapid City, S. D., June 1972. Paper UNCLASSIFIED.

area (given a constant field strength). The volume of material inside a charge carrier, such as a drop, contributes insignificantly to the charge-carrying capacity. If a hollow sphere is used as a charge-carrying particle, then a lesser volume of material is needed to deliver a given charge. Although the idea of using charged plastic spheres is theoretically feasible, delivery and pollution problems indicated that another approach should be tried.

The third approach used was contact-charging of bubbles formed by a coaxial-tube bubble generator. This method was tried since bubbles solved the hollow-sphere generating problem, the delivery problem (when used with a buoyant gas such as hydrogen, methane or, preferably, helium), and the pollution problem caused by plastic spheres. The bubble generator consisted of three coaxial tubes, the inner tube carrying inflation gas, the middle tube carrying bubble forming solution, and the outer tube carrying blowoff air (to force the bubbles off the middle tube). Efficient bubble generation required such extremely critical control of the pressure in the coaxial tubes that this approach was dropped and another one tried.

The fourth approach, and the one used during the Foggy Cloud V tests, used a prototype bubble generator in which bubbles formed by pressurized gas were contact-charged by a rotating wire mesh cylinder. Bottled nitrogen, bottled helium, and (warm) automobile exhaust were used on various tests to inflate the bubbles. This simple system produced a prolific supply of bubbles as long as a clean solution was used. The rotating mesh cylinder was approximately 1 foot in diameter and 3 feet long. The bottom of the cylinder extended into a wetting tray, and just under the top of the cylinder, on the inside, were blower tubes. The rate of bubble generation was controlled from zero to maximum by adjusting the rotational velocity of the cylinder. The maximum rate was more than 60 bubbles per second. Since a 4-inch-diameter bubble has 30 cm^2 of surface area, a bubble generator producing sixty 4-inch-diameter bubbles per second emits 18,000 cm^2 of bubble surface area per second and consumes about 1 cm^3 of solution every three seconds.

Two major problems had to be solved before testing could be attempted: producing bubbles that were durable enough to penetrate the fog, and placing sufficient charge on the bubbles. The first problem was solved by using a liquid detergent diluted with glycerine. Using a solution with about 1 part of detergent to 1 or 2 parts of glycerine, bubbles with a median life span of approximately ten minutes were generated. Some improvement, if needed, could be obtained by concentrating the solution by evaporation. Formation of bubbles from highly condensed solution was more difficult, but the bubbles thus formed appeared to be longer-lived.

The second problem was solved by charging the entire bubble generator to 15 kV or greater. Charging by use of induction rings in the vicinity of the bubble-forming area was not practical because of the ease with which charged bubbles were attracted to the induction rings.

Seven field tests of the charged-bubble generator were conducted during Foggy Cloud V. It was determined that charged-bubble generators could be designed to produce bubbles in quantities large enough to provide a reasonable potential for fog dispersal. It was found that a mixture of two parts liquid detergent and one part glycerine made the most satisfactory bubble-forming solution. Nitrogen, helium, and automobile exhaust all produced bubbles satisfactorily; each gas formed bubbles with different buoyancy characteristics. The advantages of this type of a system were defined as follows:

1. No aircraft is required; greater safety is one benefit, and lower cost is another.
2. The power requirements of the system are moderate; no high pressure pumps are required; pressurized gas bottles or an air compressor and air heater are required, but use of the latter would negate the advantage of low power requirements.
3. A given total area of surface for collecting fog droplets, if created by generating (hollow) bubbles, requires only about 1/100 of the mass of material that would be required to create the same area using droplets.*
4. The energy required to break up a liquid into small drops is saved.
5. Fog would be cleared from the ground up, a feature of special value in airport and canal fog clearing.[5]

The recommendation was to test the charged-bubble technique on a larger scale.

EVAPORATION SUPPRESSION TESTS

Visibility improvement in fog by the technique of evaporation suppression is a relatively new concept. This method should be applicable in many cases when fog derives its water for formation from underlying canal, lake, or ocean surfaces.

Evaporation suppression is achieved by spreading a monomolecular film of a higher fatty alcohol, generally C_{16} to C_{23}, over the water surface.[5] Spreading has been done from aircraft, from boats, and by other means. The alcohols have been spread as powders, emulsions, molten liquids, and solutions. Laboratory studies have shown that the evaporation suppressing ability of long-chain alcohols increases with increasing hydrocarbon chain length and decreases with increasing film temperature.[8]

---

*This computation is based on a comparison of bubbles 4 inches in diameter and droplets 100 microns in diameter.

[8]Institute of Water Utilization, Agriculture Experiment Station, Univ. of Arizona. *Evaporation Reduction Investigations Relating to Small Reservoirs in Arid Regions*, by C. B. Cluff and S. D. Resnick. Tucson, Arizona, Univ. of Arizona, October 1964. 33 pp. Publication UNCLASSIFIED.

The long-chain fatty alcohols used, such as hexadecanol and octadecanol, are nontoxic to both plant and animal life, and their films offer only slight resistance to diffusion of gases other than water vapor.

Evaporation suppression as a means of conserving water was first reported by Mansfield in 1955.[9] Since that time many similar investigations have been carried out in the western United States, mostly under the auspices of the Bureau of Reclamation in the Department of Commerce. Monomolecular films have reduced evaporation from lake surfaces by as much as 70 to 80%.

Very little work has been done to explore evaporation suppresssion as a technique for preventing the formation of fog. One of the few investigations along this line was begun in 1964-65 in Kil'skiy Bay in Russia.[10] These tests indicated a capability for fog dispersal in a bay with an area of approximately 3 km^2, using a film of surface-active substances. Visibility in the cleared zone was 10-12 kilometers, while in the adjacent fog-bound area visibility was 100-200 meters. The best fog clearing results were obtained when (1) the material utilized was a 3% solution of higher fatty alcohols of the C_{18} to C_{23} fraction dissolved in kerosene, (2) the solution was applied in a dispersed form (a spray), and (3) the wind speed was low; with winds reaching 8-12 meters per second the film broke into separate pieces and no large clearing was created. The polluting effect of the kerosene was an obvious disadvantage.

Other research has been conducted on material spreading rates, evaporation reducing efficiencies, persistence of films, bacterial degradation, ecological hazards and other basic properties of the long-chain alcohols. Laboratory and field tests together have demonstrated the effectiveness of various suppressant chemicals, as follows:

Mixtures of cetyl and stearyl alcohols (hexadecanol and octadecanol) containing 65% or more of octadecanol are most efficient for field use. Hexadecanol alone is less effective in reducing evaporation than octadecanol, but octadecanol alone does not spread effectively. The C_{20} and C_{22} long-chain alcohols (eicosanol and docosanol) are the most effective under quiet conditions, but the films are brittle and break under windy conditions. The C_{14} alcohol, tetradecanol, is useful for film spreading of octadecanol in low concentrations, but reduces the film efficiency at high concentrations. Dodecanol (C_{12} alcohol) in a mixture is detrimental to film efficiencies, but can be "squeezed out" of the film when the film is compressed.

---

[9]Commonwealth Scientific and Independent Research Organization of Australia (Ser. No. 74), *Summary of Field Trials on the Use of Cetyl Alcohol to Restrict Evaporation From Open Storages During the Season 1954-55*, 1955. Publication UNCLASSIFIED.

[10]R. A. Bakharova and others. "Results of Tests on Methods of Modifying Steam Fog," *Trudy UkrNIGMI, No. 77* (1969), pp. 144-51.

The first evaporation suppression tests by NWC were undertaken at the Panama Canal during Foggy Cloud V. Experiments were conducted to determine the feasibility of suppressing the warm fog in the Gaillard Cut area by reducing water evaporation from the Canal surface with monomolecular films. Two of the trials involved dispensing ethyl alcohol solutions of cetyl alcohol (hexadecanol); three used ethyl alcohol solutions of a mixture of predominantly cetyl and stearyl (octadecanol) alcohols. The latter mixture was purchased from Proctor and Gamble Company and carried the designation: Tallow alcohol, TA1618F. Since water from the Panama Canal, after undergoing chlorination, flocculation, and filtration, is used for human consumption, it was necessary to use a nontoxic solvent. Either ethanol or freon would have served as the reagent, but ethanol was used because its cost is less. The tallow alcohol is a more efficient evaporation suppressant than hexadecanol at the temperatures prevalent in the Canal Zone.[5]

The solutions of hexadecanol and tallow alcohol ranged in concentrations from approximately 10 to 15%. The applications during Foggy Cloud V ranged from 0.2 pound per acre to 0.7 pound per acre. When the long-chain alcohols were applied, the formation of films with adequate canal coverage was observed. On three test dates during a period of relatively high fog frequency, fog did not close the canal to ship traffic. Further testing to determine repeatability was of course necessary.

PROJECT OBJECTIVES

PRIMARY OBJECTIVES

The ultimate objective of the Foggy Cloud test series is to develop an inexpensive, reliable, rapid method of dispersing warm fog and stratus. In order to pursue this ultimate objective effectively, each series of field tests is designed to pursue a series of primary and secondary objectives. The primary objectives of Foggy Cloud VI were to measure the effectiveness of warm fog clearing by:

1. Aerial dispensing of electrically charged water and glycerine, using the B26 as a spray vehicle (Phase I).
2. Surface dispensing of electrostatically charged, hygroscopic bubbles (Phase II).
3. Evaporation suppression by application of thin films of a tallow alcohol emulsion (Phase III).

SECONDARY OBJECTIVES

Secondary objectives included:

1. Field testing new equipment and instrumentation.
2. Studies of fog properties pertinent to fog life cycles.
3. Collection of data necessary for validation of existing fog and/or fog modification models.

FIELD TEST SITES AND TEST CONDITIONS

THE ARCATA-EUREKA AIRPORT

Phases I and II of the project were conducted at the Arcata-Eureka Airport (Figure 1), McKinleyville, California. This airport is located on the California coast about 80 miles south of the Oregon border. The major portions of Projects Foggy Cloud I-IV were all conducted at this field test site. Figure 2 shows the arrangement of the test area.

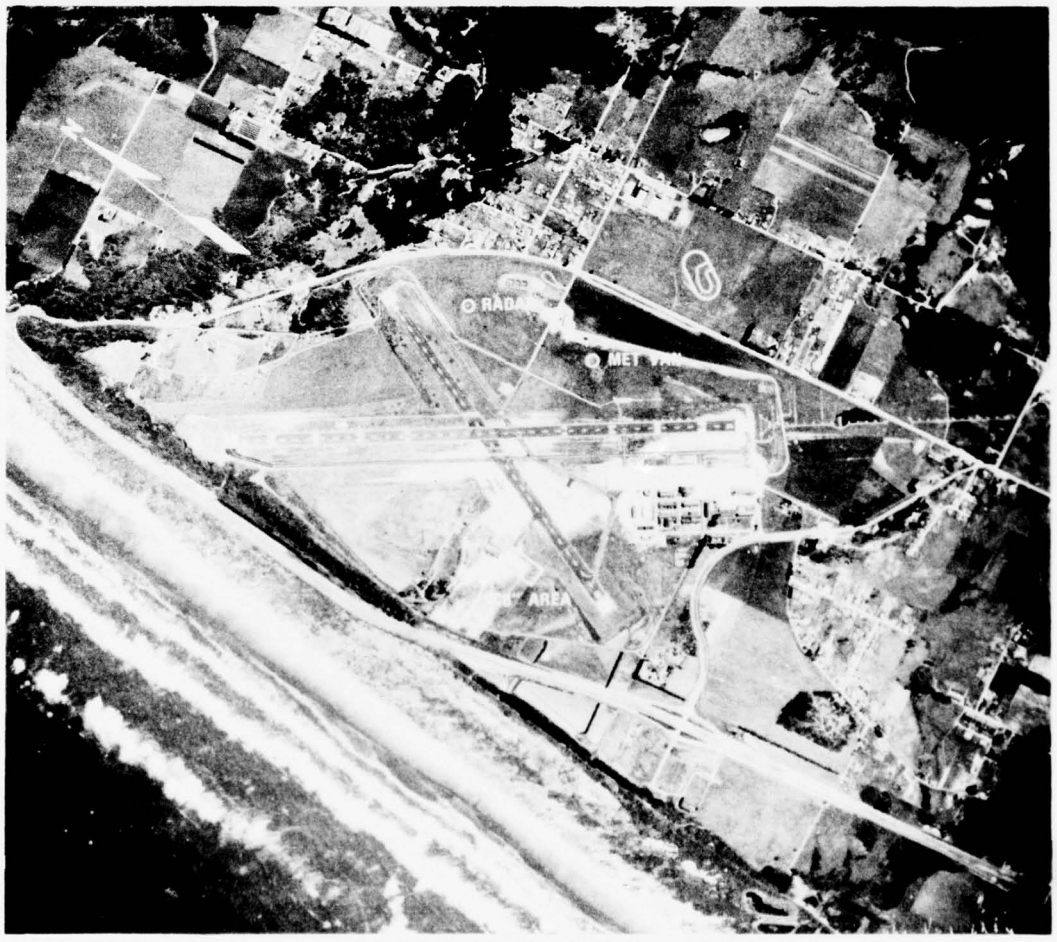

FIGURE 1. Arcata-Eureka Airport.

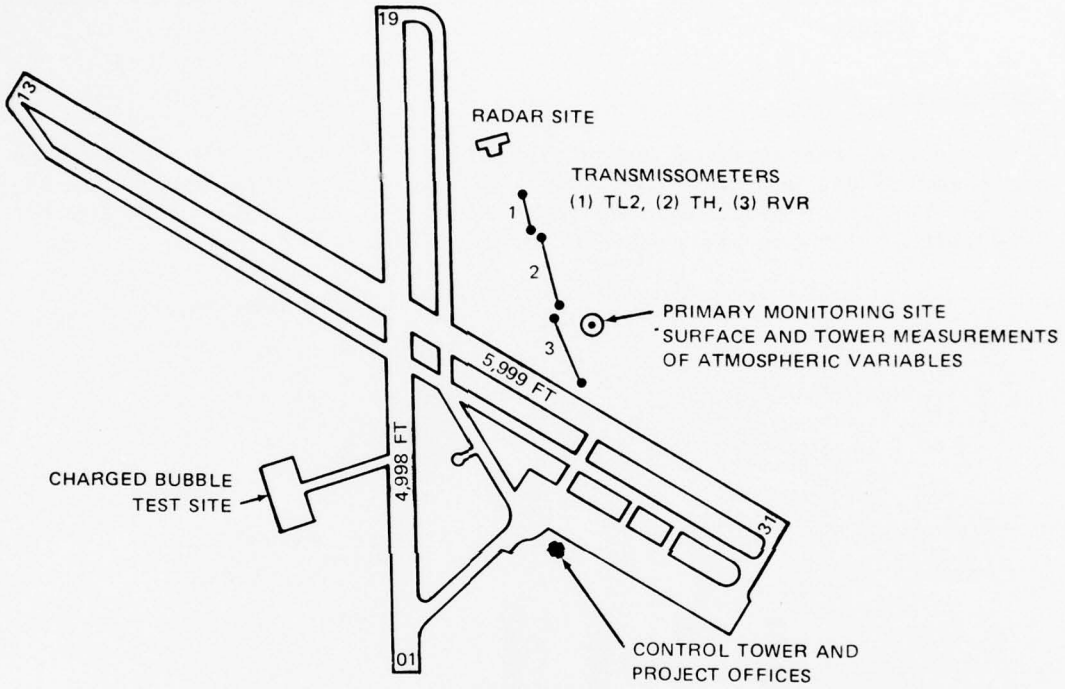

FIGURE 2. Project Site and Instrumentation Locations.

The principal reasons for selecting the Arcata-Eureka Airport as the test site were:

1. A high incidence of fog.
2. A relatively low airport traffic volume.
3. Excellent facilities, including navigational aids, office and and work space, storage buildings, and nearby alternate airfields.
4. Excellent support provided by local authorities, including the Federal Aviation Administration (FAA), the Winzler and Kelley Atmospheric Laboratory, and the Humboldt County Department of Aviation.

5. A unique array of transmissometer installations in addition to standard meteorological instrumentation, to supplement the NWC instrumentation.
6. A knowledge of the fog climatology, available from previous studies.[2,11-14]

ARCATA FOGS

The fogs that produce low visibility conditions in the Arcata area occur during all months of the year. The greatest incidence of fog is during the summer and autumn months. Climatological fog statistics for July through October are presented in Figure 3.

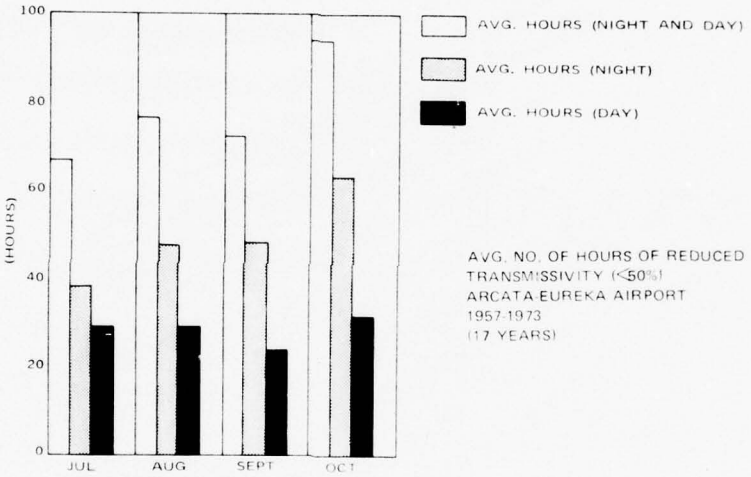

FIGURE 3. Limited Visibility Conditions at Arcata-Eureka Airport.

---

[11]National Bureau of Standards. *A Summary of Low Visibility Conditions at the Arcata Airport*, by James E. Davis and others. Washington, D.C. NBS, U.S. Dept. of Commerce, November 1968. (NBS Report No. 9958, 40 pp, report UNCLASSIFIED.)

[12]Atmospheric Research Group. *Operation Pea Soup 1959*, by T. J. Lockhart and R. J. Beesmer. Altadena, Calif., 18 December 1959, 23 pp. (ARG59 FR 58, report UNCLASSIFIED.)

[13]Aeronautical Icing Research Laboratories, Bartlett, N.H. *Fog Studies at Arcata, California, Under "Operation Pea Soup" 1960*, by G. P. Ettenheim, Jr., and others, for the U.S. Air Force, Bedford, Mass., March 1961. 34 pp. (Technical Note No. 570, AFCRL 261, Report UNCLASSIFIED.)

[14]Aeronautical Icing Research Laboratories, Arcata, Calif. *Fog Studies at Arcata, California, Under "Operation Pea Soup" 1961*, by G. P. Ettenheim, Jr., for the U.S. Air Force, Bedford, Mass., June 1962, 26 pp. (Technical Note No. 571, AFCRL 62-804, Report UNCLASSIFIED.)

Fogs occurring in the Arcata area during these seasons are generally advective in nature. These fogs form when moist marine air flows over the relatively cold coastal waters. The marine air layer is cooled to saturation by mixing and radiative processes and condensation occurs.

The proper wind flow pattern exists when the Pacific high pressure cell intensifies offshore and the interior mountains and valleys undergo intense heating. A west-east pressure gradient is established with subsequent advection of maritime air toward the coast.

Thickness of the coastal fogs varies considerably, with bases from 0 to 300 feet AGL and tops averaging 1,000 feet; however, tops exceeding 1,500 feet are not unusual. Advection fogs are cyclic in occurrence, generally appearing for three to five successive days and alternating with a similar time period of partly cloudy skies. Fog occurring during a given episode may lift and evolve to form a stratus deck after persisting for two to three days. Less commonly, stratus forms initially instead of fog. The stratus, as well as the fog, is suitable for airborne experimentation.

Radiation fogs, which are uncommon in July and August, begin to appear in late September. Although these fogs are relatively shallow, averaging about 500 feet in thickness, they are more dense at the surface, and ceilings are always at or near zero. This type of fog normally forms on the first or second day after passage of a "wet", early-season, cold front. Skies become sufficiently clear to allow radiative daytime heating and nighttime cooling of the earth's surface. Turbulent effects associated with the front must have ceased; winds must be reduced to light and variable.

Fogs on the coast occasionally form due to a combination of nocturnal radiative cooling and light advection. Further details on the formation of Arcata fogs are given in the NWC Technical Publication for Project Foggy Cloud III, Phase I.[2]

THE PANAMA CANAL

The Panama Canal must frequently be closed to navigation because of fog in the area of the Gaillard Cut (Figure 4). In 1969 the Panama Canal Company asked NWC to study the characteristics of these fogs and recommend possible means of abatement. Project Foggy Cloud V and Phase III of Foggy Cloud VI were conducted at this site.

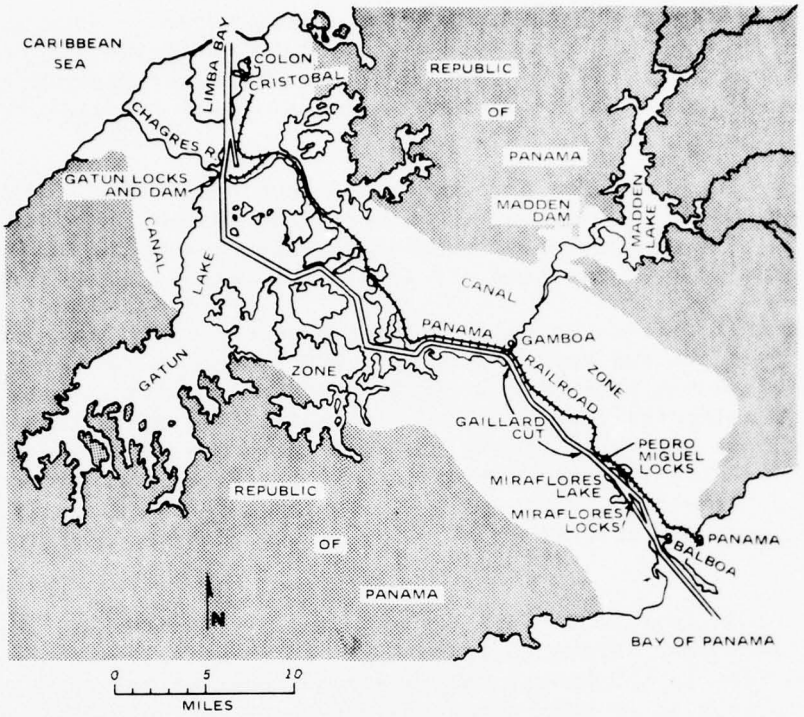

FIGURE 4. Panama Canal and Canal Zone.

PANAMA CANAL FOGS

The climate of the Canal Zone and Panama is typical of the tropics. Temperature and humidity are moderately high throughout the year. The annual north-south migration of the sub-tropical high pressure area normally divides the year into three seasons: a 4-month dry season, mid-December to mid-April; two transition months, mid-April to mid-May and mid-November to mid-December, and a 6-month rainy season, mid-May to mid-November. It is during this rainy season that fogs impede navigation through the Panama Canal.

These fogs are formed primarily by radiational cooling. They generally form during the night hours over the land areas above the canal and flow with cool air drainage to create stratus over the canal. At the same time, the air directly above the canal is being saturated by evaporation from the canal. As the cooler air from the land mixes with the wet air above the canal, the stratus lowers and fog dense enough to prevent navigation forms at the canal surface. The fog is often enhanced by condensation nuclei from a cement plant 10 miles north of Gamboa. Canal closures often last several hours and may occur three or four times

a week. From 1968 through 1971 the canal was closed an average of 236 hours per year during the months of August through November. Fogs generally occur in the region from Gamboa to Pedro Miguel Locks with the greatest density occurring along a five-mile stretch between Gamboa and Gold Hill.[5]

FIELD INSTRUMENTATION

A variety of field instrumentation was used to study the Arcata fog and monitor the effects of the fog dispersal tests of Project Phases I and II.* Descriptions of this equipment are given here. The fog dispersal devices are described in the sections on analyses of the specific Project Phases. Details of Phase I tests are given in Appendix A.

A 60-foot meteorological tower, various instruments, and a van to house data recording equipment and serve as a base for observers were located at the primary monitoring site for Phase I operations (Figures 1, 2, 5, and 6). The tower, the van and most of the following equipment were moved to the "CB area" for the tests of the charged-bubble generators (Figures 1, 2 and 7).

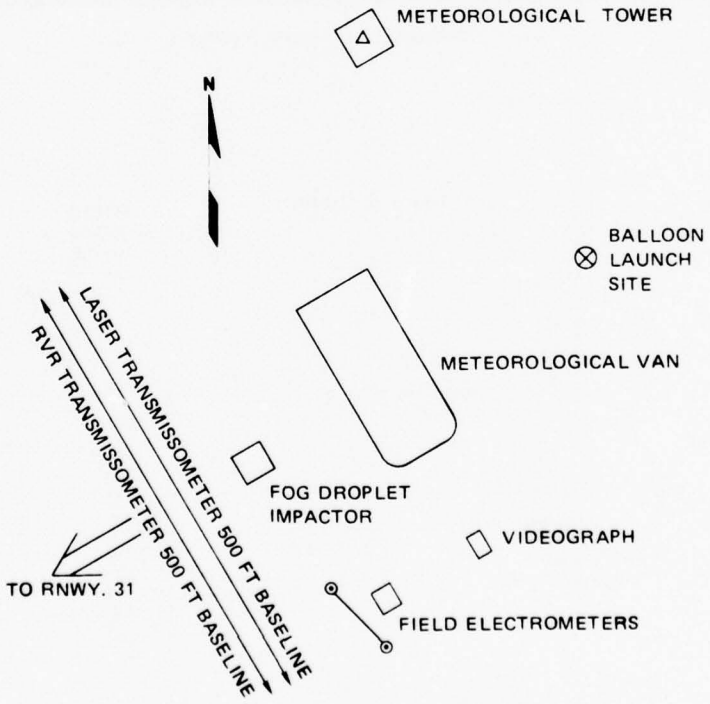

FIGURE 5. Sketch of Primary Monitoring Site.

*Materials, equipment and instrumentation used in the evaporation suppression tests in the Canal Zone are described in Phase III - Systems and Testing.

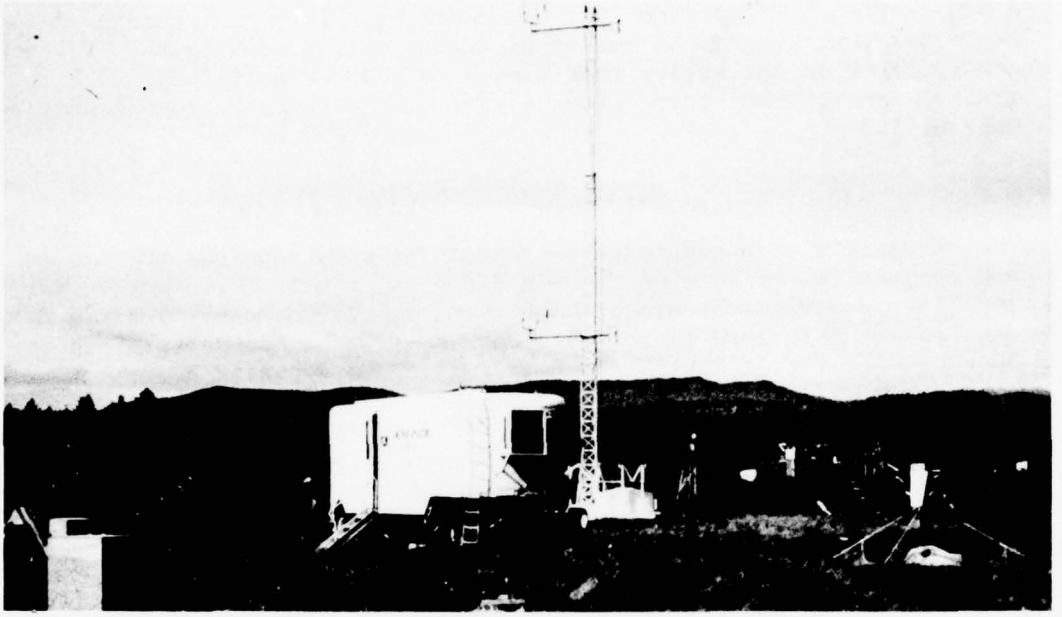

FIGURE 6. Photograph of Primary Monitoring Site.

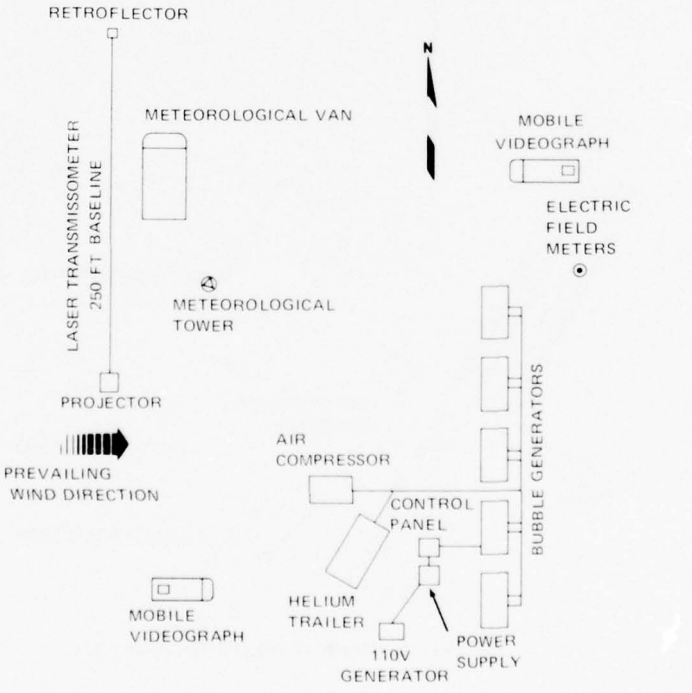

FIGURE 7. Equipment Arrangement at the "CB" Area.

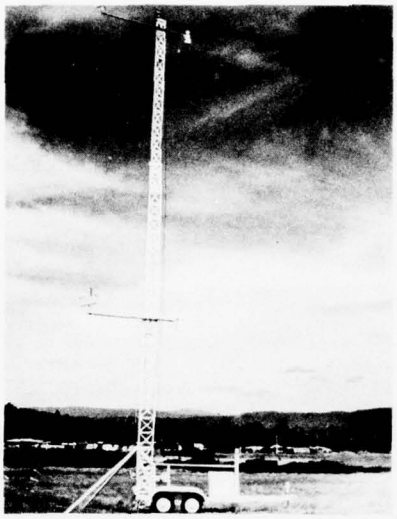

a. Temperature, dewpoint and wind sensors on tower.

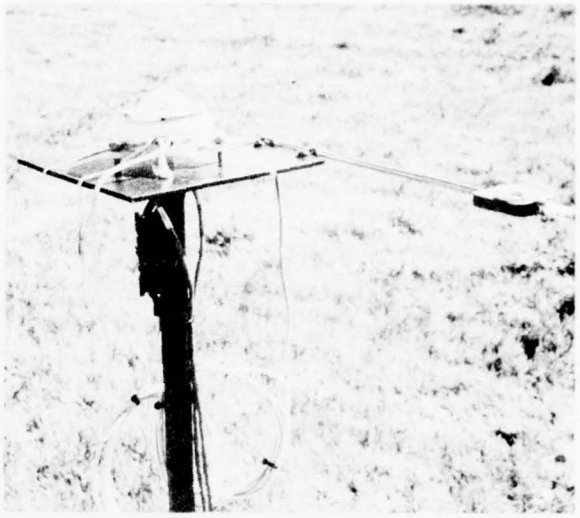

b. Solar and net radiometers.

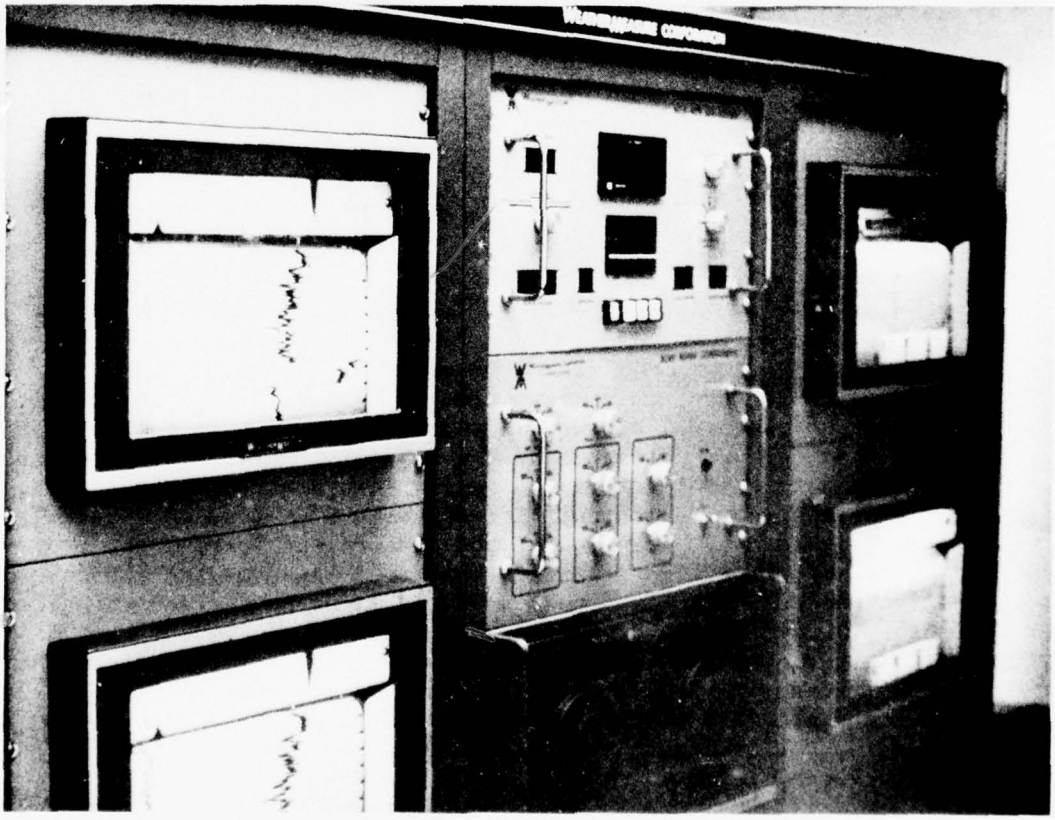

c. Data logger.

FIGURE 8. Sensing and Recording System.

A new sensor and recording system, purchased by NWC from Weather Measure, Inc., Sacramento, California, was delivered early during the field project period. This system includes instruments for measuring temperature, dewpoint and wind at two levels (20 and 50 feet AGL) on the tower, a barometric pressure sensor, solar and net radiometers, and a digital data logger which continuously records all the input parameters on strip charts and magnetic tape. These instruments are shown in Figure 8.

A new laser transmissometer from Northwest Environmental Technology Laboratories, Inc. (Figure 9), was installed in parallel with the airport

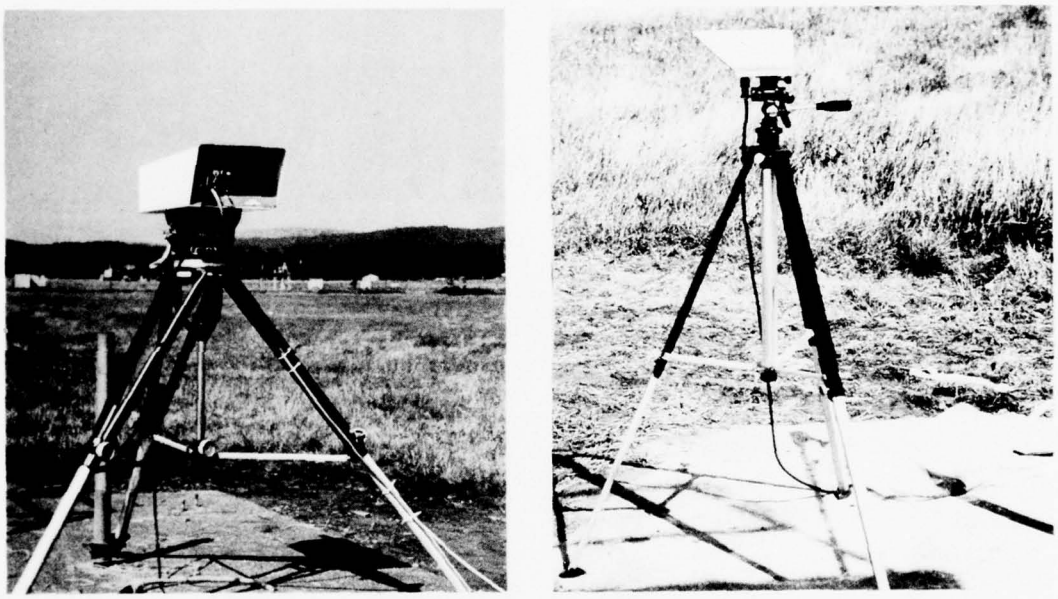

a. Right source. b. Retroreflector.

FIGURE 9. Laser Transmissometer.

Runway Visual Range (RVR) transmissometer for Phase I operations, and perpendicular to the usual on-shore advection for Phase II tests. The visibility measurements generated by the transmissometer were automatically recorded with the digital data logger. Two new videographs (manufactured by Radiation, Melbourne, Florida) were also used to measure visibility (Figure 10). The videographs measure the backscatter from a pulsed signal of white light, whereas the laser measures the attenuation of red light between the fixed points of the light source and the retroreflector. The videograph signals are recorded on continuous strip charts. One stationary videograph was used in Phase I tests. Both videographs mounted on trucks were utilized in the tests of the charged-bubble generator; the mobility allowed observers to orient the field of view of each videograph according to the airflow so as to monitor treated and untreated volumes of fog.

Fog droplet size information was obtained with a simply fabricated device that impacts the droplets on gelatin coated slides.

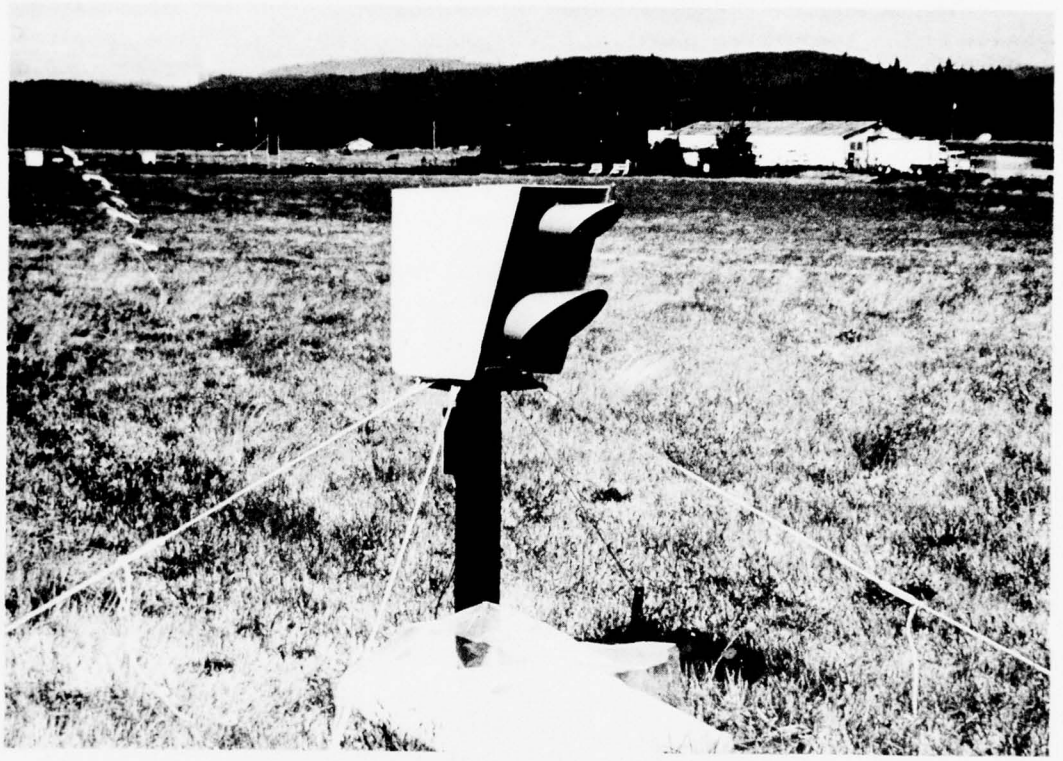

a. Installation at primary monitoring site.

b. Mobile videograph for use during charged bubble tests.

FIGURE 10. Videographs.

The number of cloud condensation nuclei (CCN) per cm^3 were determined using a MEE Industries Model 310 CCN Counter. The chemical composition of aerosols, with respect to particle size, was determined from samples collected with a model 4220 Lundgren impactor. A detailed analysis of these data is presented in Appendix B.

The atmospheric electric field was measured with two devices, a Keithley electrometer, and an experimental Dolezalek instrument (Figure 11).

a. Keithley sensor.

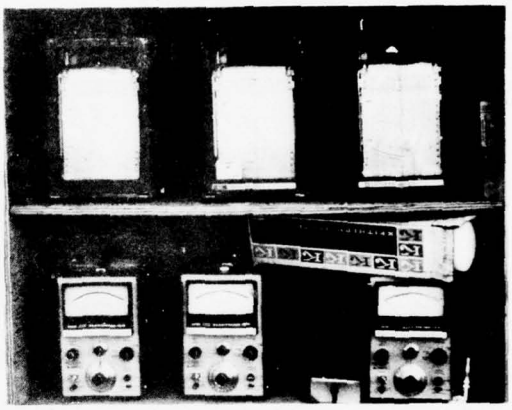

b. Keithley electrometers and recorders.

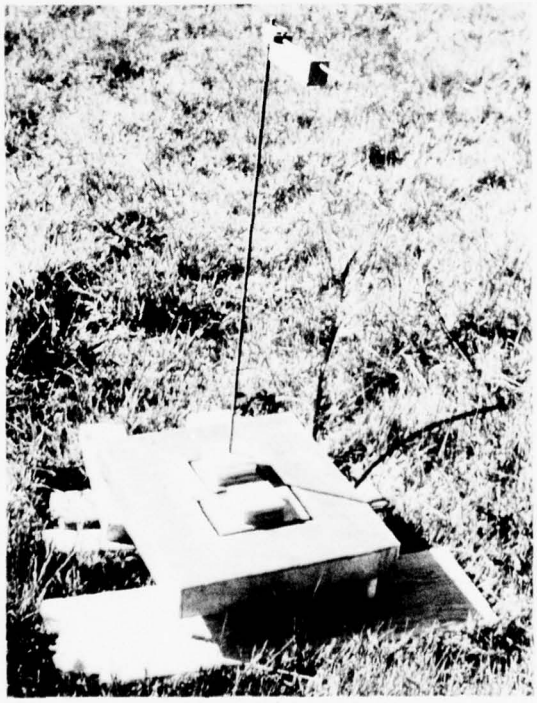

c. Experimental "Dolezalek" sensor.

FIGURE 11. Atmospheric Electric Field Measurement System.

Meteorological observers measured surface temperature, dewpoint and wind, and took visual observations of fog conditions (visibility, ceiling, clear areas, . . .) at 5-minute intervals during test periods.

Sounding balloons with aluminum reflectors were released at the point indicated in Figure 2, and were tracked through the fog layer with an M-33 radar. This operation provided wind profiles that were used to determine appropriate flight paths for targeting of the charged droplets released from the seeder aircraft.

The M-33 radar and a TPS-1D radar were employed to track and guide the seeder aircraft, and to aid in low visibility takeoffs and landings of a Navy U-3 aerial photo plane and an instrumented Cessna 337 laboratory and observation aircraft.

Aerial photos were obtained from the U-3 with a downpointing T-11 camera during daylight operations.

Observers with hand-held cameras photographed the test from the Cessna 337. A Minilab (Weather Science, Inc.) mounted in the aircraft provided continuous airborne measurements of temperature, dewpoint and fog liquid water content. The Minilab is described in detail in a Naval Weapons Center Technical Publication.[2]

Ground-to-ground and ground-to-air communications utilized portable Bendix VHF aircraft transceivers in addition to standard air traffic control communications systems.

A computer facility was set up for on-site data reduction;

Hardware included:

1. A PDP-8 computer with 4K memory, teletype and high speed reader and punch.
2. A DL-622 1/4-inch magnetic tape reader for reading Minilab tapes.
3. A Printec 100-line printer, 100 CPS.
4. A DI-503 Interface unit for use with DL-622 and Printec for raw "number dumps".

Software capabilities included:

1. FOCAL and FORTRAN II languages.
2. Programs written during past projects, including a tape dumping program with titles, a program for readout and conversion to engineering values for Minilab data tapes, and an averaging program for Minilab data passes.

Several programs were written during the project for conversion of laser transmissometer and videograph data to visibility readings, and for

modeling the droplet growth rates of the charged seeding materials. By doing the data reduction work during interim weather periods without fog, it was found that the data could be kept current.

PHASE I SYSTEMS AND TESTING - AERIAL DISPENSING OF CHARGED WATER DROPLETS

EQUIPMENT

An airborne droplet charging and spraying system on a B-26 aircraft was tested during Foggy Cloud VI. This apparatus has the same basic design as the system utilized in Foggy Cloud V. However, the mechanical structure and electrical components of the latter system were improved considerably to make the system more airworthy.

The Foggy Cloud VI spraying system is illustrated in Figures 12, 13, and 14. Water or hygroscopic solution to be sprayed is pumped into a

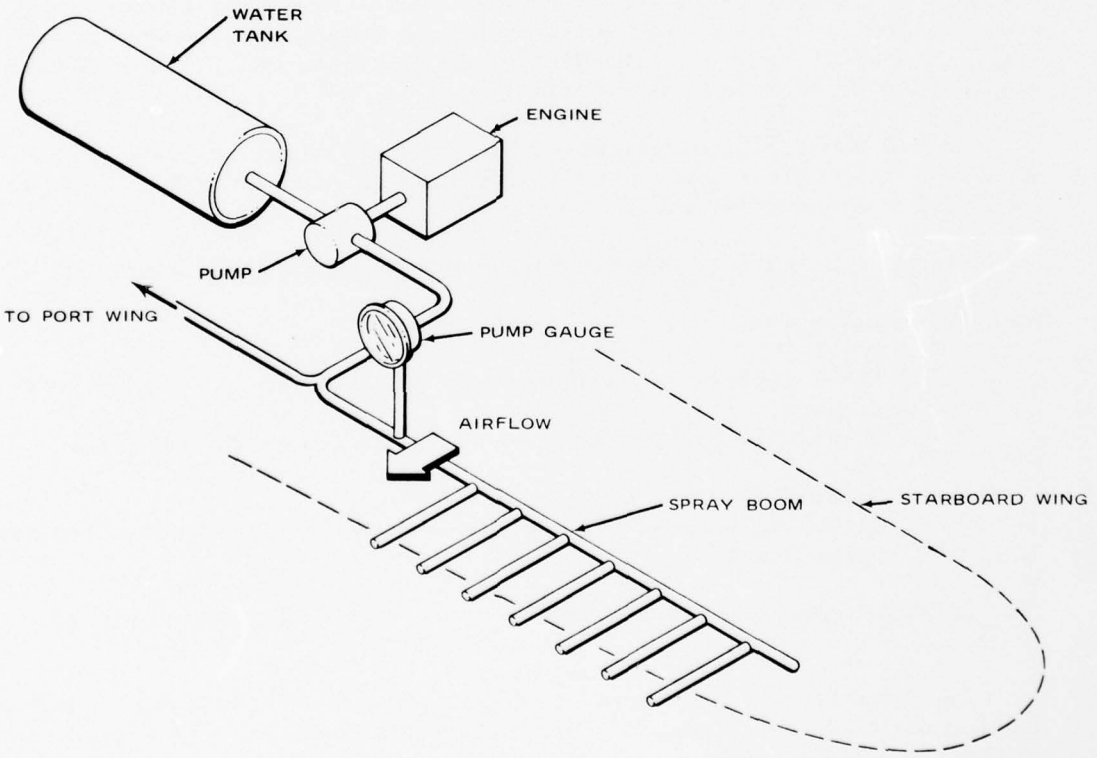

FIGURE 12. Spray System Schematic.

FIGURE 13. Seeder Taking On Water Load.

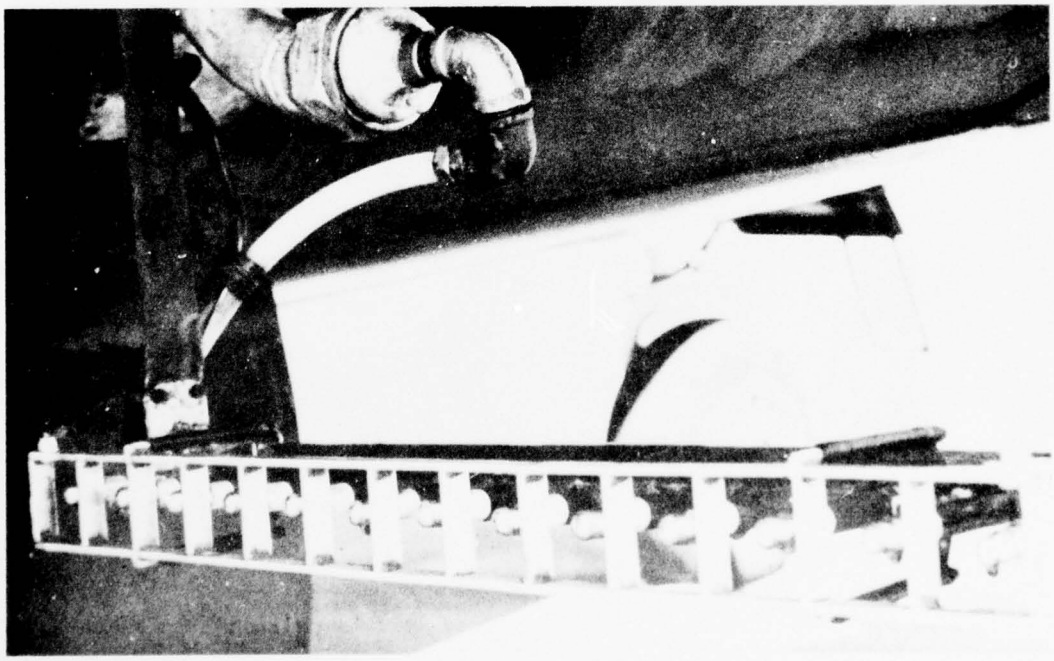

FIGURE 14. Plumbing Connecting Spray Boom at Fuselage.

1,300-gallon tank carried in the bomb bay of the B-26. An automobile engine mounted in the aircraft drives a centrifugal pump that transports the liquid into the spray booms and out the nozzles. The pressure in the booms is regulated by the rpm of the engine and is monitored on a gauge in the cockpit. The boom under each wing is fitted with 143 nozzles.

During the early stages of testing, oil spray from the aircraft engines was found to be collecting on the inner sections of the booms and possibly shorting the electrical systems. The section of each boom nearest the fuselage was therefore removed. Further tests were conducted with 130 nozzles on each boom.

Two sets of nozzles were tested.* Each nozzle of one set allows a liquid flow rate of 1 gal/hr at 125 psi; the nozzles of the other set each produce a flow of 8 gal/hr at the same pressure. The spray-droplet size distribution has a mass-median radius of approximately 40 μm for the 1 gal/hr nozzles and 66 μm for the 8 gal/hr nozzles.[15]

The droplets are charged by electrostatic induction. An induction grid on each boom serves as the induction "rings" for each series of nozzles (Figure 15). Figure 16 is a diagram of the circuits utilized.

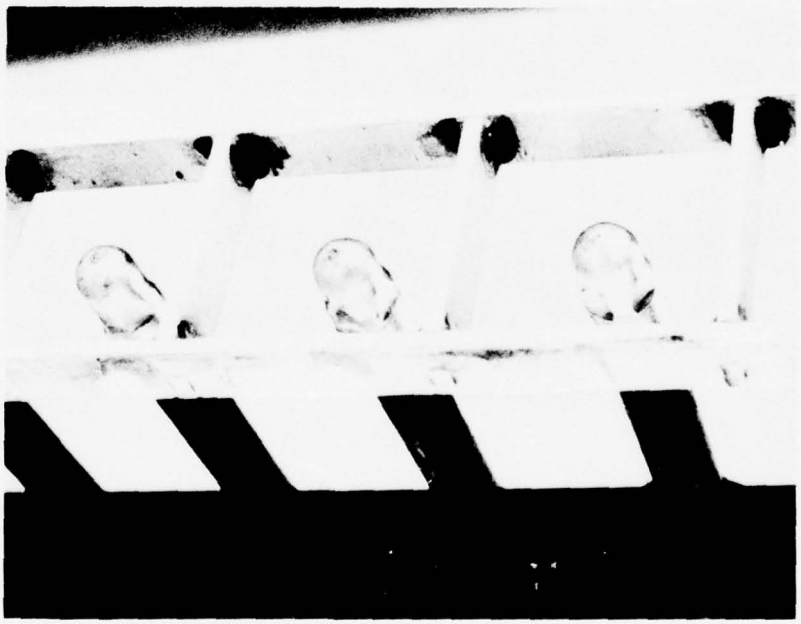

FIGURE 15. Section of Induction Grid and Nozzles.

*Delevan Manufacturing Co., West Des Moines, Iowa.

[15]R. W. Tate and E. O. Olson, "Spray Droplet Size of Pressure-Atomizing Burner Nozzles," *American Society of Heating, Refrigeration and Air-conditioning Engineers*, Vol. 4 (1962), pp. 39-42.

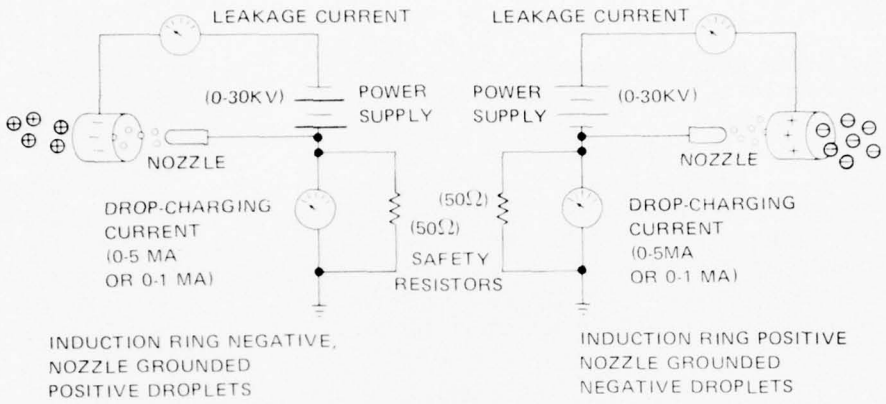

FIGURE 16. Electrostatic Induction Charging System Schematic.

Each spray boom is incorporated in a separate circuit. Induction grids on port and starboard booms are charged to opposite polarities to electrically balance the aircraft. The spray through the positively charged grid produces negatively charged droplets; and vice versa. Each 0-30 kV power supply for the charging circuits (Figure 17) is insulated from the aircraft, which serves as ground. A safety resistor in each circuit prevents buildup of any significant capacitance between ground and the power supply, should the ammeter fail and result in an open circuit.

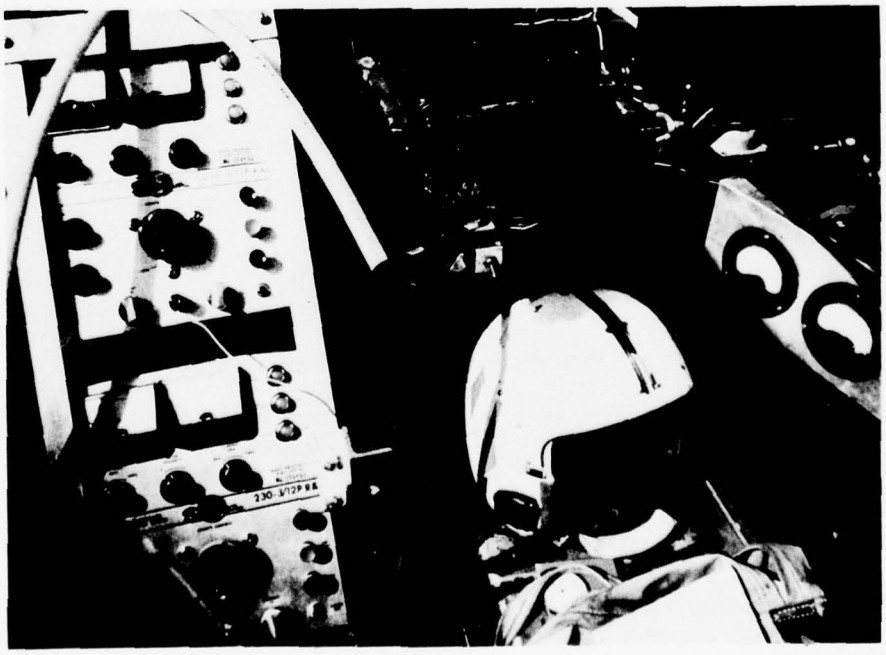

FIGURE 17. Power Supply for Induction Charging System.

PROCEDURES

Both fog and low stratus cloud cover were treated with sprays of charged droplets. Seeding was normally conducted at or just below fog (or stratus) top. A "dogbone" flight pattern (Figure 18) was used for tests under consistent wind conditions. Seeding was conducted along legs perpendicular to the wind vector. The object of utilizing this pattern was to treat the same volume of fog as it advected toward the runway. In order to allow seeding on the 10th leg to be conducted just before the drifting volume reached the runway, the distance that the first leg was offset upwind from the runway was predetermined. This distance varied from test to test in proportion to the wind speed.

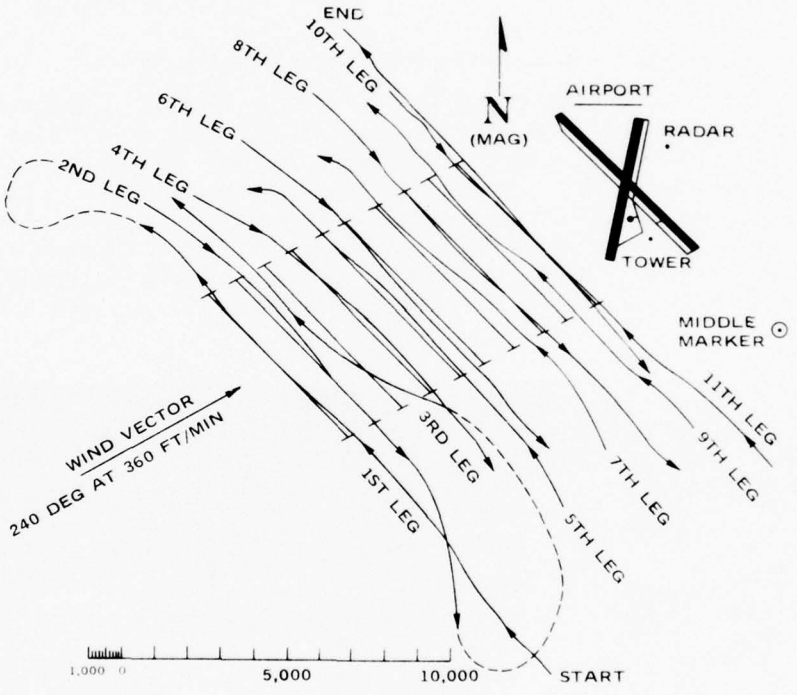

FIGURE 18. Radar Plot Showing "Dog Bone" Seeding Pattern.

Under calm conditions (i.e., light and variable winds), a "racetrack" seeding pattern was used (Figure 19). The volume of fog lying over the runway was repeatedly treated in these cases by making ten passes on the same track.

Instruments described in the Field Instrumentation Section were used to track and guide the seeding and observation airplanes, and to monitor and measure seeding effects.

The in-cloud measurements were made by the Cessna 337 laboratory aircraft along the length of Runway 31. This zone was the seeding target.

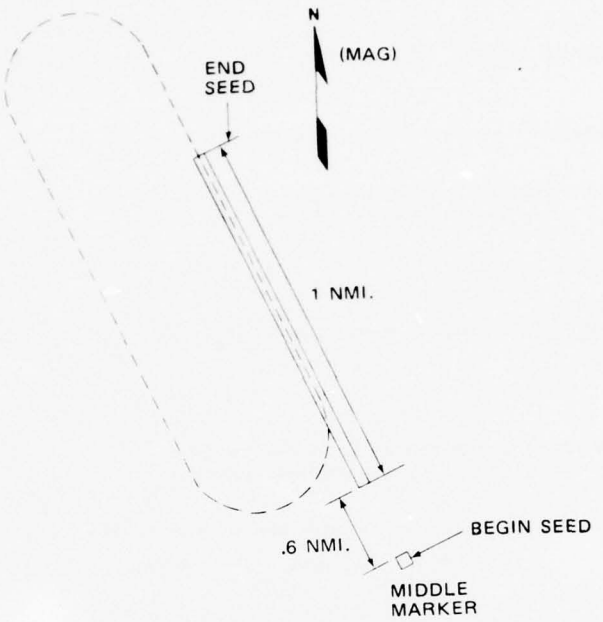

FIGURE 19. Racetrack Seeding Pattern.

When the seeder aircraft flew a dogbone pattern, the laboratory aircraft made preseed and postseed passes in the zone. When the seeder aircraft flew a racetrack pattern, the laboratory aircraft was also able to make passes following each seeding pass. The flight pattern is sketched in Figure 20. Map-view aerial photographs of the seeding operations were

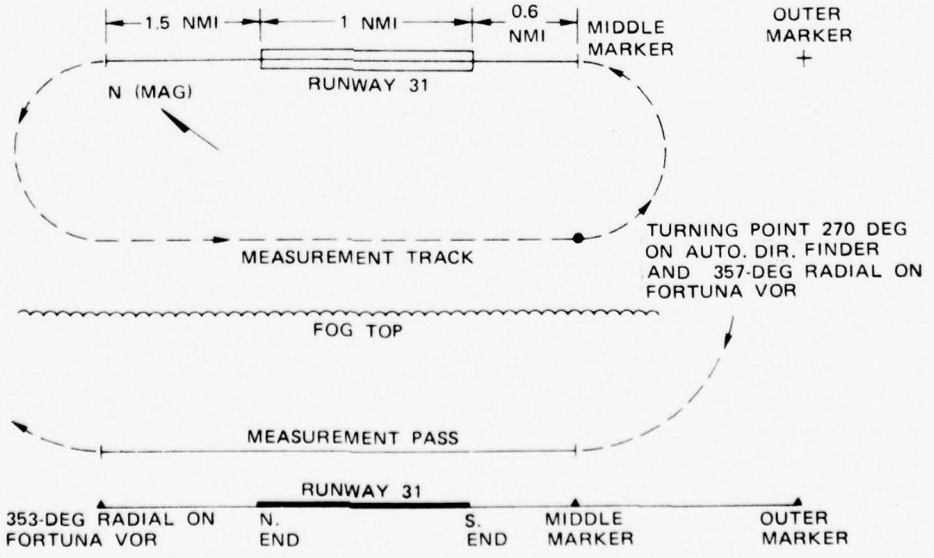

FIGURE 20. Laboratory Aircraft Flight Pattern.

taken from the U-3 aircraft at 10,000 feet above mean sea level (ft MSL). The flight pattern is shown in Figure 21. Visual observations from the primary instrument area, the tower, and the aircraft also contributed significantly.

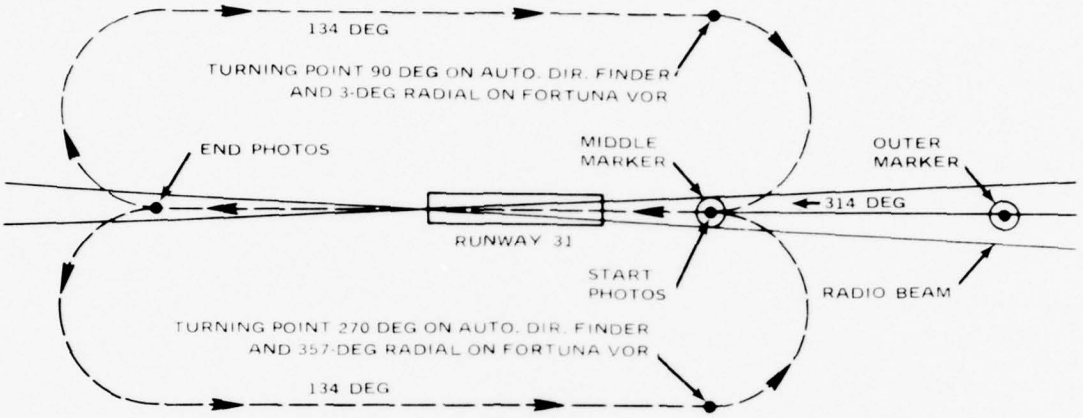

FIGURE 21. U-3 Aircraft Flight Pattern.

TEST RESULTS

The system for charging and spraying water droplets was tested extensively for its effects in dispersing fog and stratus. The primary tests of the system are designated by code letters FA(Fog, Airborne) in the following synopsis. Four extra tests of the airborne system (designated by "E") were conducted for checkout of personnel, instruments and the system, and for other special purposes. One test of the system was conducted to quantitatively determine effects of the system on cumulus clouds (designated CU-1).

Two preliminary tests, E(1) and E(2) were conducted as system rehearsal for airborne and ground crews. Then the thirteen principal tests to disperse fog and stratus were performed. The airborne electrostatic system was utilized at every opportunity. Departures of prevailing cloud characteristics from conditions ideal for testing the experimental system were evaluated for each case by utilizing parameters specified in Table 1; fog was always considered more ideal for testing than stratus because dispersal effects could be monitored with the ground-based instrumentation. The test conditions, operational aspects, and results are summarized here. Appendix A gives more details on test conditions and operations.

Basic operational aspects of each test are given in Table 2. The fog was normally treated with sprays of charged water; a glycerine-water solution was substituted in one test to add a hygroscopic effect to the droplet coalescence induced by charging. Spray nozzles designed to deliver water at a rate of 1 gallon per hour (gph) at 125 psi were used in seven of the tests; 8 gph nozzles were used in six tests. The dosage, of course, varied according to the nozzle flow rates; the nozzles with greater flow rates also produced spray droplets with greater sizes and fallspeeds.

Racetrack and dogbone flight patterns were employed to treat cloud volumes over or advecting toward the principal runway (Table 2). The fog was normally treated on each of 10 passes of the aircraft, which flew at 130-140 knots. The recorded duration of each test includes a preseed observation period, the period of treating the cloud, and a postseed observation period.

TABLE 1. Fog and Stratus Characteristics Ideal for Testing Dispersal Systems.

Parameter	Fog/Stratus
Sky cover	At least 9/10; preferably 10/10
Visibility	Less than 2,400 ft for fog; not applicable for stratus
Base	Ground level for fog; less than 800 ft for stratus
Depth	300-1,500 ft (in order to separate aircraft vortex from spray effects)
Stage of natural development	Formative or static, but not dissipating
Persistence	At least two hours before start of test; at least two hours after beginning of treatment in untreated areas
Liquid water content	Maximum 1 g/m^3
Precipitation	None, or very light drizzle at most (so natural and induced coalescence can be distinguished
Temperatures	Above freezing throughout depth of fog/stratus
Wind	Light, not gusty; preferably calm (to minimize mixing and optimize targeting)
Other clouds	Clear to scattered between top and 10,000 ft MSL (to allow visual observation from above

TABLE 2. Summary of Operations Testing the Airborne Electrostatic Fog Dispersal System

			Seeding Data				
						Altitude	
Test No.	Date Mo/Da	Time PDT	Quantity Gal.	Passes No.	Pattern	Ft/MSL	Relative to fog/cloud
FA(1)	9/3	0440-0655	28	10	Racetrack	500	Fog top
FA(2)	9/4	1320-1550	40	10	Racetrack	900-1,000	Above fog top
FA(3)	9/4	1810-2045	10	8	Dogbone (offset)	1,200-1,000	Above cloud top
FA(4)	9/10	0420-0610	140	10	Racetrack	800-600	Above fog top
FA(5)	9/10	0610-0805	140	10	Racetrack	500-400	Above fog top
FA(6)	9/11	0540-0705	320	10	Dogbone (offset)	1,900-1,700	Above cloud top
FA(7)	9/11	0705-0855	240	8	Dogbone (offset)	1,900	Cloud top
FA(8)	9/12	0520-0650	320	10	Dogbone (offset)	1,900	Above cloud top
FA(9)	9/12	1340-1635	50	13	Dogbone (offset)	1,300-1,100	Above cloud top
FA(10)	9/15	0540-0715	40	10	Dogbone (over runway)	1,400-1,200	Fog top
FA(11)	9/15	0715-0905	55	14	Dogbone (over runway)	1,300-1,100	Above fog top
FA(12)	9/25	0900-1100	40	10	Racetrack	800-400	In fog and fog top
FA(13)	9/29	0620-0815	200	9	Dogbone (offset)	1,100-900	Fog top

The performance of the spray-charging system is summarized in Table 3 and Figure 22.

TABLE 3. Performance of the Spray-Charging System.

Test #	Performance
FA(1)	System OK in clear air, shorted electrically upon entering fog, indicating heavy leakage currents. Spray dispensed just above fog on final passes. Potentials achieved on positive and negative booms somewhat below that desired. (See Figure 22 for actual potentials.)
FA(2)	Seeder attempted to fly as close to cloud top as possible while keeping boom dry, thus avoiding shorting/arcing.
FA(3)	All seeding passes made just above stratus top; no shorting/arcing.
FA(4)	Same as FA(3), but potential dropped considerably on positive boom (Figure 22).
FA(5)	Seeding accomplished just above fog, except for one pass in fog. Negative power was arcing at all times.
FA(6)	Seeder aircraft just above stratus top; arcing apparent only on last pass. Potential on negative boom slightly improved.
FA(7)	Excessive arcing in flight at stratus top. Fuse in charging system burned out on pass 5.
FA(8)	Excessive arcing of negative boom in flight above stratus top. Very low potentials realized on both booms.
FA(9)	All sharp points on nozzles and boom filed and smoothed before test to reduce arcing. Significant improvements in potentials on both booms realized (Figure 22), although positive potential fell off when aircraft entered stratus top on last passes.
FA(10)	Negative boom arcing on first pass, but good potential maintained.
FA(11)	Potentials maintained (Figure 22), but arcing loud enough to hear in cockpit on one pass. Arcing still causing uncertainty in magnitude of charge actually delivered to spray.
FA(12)	System improved prior to this test by 1) disconnecting and bypassing the boom and grid sections next to the fuselage which were fouling with engine grease and emissions, and 2) by coating the booms, grids, and electrical insulators with silicone grease to bead collected fog water and disrupt paths permitting leakage currents. System arced on only two of the ten passes within the fog.
FA(13)	Arcing problems experienced again as silicone coating deteriorated.
CU(1)	Charging potential held at high values during this test in (wet) cumulus clouds. (This test was conducted after the modifications of the system for test FA(12) were completed.)

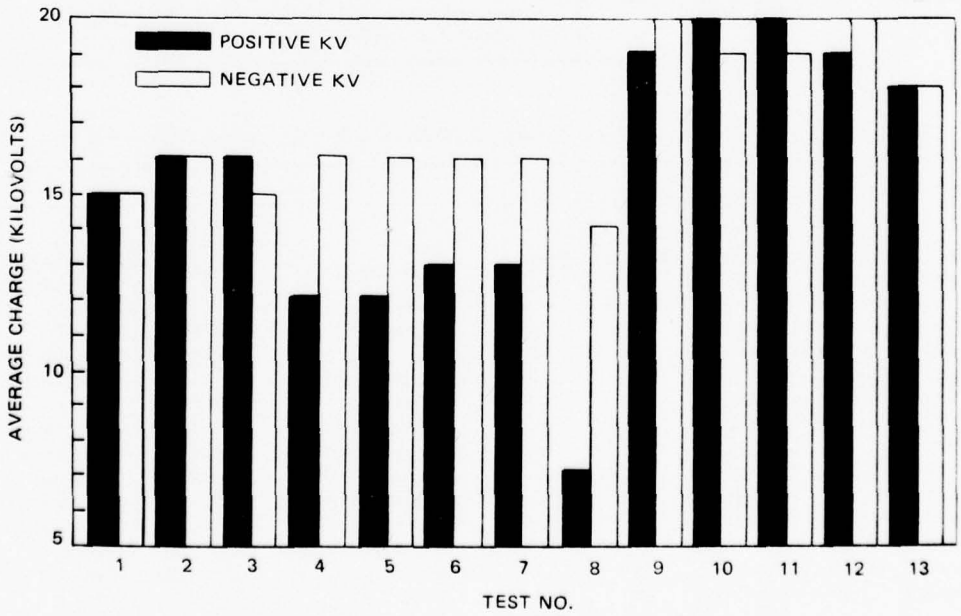

FIGURE 22. Electrical Potentials Between Spray Booms and Grids.

Table 4 is a summary of results of the fog dispersal effort test by test. The observed suitability of the clouds for testing is presented with the results.

TABLE 4. Test Results of the Airborne Electrostatic Fog Dispersal System.

TEST	TARGET	SUITABILITY*	RESULTS
FA(1)	Fog	Nonideal	Microscale clearings visually suggested, but no significant change in measured visibility during seeding. Effects competing with natural variability in visibility soon after seeding; wind drift carried effects away from point of measurement.
FA(2)	Fog (at sea)	Nonideal	Advection and mixing obscured most visual evidence of dissipation except for distrails in fog top; size of swath cut by seeder aircraft varied, possibly with height of aircraft above fog.
FA(3)	Stratus	Nonideal	Positive effects visually indicated; but much natural cloud variability.
FA(4)	Fog	Good	Measured visibility steady before, throughout, and after seeding period.
FA(5)	Fog	Very Good	Seeder aircraft cleared narrow swath through 200-300 ft of fog to runway (Fig. 23); warm air driven down by aircraft vortices and charged spray together produced clearing. Measured visibility (Appendix A, Fig.) shows steady visibility of .2 nmi in unaffected area outside of swath.
FA(6)	Stratus	Very Good	Troughing occurred behind seeder in deep stratus, closing in 1-3 minutes; seeded swaths appeared deeper than unseeded distrails; drizzle followed start of seeding.
FA(7)	Stratus	Very Good	Indeterminate effect; distrails.
FA(8)	Stratus	Very Good	Seeder aircraft too high above stratus top; spray evaporated before reaching cloud top; distrails.
FA(9)	Stratus	Good	Thick (700 Ft) stratus deck became mottled throughout the treated swath. Seeder could be seen from ground on final pass; solar radiation measured at the ground increased during this period and later decreased again.
FA(10)	Fog	Good	Fog top dropped sharply in seeded swath; variability of measured visibility increased as seeding progressed and continued to increase after treatment ended, as expected, allowing time for coalesced droplets to settle out; targeting good.
FA(11)	Fog	Good	Visibility still improving from FA(10) when seeding began. Further improvement continued followed by a dramatic decrease in visibility when light winds arose and carried treated volume away from point of visibility measurement.
FA(12)	Fog (at sea)	Nonideal	Swaths/distrails caused by seeder aircraft extremely variable because of uneven fog tops; between "ridges" much of spray evaporated before reaching tops; effects indeterminate.
FA(13)	Fog	Very Good	Measured visibility increased by 20% during this test with a charged spray of glycerine/water solution; darkness prevented accurate visual observation from the ground and aloft.

*See text and Table 1.

Results of the fog dispersal effort were variable, even when the fog or stratus conditions were very good for testing. However, some positive indications that dispersal effects were induced are evident from the data.

A swath was opened in a shallow fog during Test FA(5) (Table 4 and Figure 23). Drizzle occurred at the right times during Tests FA(6) and FA(9) to be correlated with coalescence induced by the treatments.

The charge-inducing potential achieved on the spray system was substantially improved by making basic modification during the course of testing. The first and most effective improvements in the systems were made prior to Test FA(9); the increased potentials for FA(9) and subsequent tests are recorded in Figure 22. Improvements in visibility and other physical indications of success increased with the improvements in the charging system, as shown by the results of tests FA(9), FA(10), and part of FA(11) (Table 4 and Appendix A).

FIGURE 23. Clearing Over Runway Through Fog of ~ 300 ft. Depth.

A special clear-air test (E4) was conducted after Test FA(12) to verify electrification of the cloud of spray from the seeder aircraft, after the improvements in the system were made. The aircraft sprayed charged water above the instrumented observation site. The devices for measuring the atmospheric electric field responded to the charge carried by the spray, and not to the seeder aircraft itself, as was required and expected.

Positive effects were more consistently observed when the 1 gph nozzles, rather than the 8 gph nozzles were used. Generally, higher charging potentials were maintained when the 1 gph nozzle was utilized. Also, the droplets of spray from the 1 gph nozzles are smaller than those produced by the nozzles with the higher flow rate; perhaps the greater mobility of the charged smaller droplets causes more initiation of fog droplet coalescence.

The use of glycerine-water solution instead of just water in one test [FA(13)] did not improve the fog dispersing capability.

The major problem encountered during the testing was the arcing of the charging system (Table 3). This caused substantial drains on the charging current and necessitated in-flight adjustments to the system. The system arced from very minor but sharp metal points on the boom and the grid. The arcing was most prevalent when the system was wetted by the fogs, so the sprays were released from slightly above cloud top in many test cases (Table 2); the effectiveness of the system was, consequently, reduced by partial evaporation of the charged spray in the warm air of temperature inversions before it was driven into the fog by the wake of the aircraft. The sharp points on the system were filed smooth prior to Test FA(9); this modification seemed to improve both the charging potential and the consistency of the results significantly. However, all arcing was not prevented in the remaining tests.

The recording system for monitoring the charging currents and potentials during flight was detrimentally affected by the arcing and by aircraft vibration, so it proved to be inadequate. The need for an improved and automated system to record these parameters was immediately recognized.

The tests demonstrated that the airborne electrostatic fog dispersal system was promising, but inadequate to induce complete clearing of an airport. The principles of electrostatically enhanced coalescence are sound, so an improved version of the present airborne system may be very effective. Elimination of arcing in the charging system is mandatory. Greater quantities of spray and/or spray droplets carrying higher charges are needed.

PHASE II SYSTEMS AND TESTING - CHARGED, HYGROSCOPIC BUBBLES

COMPARISON OF CHARGED BUBBLES AND CHARGED DROPLETS

Electrically charged bubbles clear fog by attracting fog droplets to collision and coalescence. Bubbles that are hygroscopic have the added effect of drawing water vapor out of the foggy air. The principles are the same as those applicable to charged droplets. However, the collecting areas per unit volume of material, the terminal velocities, and the collection efficiencies of bubbles differ from those of droplets.

Let the material composing treatment droplets and bubbles be designated as the "agent". Consider a bubble with its wall composed of a unit volume of agent. This bubble exposes a greater surface area for vapor and fog droplet collection than does a droplet composed of the same amount of agent. Conversely, the amount of agent required to create a given surface or cross-sectional area is less for (thin-walled) bubbles than for treatment droplets. This advantage of bubbles is demonstrated by the following calculation:

The cross-sectional area is considered in basic theory to be the area which determines fog droplet collection. The effective collecting area per unit volume of agent, ϕ, for a treatment droplet is

$$\phi_d = \frac{3E}{4r} ,$$

where E is the collection efficiency and r is the droplet radius. The wall volume of a bubble is approximately $4\pi R^2 \tau$ for a bubble of radius R and wall thickness τ, since $R \gg \tau$. Thus, for a bubble.

$$\phi_b = \frac{E}{4\tau} .$$

Consequently, for a given E,

$$\phi_b = \frac{r}{3\tau} \phi_d$$

The thickness τ is approximately 0.5 μm, and optimally r ≃ 20-100 μm.

Thus,

$$\phi_b \simeq 13\phi_d \text{ to } 67\phi_d ;$$

this difference is substantial.

The condition, $\phi_b = \phi_d$, could occur only with droplets of radius 3τ or approximately 1.5 μm. Such small droplets cannot grow sufficiently to settle to the ground within the time restraints of fog clearing.

Now compare basic settling characteristics of bubbles and droplets. Droplets of seeding agent fall at rates approximated by Stoke's Law. A droplet of 20 μm radius has a fallspeed of about 12 cm/sec [16] and will settle through a fog 1,000 feet deep in about 42 minutes. This time approximates the maximum allowable in fog seeding, so a usable droplet of agent can be defined as anything larger than about 20 μm. Droplets larger than about 100 μm in radius have small cross-sectional areas per unit volume of agent, so the mass of material required becomes excessive. These factors determine the approximate optimal charged droplet radii of 20 to 100 μm.

The Stokes terminal velocity of an air filled bubble is

$$V_b = \frac{2R\tau\rho_{ag}g}{3\mu}$$

for $R > \tau$; here ρ_{ag} is the density of the agent, μ is the dynamic viscosity of air and g is the acceleration of gravity. A 1-mm-radius air-filled bubble of an agent with a density of 1.146 g/cm^3 (as utilized) and $\tau \simeq 0.5$ μm will settle at 21 cm/sec in still air; V_b is directly proportional to R, so a 10-cm-radius bubble will settle at 21 m/sec. Air-filled bubbles of radii 1 mm and 10 cm, if released at the top of a 1,000-ft deep fog in still air would settle to the ground in roughly 33 minutes and 0.33 minute (20 seconds), respectively, neglecting increases in τ and V_b due to collection of fog droplets. These times required for fallout approximate practical limits appropriate for fog clearing, so 1-mm to 10-cm air-filled bubbles should be usable for this purpose.

Bubbles that are released from the ground must initially have a positive buoyancy (negative fallspeed) to be effective; that is, they must rise into the fog, collect fog water, and then settle back to the ground under the weight of the water. The condition for positive buoyancy is that

$$\rho_b < \rho_{air}$$

where ρ_b represents bubble density. Positive buoyancy is provided by filling the bubbles with helium rather than air; the buoyancy condition may thus be rewritten as

---

[16] J. H. Perry and others. *Chemical Engineers' Handbook*. New York, McGraw-Hill, 1963. Pp. 5-59 to 5-62.

$$\frac{3\tau\rho_{ag}}{R} + \rho_{He} < \rho_{air}$$

or

$$\frac{3\tau\rho_{ag}}{R} + \frac{4}{29}\rho_{air} < \rho_{air} .$$

Thus the requirement on bubble radius is that

$$R > \frac{3\tau\rho_{ag}}{(1 - \frac{4}{29})\rho_{air}}$$

for positive buoyancy. For representative ambient conditions of 10°C (50°F) and 1,000 mb, such that $\rho_{air} = 1.23 \times 10^{-3}$, gm/cm^3, bubbles with a wall thickness $\tau = 0.5$ μm and $\rho_{ag} = 1.146$ g/cm^3 will initially rise if

$$R > 0.16 \text{ cm}$$

Usable helium-filled bubbles thus range in radii from about 2 mm upward.

A bubble will collect a certain mass of water from the fog. The mass of water that must be collected to change bubble buoyancy from positive to neutral may be calculated as follows:

Bubble terminal velocity may be expressed as

$$V_t = \frac{2g}{9\mu} R^2 (\rho_b - \rho_{air})$$

where the bubble density with mass m of water collected is

$$\rho_b = \frac{3\tau\rho_{ag}}{R} + \rho_{He} + \frac{3m}{4\pi R^3} .$$

For neutral buoyancy, $V_t = 0$ and

$$m = \frac{4}{3}\pi R^3 \left(1 - \frac{4}{29}\right)\rho_{air} - \frac{3\tau\rho_{ag}}{R} .$$

Mass m as a function of bubble radius R is given in Table 5. When collected fog water exceeds the m for neutral buoyancy by one percent, or even less, substantial fallspeeds are introduced, and the bubbles settle from the fog.

TABLE 5. Collected Water Required to Produce Neutral Bubble Buoyancy.

Bubble radius		Water mass
R(cm)	R(in)	m(g)
1	0.4	0.00372
2.5	1	0.0649
5	2	0.537
7.5	3	1.83
10	4	4.37

A helium-filled bubble released at the surface will rise until the weight of water it has accumulated is equal to the lift of the gas inside it, and then it will fall through the same vertical distance back to the surface, accumulating roughly an equal amount of water by the time it hits the earth. Therefore, masses twice those in Table 5 reasonably approximate the fog water collected and removed when a given helium-filled bubble falls to the ground; the quantity, 2m is graphed as a function of R in Figure 24. Arcata fog liquid water contents are normally of the order of 0.1 to 0.3 g/m^3, so a 2.5-or 3-cm radius bubble will collect about the same amount of water present in a cubic meter of fog before it settles out. Larger bubbles collect more water.

The collection efficiency, E, of a bubble due to its electrical charge may be calculated in the same manner as for charged droplets (see Appendix A in NWC Technical Publication, Project Foggy Cloud V).[5] Thus

$$E = \frac{50^2 r^2}{8R^5 \mu |V_b - V_d|}^{2/5}$$

where Q = charge (esu)
r = fog droplet radius

$|V_b - V_d|$ = difference in fall velocity between bubble and fog droplet

Consider helium-filled bubbles as they rise into a fog. Their rates of rise in this non-neutral buoyancy condition may be calculated using the equation,

$$V_t = \frac{8}{3} \frac{g(\rho_b - \rho_{air})R}{C\rho_{air}}^{1/2}$$

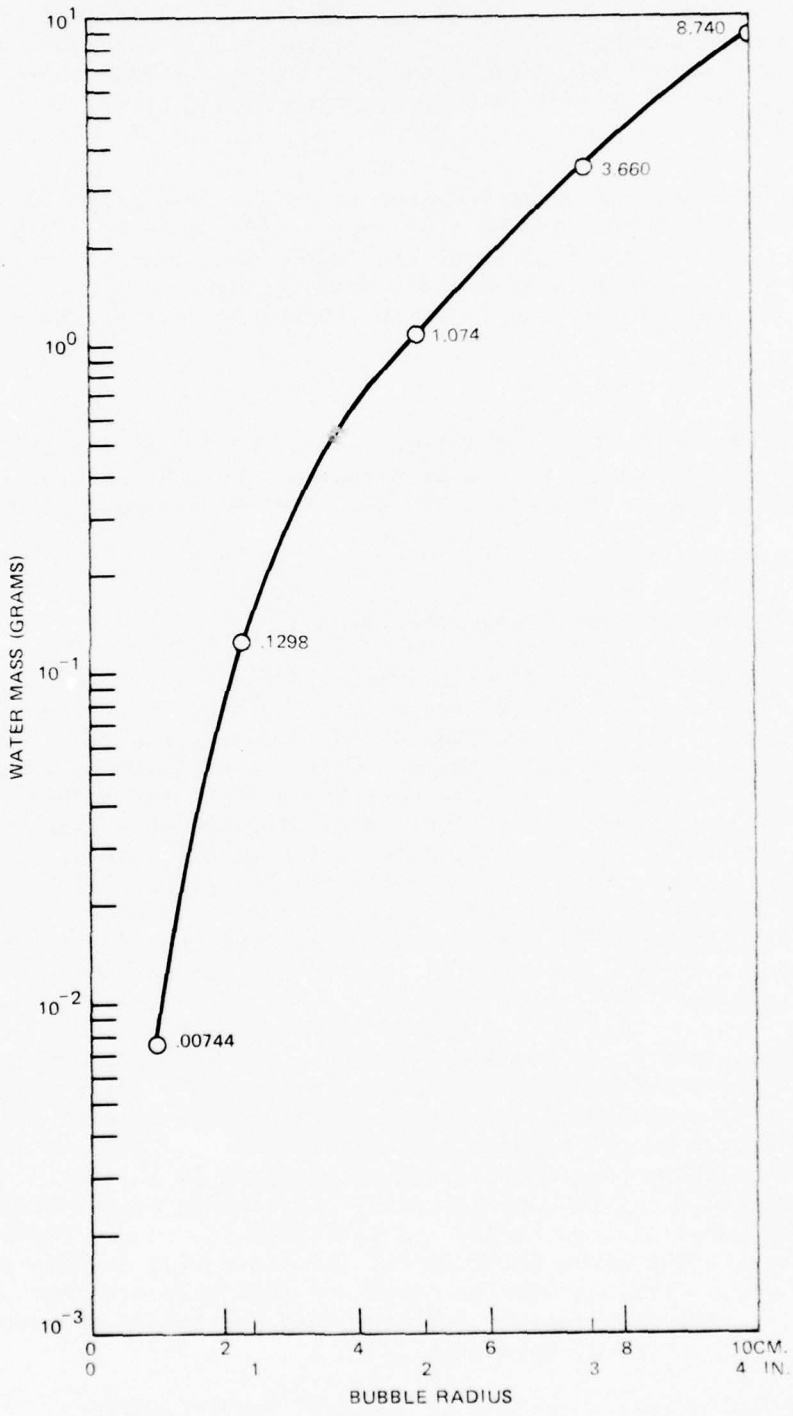

FIGURE 24. Estimate of Fog Water Collected and Precipitated.

which is more general than Stoke's Law. The drag coefficient, C, for 1- and 10-cm radius bubbles are respectively about 1.35 and 0.39, as determined from data in Chemical Engineers' Handbook[16]. Thus 1-cm bubbles and 10-cm bubbles will rise at 37 and 75 cm/sec, respectively, prior to collecting water loads.

The bubble generating device used in Foggy Cloud tests has a voltage output of V' of 120 kV. Assume that each bubble picks up the maximum charge possible in air without breakdown, or 120 kV, whichever is smaller. Air becomes conducting at an electric potential gradient, E_m, of about 3×10^5 volts/m. The maximum voltage to which a bubble in air can be raised is

$$V'_m = RE_m$$

which has a value of 30 kV for a 1-cm bubble and 300 kV for a 10-cm bubble. Hence it is assumed that a 1-cm-radius bubble is charged to 30 kV and a 10-cm bubble is charged to 120 kV. The charges on each bubble,

$$Q = 4\pi\varepsilon_0 rV',$$

are then 100 and 4000 esu, respectively.

The efficiency for collecting a 5-μm-radius fog droplet is then 0.56 for 1-cm-radius bubble and 8.03 for a 10-cm-bubble; i.e., these bubbles respectively will sweep 56 and 803% of the volume projected from the geometric cross-sections of the bubbles. Thus the efficiences increase dramatically with bubble size and are very large for large bubbles. As the bubbles pick up fog water by collection of droplets as well as by vapor deposition due to the hygroscopic effect, the bubble rate of rise will gradually decrease to zero; subsequently the bubbles will fall at increasing rates. During this process, the collection efficiency due to the charge on each bubble will vary through a maximum that is larger than the above values; this will occur while fallspeed V_b is at and near zero, because E increases as $V_b \to 0$.

A charged droplet of seeding agent, as compared to a bubble, does not go through this transition in fallspeed. A droplet's fallspeed is always positive (i.e., downward relative to vertical motion of air). A comparison of parameter values used to calculate efficiency E for a droplet and E for a bubble shows that while E due to charging is initially much higher for the droplet, E for the droplet falls off rapidly as the droplet collects fog water and the radius and fallspeed increase. The bubbles are much larger than agent droplets (of the order of 5 cm versus 5×10^{-3} cm), and individual bubbles sweep out much more area per unit volume of agent. All calculations indicate that the larger the bubble, the greater the collection of fog water.

The volume of fog swept out by a single bubble, whether the fog is moving or stationary, is determined only by the height to which the bubble

rises, and from which it falls, by its capture cross-sectional area (EA), and by its residence time in the fog. Once the bubble is free from its source, it can only move vertically with respect to the medium it is in, although both it and the medium may be moving horizontally with respect to a fixed point on the earth. If the bubble collects sufficient water to balance its lift before escaping from the top of the fog, it will fall back through the depth it has risen, collecting more fog droplets before it hits the ground. As large numbers of bubbles reduce the average density of the fog, the vertical trajectories will become higher and higher until the bubbles begin to escape. The effect of charging the bubbles is to increase the rate of collection of fog droplets. This reduces the number of bubbles that escape and so increases the total water collected by each bubble.

It is assumed that the bubbles do not shed drops of collected water. The shedding of drops, if it occurs, will increase the residence time in the fog, and result in collection of more fog water, if escape is controlled. In this case, the drops that are shed would be large enough to precipitate.

BUBBLE GENERATOR DESIGN

Several bubble generator designs were tested during Foggy Cloud VI prior to going to the field. The small wheel design (Figure 25) was the

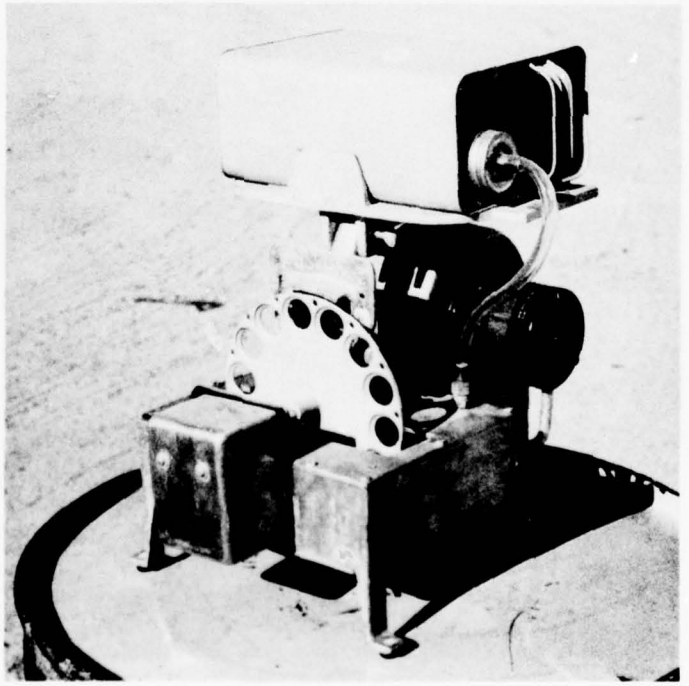

FIGURE 25. Small Wheel Bubble Generator.

best for bench testing. Different solutions, gases and wheel designs were tested. One small wheel design was fabricated specifically for the purpose of investigating gases and gas combinations, and how the gases affected bubble flight characteristics in a dry-air medium. The design consisted of a series of tubular spokes extending radially from a hollow hub (gas mixing chamber). The tubular spokes alternately dipped into the bubble solutions, and bubbles were formed at a specific point during the rotation of the hub. A 10% solution of helium in air resulted in neutral buoyancy for bubbles with approximately 1-inch diameters. An effort was initiated to design an apparatus to dispense bubbles from aircraft at airspeeds greater than 40 knots, but time did not allow this to be carried to completion.

The large wheel design (Figure 26) was developed to reduce costs and to increase the output and ruggedness of the bubble machine. This design functioned satisfactorily in fog and produced a substantial number of bubbles. One fan was used to blow air through the screen; one or two other

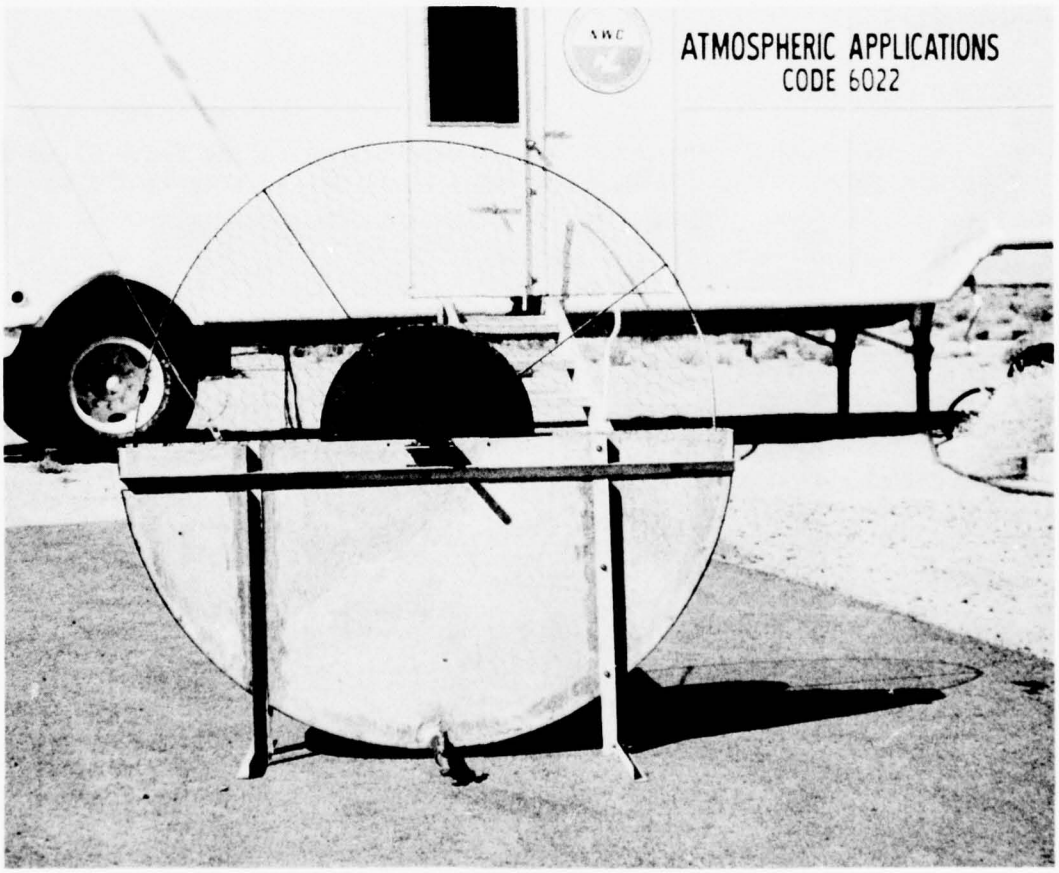

FIGURE 26. Large Wheel Bubble Generator.

fans were used to lift the bubbles above the ground (Figure 27). When two fans were used and the wind was 5 knots or less and in line with the fans, there was good bubble production and the bubbles rose over 50 feet into the air. When the wind shifted out of line or only one fan was used, many bubbles were broken by the fan and many bubbles were not lifted. This design showed at least as much promise as the tray design, so future efforts could be directed toward improving this system.

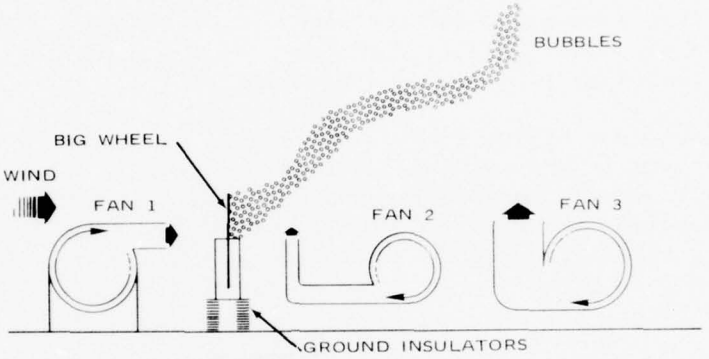

FIGURE 27. Large Wheel Bubble Generator and Fan Arrangement.

The tray design was used in the field tests of Foggy Cloud VI. This design, shown in Figure 28, is very similar to the smaller apparatus (Figure 29) used in Foggy Cloud V.[5] Each tray is 10.5 feet long, 1-foot

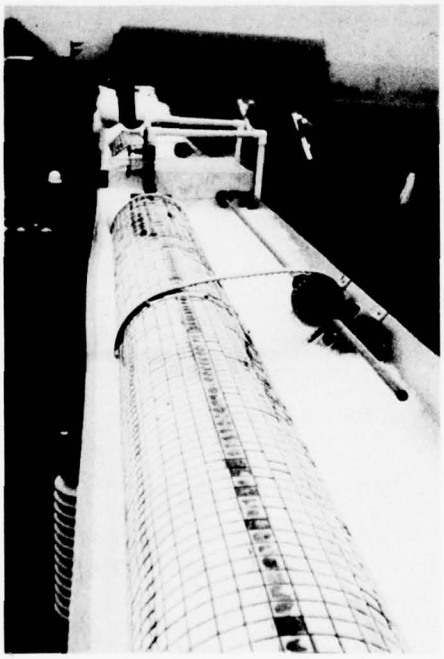

FIGURE 28. Tray Design Bubble Generators.

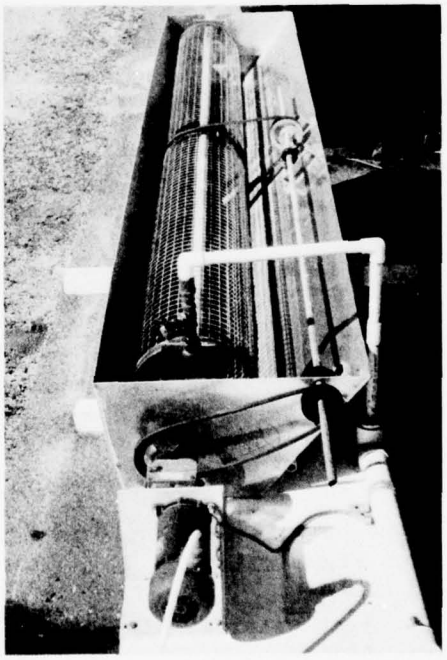

FIGURE 29. Bubble Generator Used on Project Foggy Cloud V.

wide at the bottom, and 1-foot deep. Bubble solution fills each tray to a depth of 3 inches; a rotating screen dips into the solution. Each screen, which is made of heavy wire with 1-inch square holes between wires, is 9.5 feet long and 12 inches in diameter. Each bubble generator has two trays and screens. A 12-volt battery and a geared-down DC motor drives the two screens at 16 rpm. Exhaust gas blows bubbles off the top of each screen as it exits from a 1-inch blow pipe through counter-sunk, 1/8-inch-diameter holes that are 1 inch apart. The blow pipe runs the length of the screen. The blow pipes for any number of trays used are connected to a 2-inch main gas line. The flow of gas from the main line to each blow pipe is controlled by 1/2-inch needle valves.

A multicylinder helium trailer and an air compressor are connected to the blow pipes in the trays via a 2-inch polyvinyl pipe. This pipe electrically insulates the trailer and compressor from the bubble generator. The capacity of the helium trailer is 30,000 cubic feet; the air compressor is rated at 600 CFM. Pure helium, air, or a controlled mixture of the two, may be piped to the trays. Figure 30 is a schematic of this bubble generating system.

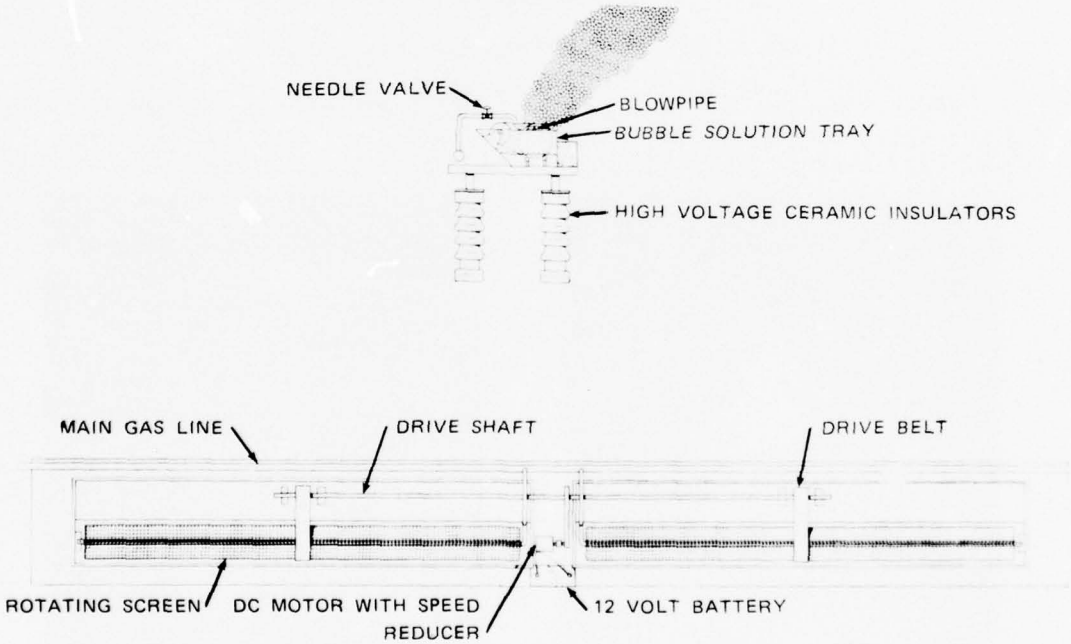

FIGURE 30. Sketch of Bubble Generating Device Used on Project Foggy Cloud VI.

The bubble solution consists of 4 parts (by volume) glycerine and 3 parts Light Water^{R*}. Light Water^{R} is used by the Navy fire departments

*Light Water^{R}: (MIL-F-24385)FSN-4210-152-0949, Fire Extinguishing Agent, Minnesota Mining and Manufacturing Co., Aqueous film-forming foam liquid concentrate.

as an additive to water for making foam for fighting fuel fires. About 10 gallons of bubble solution are poured into each tray.

The Light Water^{R} replaces Ivory liquid soap used in previous tests. Preliminary tests with an Ivory liquid and glycerine solution gave very poor results, contrary to previous experience; the Ivory liquid formulation, although unknown, appeared to be different from that used in Foggy Cloud V.

A Kilovot Corporation (Hackensack, N.J.) 120-130 kV power supply is used to electrically charge the trays, the screens and emanating bubbles. The power supply can charge the trays from 0-120 kV and is rated for 30 milliamps; the output polarity is reversible.

Ten bubble-solution trays with charging screens (i.e., five complete bubble generators) were utilized in the field tests. The trays were set end-to-end to provide 117-ft north-south line source of bubbles. The north-south orientation paralleled the coast and took advantage of both onshore (westerly) and offshore (easterly) airflow. The prevailing winds are westerly at Arcata during the advection fogs, but weak intermittent easterlies are not uncommon (see Figure 7).

RESULTS--ELECTRICAL

In the field good electrical charging was developed. The power supply charged the bubble generators to 120 kV positive drawing 0.75 milliamps, and to 118 kV negative drawing 0.9 milliamps. Current readings were the same with and without bubble production; even at the Rayleigh limit the charge carried by all of the bubbles is much less than the charge lost by leakage. The current held at these low values if the insulators between the trays and the ground were kept clean and dry; wet insulators encountered during the first fog dispersal test reduced the attainable charging to 92 kV at 5 milliamps, so the insulators were subsequently wrapped in plastic to keep them dry between tests. The full charging capability was realized during further testing. Judging from the length of sparks to a grounded wire, the voltage on the screen was 100 kV on the ends of the screen and 80 kV at the centers. Observers could physically detect more voltage when it was negative than when positive: Our hair stood on end when we were 10 feet from the trays charged 118 kV negative; this distance dropped to 5 feet with a positive voltage. Some 800 volts were measured 5 feet from the trays at 8 feet above the ground.

RESULTS--BUBBLE PRODUCTION

The bubble generators in operation are illustrated in Figure 31. Each screen blew about the same number of bubbles. However, the gas, pressurized to 80 psi if air or air mixed with helium, or 40 psi if pure helium, did not flow evenly from the row of the holes in the blowpipe. From the half of each screen nearest the feeder valve, an average of two bubbles were produced per hole per pass over the blowpipe; from the half of the

FIGURE 31. Bubble Generators in Operation at "CB" Area.

screen farthest from the valve, about one-fifth of the holes each produced one bubble per pass. This variation in bubble production along the length of individual screens is evident in Figure 31. The total bubble production rate for the ten screens utilized was thus about 378,400 bubbles per minute.

The size distributions of generated helium-filled bubbles were determined by photographing the bubbles rising in front of a 2-inch grid placed next to a tray, as shown in Figure 32. The 35 mm slide photographs were

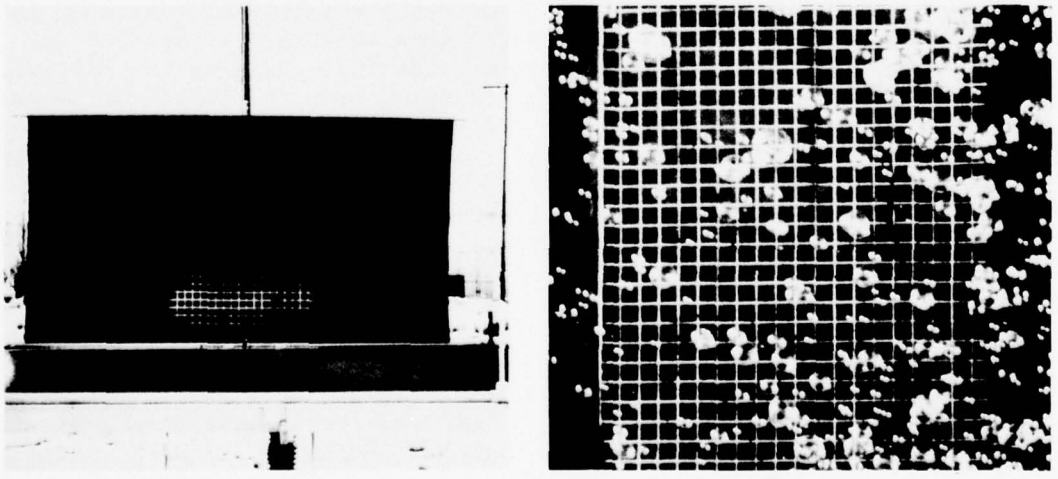

a. Full view. b. Close-up.

FIGURE 32. Grid Used To Measure Bubble Size Distribution.

then projected on a screen where bubble sizes were measured. The size distributions for uncharged and positively- and negatively-charged bubbles are shown in Figure 33. Corresponding statistics are given in Table 6.

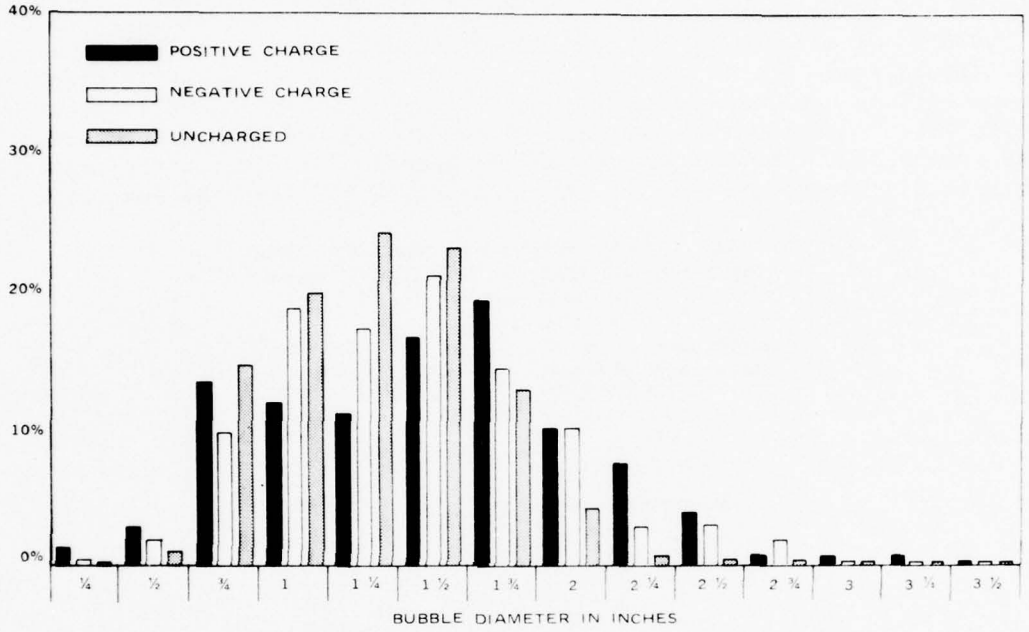

FIGURE 33. Size Distribution of Charged and Uncharged Bubbles.

TABLE 6. Size Characteristics of Charged and Uncharged Bubbles

	+ Charge	- Charge	Uncharged
No. bubbles sized	287	360	395
Median diameter (in.)	1.5	1.5	1.25
Diameter range (in.)	0.25-3.25	0.25-2.75*	0.5-2.75
% < 1 in. (2.5 cm) dia.	17.4	11.7	15.4
% 1 in. (2.5 cm) to 2 in. (5 cm) dia.	68.9	81.1	83.5
% > 2 in. (5 cm) dia.	13.5	7.3	1.1

*One bubble measured at 5.25 in. dia.

The percentages of bubbles in each of the three size categories in the table may be combined with the total bubble production rate calculated above to estimate the water removed from fog by an entire population of bubbles. Bubble diameters of 3/4 inch (1.9 cm), 1.5 inch (3.8 cm), and 2-1/2 inches (6.3 cm) may be used to represent, respectively, bubbles with diameters less than 1 inch (2.5 cm), 1 to 2 inches (2.5 to 5.1 cm) and greater than 2 inches (5.1 cm). Data in Figure 24 indicate that individual bubbles of these sizes will respectively collect and precipitate 0.017, 0.068, and 0.26 g of water during transit through a fog. Corresponding

estimates for a bubble population are given in Table 7. These estimates apply for each minute of operation of the bubble generators. Size distribution and total water collection are not significantly different for bubbles with positive and negative charge. The data in the table indicate that the bubbles generated in 1 minute would clear the equivalent of about 300,000 m^3 of a fog with 0.1 g/m^2 liquid water content, or 100,000 m^3 if the liquid water content is 0.3 g/m^3. The expected clearing is proportionally less for larger volumes; the actual clearing accomplished at a given location depends on the flux of fog (wind) past the generators, the dispersion of the bubble plume, and the duration of generator operation. This is discussed further with the analyses of the fog-clearing tests.

TABLE 7. Estimates of Mass of Water Precipitated From Fog by a Population of Bubbles Generated in One Minute.

Bubbles with positive charge (diameter)	Fog water collected (g)
< 1"	1,119
1"-2"	17,729
> 2"	13,282
Total fog water collected	32,130
Bubbles with negative charge (diameter)	**Fog water collected**
< 1"	753
1"-2"	20,868
> 2"	7,182
Total fog water collected	28,803

A comparison of charged and uncharged bubbles in the field revealed that charging caused more bubbles to be drawn to the ground upon leaving the trap. After the charged bubbles rose 6 feet or more they were no longer attracted to the ground. The charged bubbles, although of the same sign, had a greater tendency to coalesce with one another. C. V. Boys[17] also noted this tendency. Differences in the surface properties of charged and uncharged bubbles, and induced dipole-interactions of the charged bubbles may be responsible. In any case, the coalescence occurs with only a minor fraction of the bubbles and does not significantly reduce the population. Even when bubbles were highly charged with respect to ground, aerodynamic forces prevented most of the bubbles from crossing air streamlines to collide with grounded objects; for example, a cloud of charged bubbles would follow the airflow around the helium trailer. However, clear-air field tests demonstrated that bubbles blown with just air spilled out of the trays; too many were lost by bursting as they touched the ground, although those caught in updrafts were carried more than a quarter mile downwind.

[17] C. V. Boys. *Soap-Bubbles, Their Colors and the Forces That Mold Them*. New York, Dover Publications, Inc., 1959. 192 pp.

Helium provided the lift required to minimize ground losses. On a clear but stable morning, a bevy of helium-filled bubbles was released. These bubbles rose rapidly, stayed together, and were still visible ten minutes later when they reached an altitude of about 2,000 feet above the ground. This test demonstrated that the helium-filled bubbles have a long life expectancy and such significant buoyancy that they would be prevented from rising through and out the top of a fog only by collecting significant water loads. The latter conclusion provided a technique for verifying fog water collection by the bubbles.

RESULTS—FOG DISPERSAL TESTS

Two fog dispersal tests were conducted using the bubble generators, Test VI-B(1) on 10 October and Test VI-B(2) on 11 October 1973.

For the first test, the decision was made to use bubbles buoyed by a helium/air mixture. The plan called for 5-minute releases of bubbles at approximately 10-minute intervals, so as to produce pulsating changes in visibility.

The fog for the test situation formed by a combination of radiative and advective processes, and was consequently wetter than the purely advective fogs previously observed. The fog was locally dense, but visibility was variable within the 0.2-0.5 nmi range. Some rifts were observed from the observation aircraft. Five charged bubble bursts, each of 5-minute duration, were released at 10-15 minute intervals as planned. The first three releases carried positive charge; the fourth and fith carried negative charge. The level of charging was less than desired due to the wetting of the insulators as discussed above. Wind speeds were ideal (0-3 mph) but the direction of drift changed frequently, by as much as 180° as shown in Figure 34. This latter factor made both visual and instrumented observation difficult. The mobile videographs had to be repositioned frequently, so that visibility measurements in the plume before, during, and after releases were not always possible. However, the visibility measuring devices were in proper positions throughout two of the releases, the first and the fourth.

During the first release of bubbles, visibility in the plume did increase by about 19% (Videograph #1, Figure 34), while the visibility in the control fog volume remained essentially constant. The visibility remained at the higher level through the second release and until the wind shifted dramatically to a westerly direction at 0838 PDT, some 30 minutes after the beginning of the first release. Minor wind shifts put the field of view of Videograph #2 out of the plume during release 2. The duration of the better visibility is long relative to the 5-minute initial bubble release and the likely duration of effects; thus there is no convincing separation of induced and natural fluctuation in visibility. (Initial differences in visibility recorded by the two videographs as depicted in Figure 34 are largely instrumental).

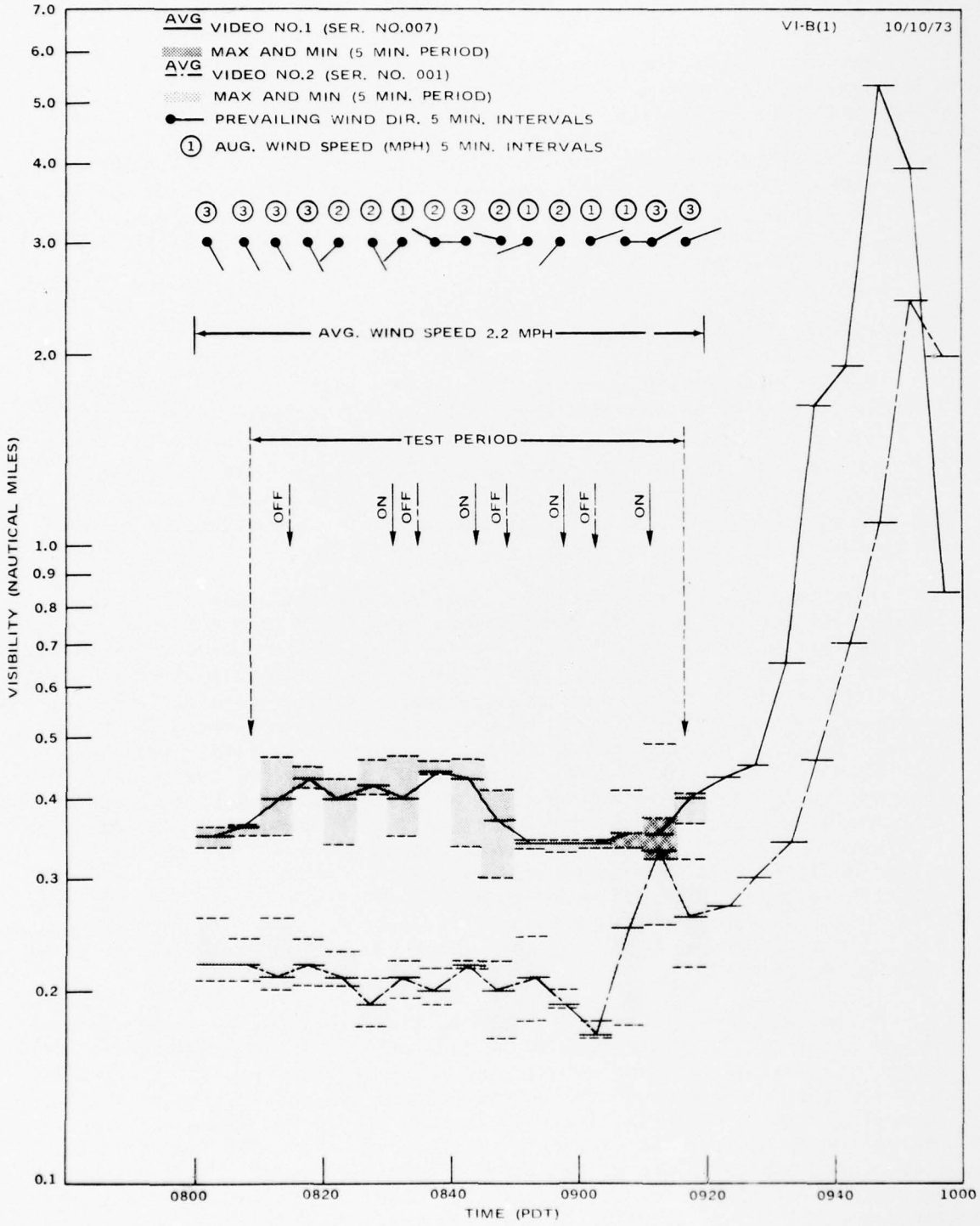

FIGURE 34. Visibility Variations With Time and Compared With Wind Flow - Test B(1).

The most significant visibility perturbation during the first testing occurred with the fourth release of bubbles, when Videograph #2 was oriented into the plume and Videograph #1 was used as the control. Visibility in the plume rose by about 94% (0.17 to 0.33 nmi, Figure 34) over the 10-minute period immediately following the release, while visibility in the control volume remained approximately constant; however, the visibility in the plume temporarily dropped by 21% during the last release, so the results were again inconclusive.

No bubbles were observed penetrating to above the fog top which rose from 350 feet to 700 feet AGL during the course of the testing; the bubbles were collecting and descending with water and simply impacting on the ground without rising. Due to the wind shifts of more than 180°, some bubbles were observed settling to the ground near the trays as long as 10 minutes after the generators were turned off. The bubble buoyancy was observed to be less than desired; ground losses were so great that the treatment densities (bubbles per unit fog volume) were far less than desired, although this was improved somewhat by increasing the helium-air ratio in the latter releases.

Many bubbles with nearly neutral buoyancy were produced using the helium-air mixture. These followed the air currents closely. Changes in the vertical wind component caused whole clouds of bubbles to rise or fall as a unit, often more rapidly than individual bubbles settled as they picked up fog water, and occasionally they lost weight and rose as excess bubble solution or water dripped off the bottom. Depending on the wind, the bubbles struck the ground near the trays and at distances ranging to several hundred feet downwind. To overcome the inadequate buoyancies, it was decided to use helium in the next test.

The plan for the second test (VI-B[2]), as in the first, called for releases of bubbles separated by non-seeded intervals of approximately 10 minutes. This test was conducted under more ideal and observable conditions. Wind was light (1-3 mph) and fairly consistent in direction ((Figure 35).

Three bevies of bubbles, two of 3-minutes duration and a third of 7-minutes duration, were released. Good charging was attained, as noted previously. The first release carried negative charge; the second and third carried positive charge.

The helium-filled bubbles rose more efficiently into the fog; ground losses were significantly reduced. Water laden bubbles of all sizes were observed falling out in significant numbers after rising into the fog.

Helium-filled bubbles released during the clear-air demonstration of the bubble generator rose at least 2,000 feet, as noted earlier. However, the helium-filled bubbles released into this fog did not rise to the fog top at 700 ft AGL despite their initial buoyancy. This factor supports the observation that significant fog water loads were collected by the bubbles.

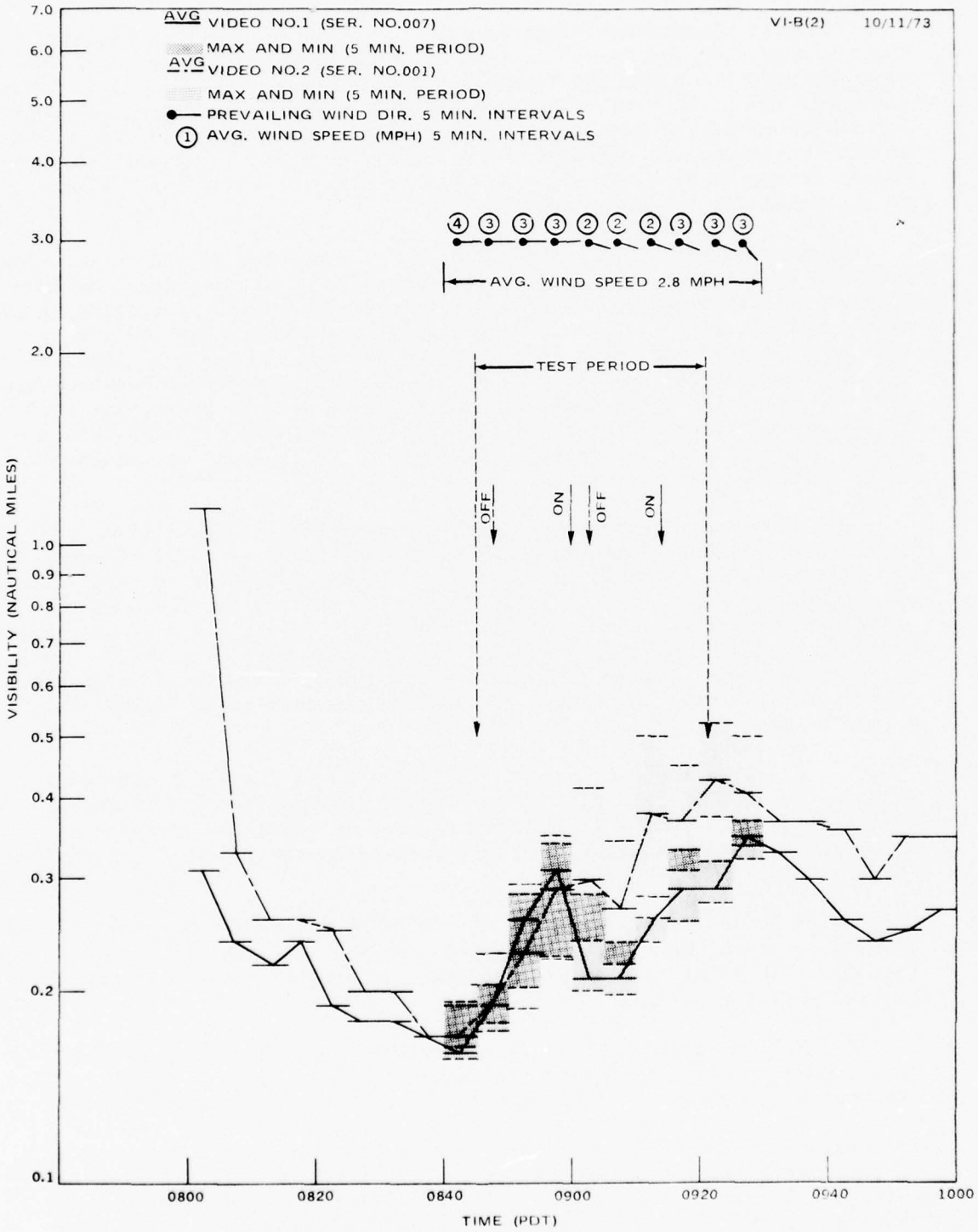

FIGURE 35. Visibility Variations With Time and Compared With Wind Flow - Test B(2).

At an observer's position 500 feet downwind from the trays, it appeared that predominantly the larger of the bubbles (2-3 inches in diameter) were falling out, whereas predominantly 1 inch in diameter bubbles were settling out water loads more quickly, as predicted earlier by the calculations of larger collection efficiencies for larger bubbles.

The trajectories of the bubbles may have been influenced not only by the weight of collected water, but also by the aerodynamic effect of the water on bubble shape. After rising into the fog for a few seconds, even the helium-filled bubbles often flowed in what seemed to be horizontal lines, contrary to the rapid and continuous rise observed in stable, clear air. A possible explanation is that a drop of liquid on the bottom of a bubble would cause the bubble to have a non-spherical shape. The bubble could thus act as an airfoil having a longer path of airflow around the bottom than across the top; this would cause a downward aerodynamic force on the bubble, counteracting the lift of the helium, during velocity differences between the wind and the bubble. When the bubble's horizontal velocity increased to that of the wind, there would be no net force. A variable wind would induce forces of variable magnitude, with the bubble continually adjusting its velocity to that of the wind. The aerodynamic force would always be downward because the collected water always drained to the bottom of the bubble. The observed quasi-horizontal trajectories of some bubbles may thus be further evidence that the bubbles did collect fog water.

Beginning with the second release of bubbles, visibilities recorded by the videograph oriented into the plume were more improved than those recorded in the control fog volume (Figure 35). However, the 2-3 mph wind carried the treated fog volumes beyond the 75-foot videograph viewing range within 20-30 seconds after each release, and the fog was then replenished by advection in each case. Consequently, it is difficult to explain the better visibilities that also occurred in the direction of the plume between releases.

Beyond the videograph range, the major portion of the treated volume rose overhead where visibility observations were, of course, precluded. Downwind observers did report visibility improvements at the surface that appeared to be correlated with the bubble releases; however, a positive separation from natural variations cannot be verified. The durations of the bubble releases and/or densities of bubbles in the plume were evidently inadequate to produce significant and sustained increases in the visibility in the vicinity of the trays. (The bubbles themselves are so large and widely separated that they do not significantly backscatter or reduce visibility.)

Apparently for the same reasons, the treatments were insufficient to cut holes through the whole fog depth so as to make either the sky visible from the ground or the ground visible from the observation aircraft.

The fact remains that significant numbers of the helium-filled bubbles did indeed collect enough water to settle back to the ground, thus removing the water from the fog.

RESULTS - GAS CONSUMPTION

The 30,000 cubic feet of helium in the supply trailer was utilized as follows: Pretesting and clear-air testing, 6,100 cubic feet; Test VI-B(1), 10,700 cubic feet; Test VI-B(2), 10,900 cubic feet; unusable remainder, 300 cubic feet.

The helium flow rate during Test VI-B(2) (helium only) was about 900 cubic feet/minute.

The flow rates of the air-helium mixtures (Test VI-B(1) were not measured. However, the air compressor, rated at 100 psi, 600 CFM, could maintain only 80 psi when blowing bubbles with air only, so the flow rate must have been of the order of 700 or 800 cubic feet/minute.

PHASE III SYSTEMS AND TESTING--EVAPORATION SUPPRESSION

MATERIAL AND EQUIPMENT

As previously stated, ethyl alcohol solutions of cetyl (hexadeconal) and stearyl (octadecanol) alcohols were used during Foggy Cloud V evaporation suppression tests. Preliminary studies for Foggy Cloud VI suggested that a better method of spreading the monomolecular films was needed; ethyl alcohol is too expensive for large scale use. Alternate techniques considered were as follows:

1. Melt spraying with or without small additions of ethyl alcohol. This technique requires the spraying of small amounts of material per day (~200 pounds) over large averages and would necessitate precise metering through small spray nozzles. The possibility of nozzle clogging and subsequent solidification of the material in the spray booms was unattractive.

2. Dispensing of powdered alcohols employing a grinder-blower technique. While successfully tested in Australia, the technique has been limited to hexadecanol. Mixtures of hexadecanol and octadecanol are low melting and too "sticky" for dispersion by this technique, and octadecanol alone will not spread efficiently over the water surface.

3. Dispensing of dilute aqueous dispersions of tallow alcohols using spray booms. This technique was chosen for the operational phase. It offers the greatest versatility; boat or aircraft operations are possible. The ultimate cost of the technique would be low, particularly if the dispersions could be manufactured in the Canal Zone.

Trial formulations were prepared by personnel of the Polymer Sciences Branch, Chemistry Division, Naval Weapons Center. Particular efforts were made to prepare a fluid formulation containing a maximum of tallow

alcohols and a minimum of surfactants and dispersants, which would be stable in storage and shipping, and which could be diluted to spreading concentration without rapid separation of the tallow alcohols.

Thirty-thousand pounds of a concentrated stable dispersion of tallow alcohols were prepared by a contractor, Michelman Chemical Company, Cincinnati, Ohio, using the formulation developed at NWC. Due to the current shortage of tallow alcohols, the total quantity was prepared in several production lots, each dependent on the amounts and types of tallow alcohols available. The basic formulation used is as follows:

Material	Weight %
Water	79.900
Tallow Alcohol	19.970
IGEPON AC 78[a]	0.065
IGEPAL CO 880[a]	00.065

[a] Surfactants and emulsifiers manufactured by Antara Chemicals Division of GAF Corporation.

The emulsion was shipped to the Canal Zone in 55-gallon barrels, each containing 80 pounds of tallow alcohol.

These concentrated dispersions are stable to storage and are readily diluted from 20% to 2% by weight of tallow alcohol content. The dilute dispersions are reasonably stable; simple circulation or stirring will maintain a homogeneous mixture suitable for spraying.

Spraying equipment was designed and fabricated by NWC and shipped to Panama on 16 August 1973. The Panama Canal Company (PCC) provided a suitable small boat to carry the emulsion storage and spray dispensing system (Figures 36, 37, and 38).

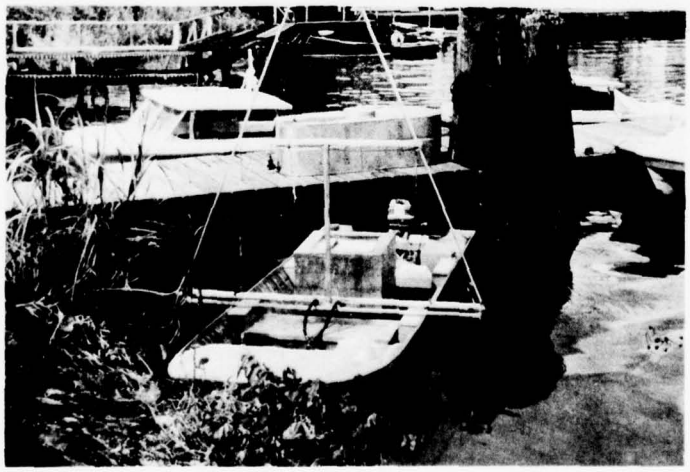

FIGURE 36. Spray System Installed and Loaded With Booms in Standby Position.

FIGURE 37. Spray System in Operating Position.

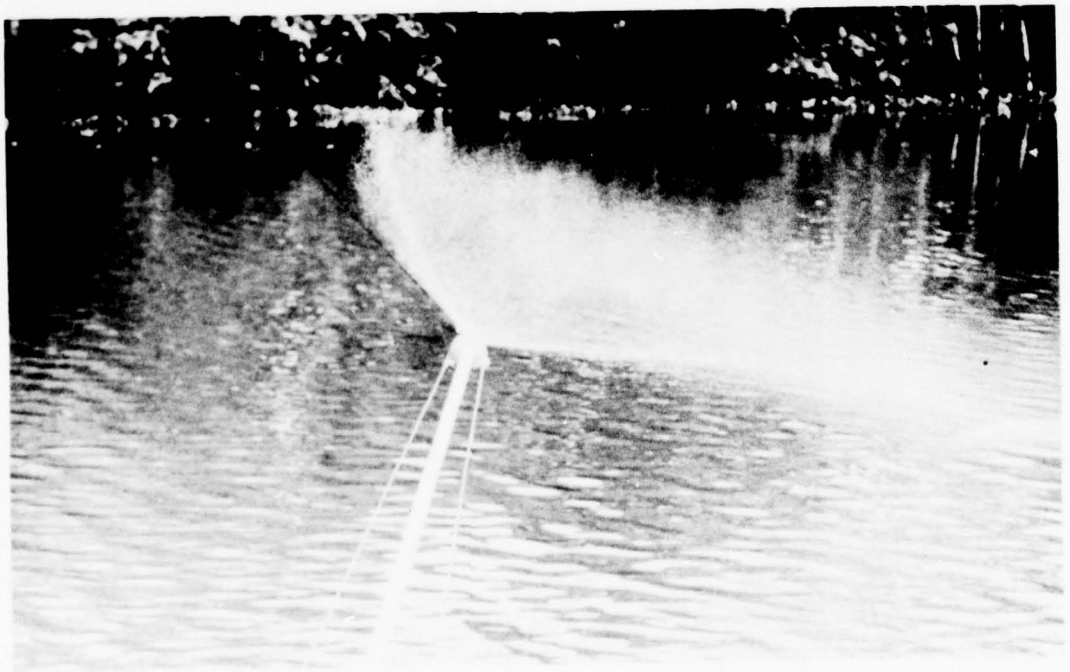

FIGURE 38. Emulsion Spray From 0.8 GPM Nozzle.

PROCEDURES

The first film coating operation was conducted on Thursday, 13 September. It had been decided that an initial coat of 0.2 lb/acre would be applied; subsequent patching coats would be at the rate of 0.1 lb/acre if possible. Panama Canal Company personnel requested that film be applied to (1) the Gaillard Cut from the Chagres River to Gold Hill; (2) up the Chagres River from the bridge to a point above the log boom opposite the Gamboa Golf Club and (3) in Gatun Lake to a point opposite the dredging. Since these areas [(1) 387 acres, (2) 225 acres, and (3) 360 acres] totaled 972 acres, NWC personnel suggested that Gatun Lake coverage be omitted initially. Indications were that film moving down the Chagres would flow northward into Gatun Lake. Figure 39 depicts the experimental area.

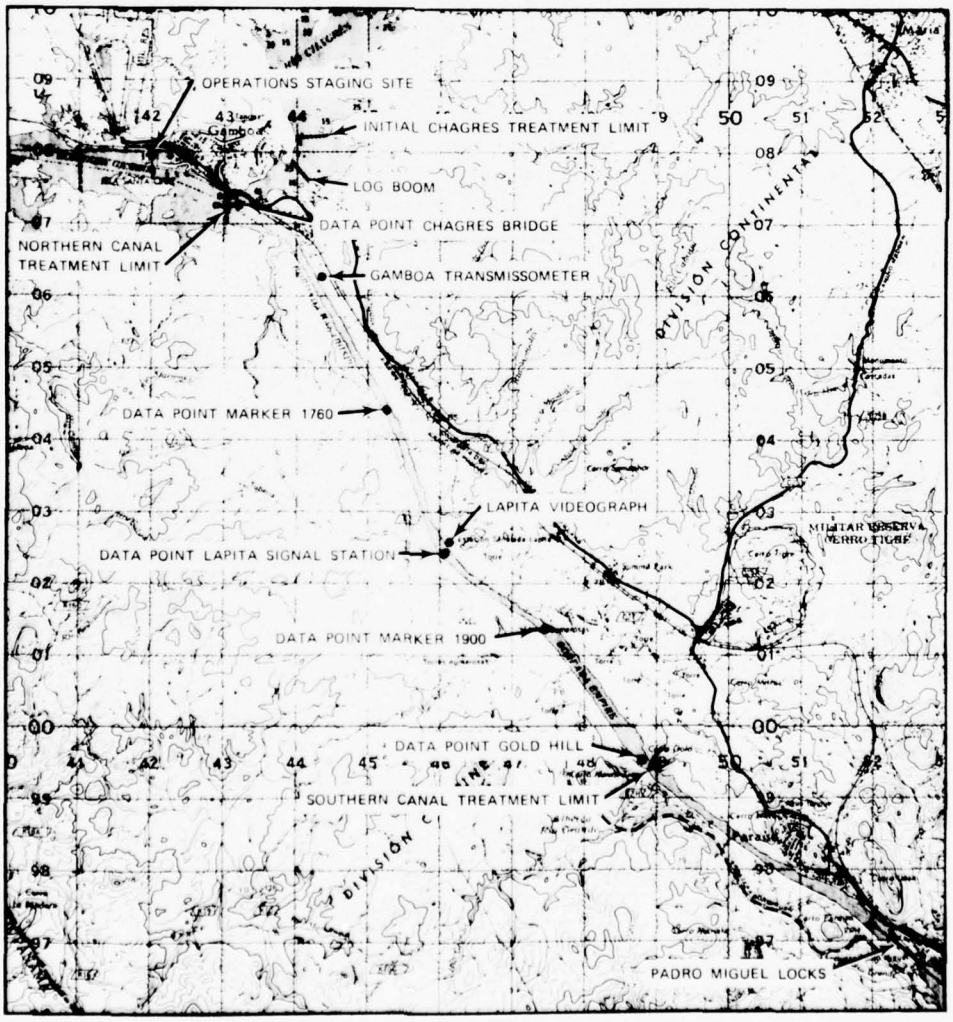

FIGURE 39. Map of Evaporation Suppression Experimental Area.

The boat was loaded with 137.5 gallons of 10% dispersion containing 100 pounds of tallow alcohol and departed the dock at 1330. Spraying commenced at 1342 at the entrance and on the west side of the Cut and finished at 1535, 0.5 mile short of the entrance on the east side of the Cut. Difficulties were encountered with nozzle-plugging due to miscellaneous trash in the dispersion from the mixing and transfer operations. Film spreading was readily observed (Figure 40). The two film slicks initially generated spread rapidly, joined about 1,500 feet aft of the boat and appeared to cover about half of the Cut width about one-half to one mile aft of the boat. After turnaround at Gold Hill it became obvious that a complete coverage would be attained on completion of the return trip.

After the spray run down the Gaillard Cut, the boat was reloaded with 50 pounds of tallow alcohol (137.5 gallons of 5% dispersion) for the spray run up the Chagres River. Spraying occurred from 1630 to 1800 hours (Figure 41). Many nozzle clogs occurred; the spray booms were ultimately fitted with large nozzles and the balance of the dispersion pumped out during the return run to the dock.

Fog was reported in the Cut from 0535 to 0755 hours on 14 September. No observations of fog intensity, visibility, or ceiling were made during the fog incident since arrangements for a qualified boat operator for early morning observation runs had not been made. Winds during the spray operation were light and variable from the north (down the Cut toward Pedro Miguel). On Friday, 14 September, the spray system was fitted with copper gauze filters to prevent nozzle plugging and the top of the dispersion tank was cut out to permit stirring with a paddle. Spraying operations on Friday, Saturday, and Sunday, the 14th, 15th, and 16th, were identical. After loading 110 gallons of 5% dispersion (40 pounds tallow alcohols), the boat departed the dock for the Chagres River operation at approximately 1500 hours. The dispersion was sprayed above and below the log boom in a ratio of about 2/3 to 1/3 by surface area. Visual observations of film coverage were made from the Gamboa Gold Club overlooking the upper Chagres River by NWC and/or PCC personnel as available. On return to the dock, the boat was reloaded with 165 gallons of 5% dispersion (60 pounds tallow alcohols) and departed for the Gaillard Cut spray run.

Operations were generally completed by 1830-1900 hours. Observations of film coverage were made from the LaPita Station by personnel as available. Good film coverages were attained in the Gaillard Cut on these operations, although the previous day's film coverage appeared spotty and incomplete prior to operations each day. Film coverage in the Chagres did not appear to last more than two or three hours due to a combination of daily winds and, more importantly, river current carrying the film out of the river. Considerable rain fell during the afternoons on these three days; the winds remained light from the north and east.

On Monday, 17 September, it was learned that fog had closed the Gaillard Cut from about 2130 hours, 16 September, to 0755, 17 September.

FIGURE 40. Portion of Gaillard Cut - Partially Coated.

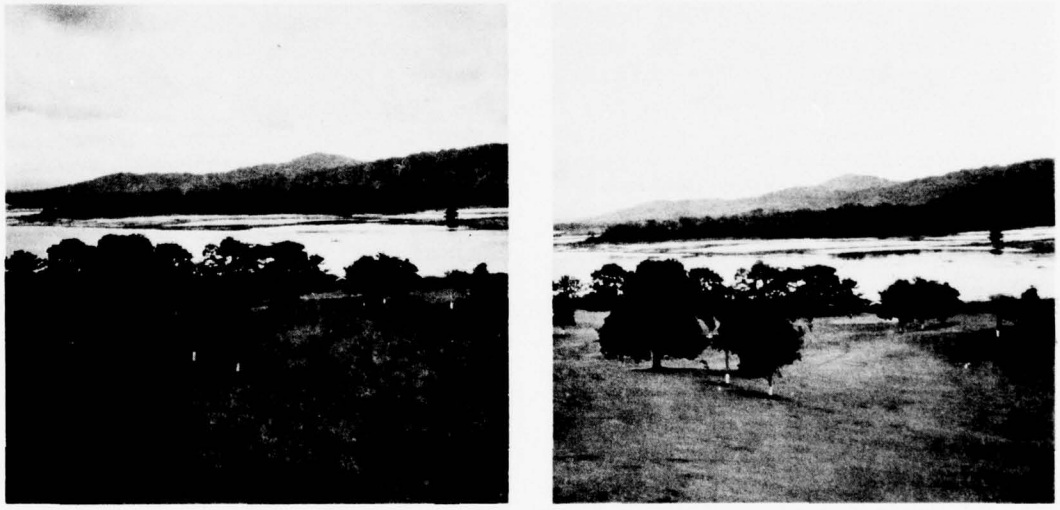

a. In progress. b. Complete.

FIGURE 41. Film Coating Operation on the Chagres River.

The fog was very dense and down to the water. The afternoon film spreading runs were the same as the preceding three days; 40 pounds tallow alcohol in the Chagres River and 60 pounds in the Cut. Difficulties were encountered in achieving a good film coverage due to strong winds (∿ 10 knots or more) from the south-southeast (an easterly wave had passed through the Saturday before). It appeared that the film was being blown north out of the Cut and also against the west bank of the Canal.

On Tuesday, 18 September, project personnel began daily observations and data collection in the Gaillard Cut between 0430 and 0700 hours. It was estimated that Canal film coverage was about 60% complete from the previous day's operation. Film-coating operations this day involved a double coat of the Cut (120 pounds tallow alcohols) and increased coverage of the Chagres River (60 pounds tallow alcohols) to counter the effects of the strong southerly winds. It had become apparent that maintaining long duration coverage of the Chagres River above the log boom was impossible; the river current quickly moved the film down toward Gatun Lake. Panama Canal Company personnel, nevertheless, requested coverage below the Chagres River boom since the mosquito control program was being conducted in the area.

On Wednesday, 19 September, the film operation was modified so as to cover the Chagres River from the Gamboa bridge to the log boom with approximately 20 pounds of tallow alcohols and the Gaillard Cut with 80 pounds of alcohols. The spray operation was reduced to one trip starting at 15001530 hours and finishing at 1800 hours. The winds were light from the south as before. Film from the previous day's operation was observed in Gatun Lake as far as the Dredging Division docks.

The operation was repeated in the same manner on Thursday, Friday, Saturday, and Sunday (2023 September). Fair to excellent film coverage was obtained each day. The winds shifted to the north on Friday and film was observed in the Gold Hill to Pedro Miguel area in the afternoons. Fogs occurred in the Cut on the 20th and 21st from 0010 to 0750 and 0420 to 0615, respectively, as reported by Marine Traffic Control. Our observations on the 21st, morning run, indicated poor film coverage at 0600 over much of the Cut.

The second shipment (24,000 pounds) of tallow alcohols dispersion was delivered to Gamboa on Monday, 24 September (the last of the first shipment of 6,000 pounds was used up on Sunday, 23 September). Coverages achieved daily during the prior week, while increasingly good during and immediately after the afternoon operation, were found to be reduced to only partial coverages at 0600 the following day. Bacterial counts on the raw water supply at Pedro Miguel had remained low during the operation, suggesting that degradation of the film was not a factor responsible for the poor film maintenance. Film was observed in Gatun Lake despite the shift to north-northeast winds, suggesting that water currents had shifted or increased in magnitude toward the north. (Heavy rains had raised the lake level, permitting more power generation at Gatun Dam.) It was decided that increased tallow alcohol dosage rates might counter the tendency to film breakup, therefore the coverage was raised to 0.47 lb/acre.

Operations starting Monday, 24 September, then involved loading the boat with 100 pounds of tallow alcohols in 165 gallons (3 drums) of dispersion, spraying the Chagres River area for 20 minutes (20 pounds alcohols), then spraying the Gaillard Cut to Gold Hill and back to the

Chagres River with the remaining 80 pounds of tallow alcohols. The boat was then reloaded with another 165 gallons of dispersion containing 100 pounds of tallow alcohols and the Cut was sprayed again from the Chagres River bridge to Gold Hill and back. Generally one run up and back the Cut covered the water adjacent to the Canal banks, the second run being up and back the center of the Cut, ship traffic permitting. This procedure was followed until Thursday, 27 September, when the Chagres River coverage was abandoned and the Cut was treated with 200 pounds of alcohols.

Fog occurred in the morning hours of the 24th, 25th, 26th, and 27th of September in the Gaillard Cut and Chagres River areas. The characteristics of the fog as observed between 0430 and 0600 hours, suggested strongly that the desired effect was being achieved. In general, where 100% film coverage was established, the fog ceiling was at 100-200 feet and the visibility was unrestricted. An unusual clarity (complete absence of droplets or other particulates) characterized the air below the fog ceiling. Reflections of the Canal bank lights in the water were sharp and the water surface smooth. In areas where the film coverage had been broken by current, winds, ship-lockages at Pedro Miguel, or unknown reasons, the fog ceilings tended to lower and visibility decreased. While the Canal was closed to shipping on these four days, our observations were that Canal traffic would have proceeded on the 24th, 25th, and 27th. The Dredging Division did, however, utilize all four nights to pull large boulders out of the Cut with a large floating crane and barges. This operation probably could not have been carried out simultaneously with shipping transits or in dense fog.

With operational problems resolved, NWC personnel departed Panama following operations on 27 September with the recommendation to PCC personnel to continue the daily treatment of 200 pounds (0.52 lb/acre) of tallow alcohol to the Gaillard Cut. Panama Canal Company personnel, however, reduced the treatment to 160 pounds (0.41 lbs/acre) of tallow alcohol daily. This was probably done for ease of handling since there were 80 pounds of tallow alcohol per barrel. This treatment (0.41 lbs/acre) was continued until the material was exhausted on 22 October.

DATA ACQUISITION

It was initially planned to use the Marine Traffic Logs as evidence of fog formation and intensity; however, it was learned early in the project that a better method of documentation was needed. The marine traffic controller frequently closed the canal when fog threatened the Canal and rarely was the Canal reopened during the night even though visibility was adequate. Additionally, some nighttime closures were for Canal maintenance but the logs did not so indicate. Consequently, commencing on 18 September and continuing until the end of the fog season (4 November) project personnel made daily early morning observation boat runs down the

Gaillard Cut from the staging site to Gold Hill and return. These observations were routinely made between 0430-0700, the time when fog would most likely exist. These observations were not made on four days, 19, 20, 22 and 28 September, due to the unavailability of a boat. By continuous observations until the end of the fog season a thirteen-day control period was made available. Project observers recorded observations of ceiling and visibility, air temperature and relative humidity at one meter above the water surface and water temperatures at the surface and 12-inch depth. Additionally, the observer summarized the film coverage and general weather conditions (Figure 42). It was hoped that the temperature and moisture

TIME	POSITION	CIG.	VSBY (EST. NM)	DB (°F)	WB (°F)	RH %	SFC WATER TEMP (°F)	12 INCH WATER TEMP (°F)
0500	DEPART DREDGING							
0515	CHAGRES BRIDGE	200	0.5	75.2	75.0	99	79.7	80.0
0535	MARKER 1760	100	UNRES.	75.2	75.0	99	79.8	80.0
0550	LAPITA	200	UNRES.	75.8	75.0	96	79.7	79.9
0605	MARKER 1900	200	UNRES.	75.9	75.2	97	79.5	79.8
0615	GOLD HILL	200 BRKS	UNRES.	76.0	75.0	95	79.4	79.8
0655	ARRIVE DREDGING							

Film Summary (Gold Hill to Dredging): Solid 100% film coverage from Gold Hill to the Mandingo River. 90% coverage from the Mandingo to Dredging.

Weather Summary: Driving to Gamboa from Panama City intermittent patches of light to dense fog were encountered north of Paraiso. At the first data point (mouth of the Chagres) visibility was reduced to one half mile. Entering the Cut was like entering a tunnel. A ceiling of 100 to 200 ft existed throughout the Cut with a very even base and excellent underlying visual clarity with brilliant Canal light reflections on the surface film. At 0615 (at Gold Hill) the first patches of blue sky were noted directly overhead and at 0630 (adjacent to 800 ft tower) a band of blue sky directly over and paralleling the Cut began to appear. Upon return to Dredging at 0655 break-up in general was in progress, however, remnants of fog (down to water surface) with poor visibility were observed in the Chagres River and north in Gatun.

Discussion: This was the first morning's observation in which the film was sustained intact over the area of concern during the night and followed tallow alcohol treatment increased to 4 .47lb/acre. Indications are that film is maintained ceiling and visibility will remain above that required for safe navigation.

FIGURE 42. Sample Observation Log.

measurements would be indicative of the evaporation suppression film efficiency and, while this seemed to be true in some instances, there was too much uncertainty as to film coverage at the data collection points, since these data were collected prior to daylight. A summary of observed film coverage and weather conditions is included in Table 8, while the continuation observations during the control period are shown in Table 9. In addition to the routine observations, photography was attempted in a few instances, lighting conditions permitting (Figures 43(a) and (b)).

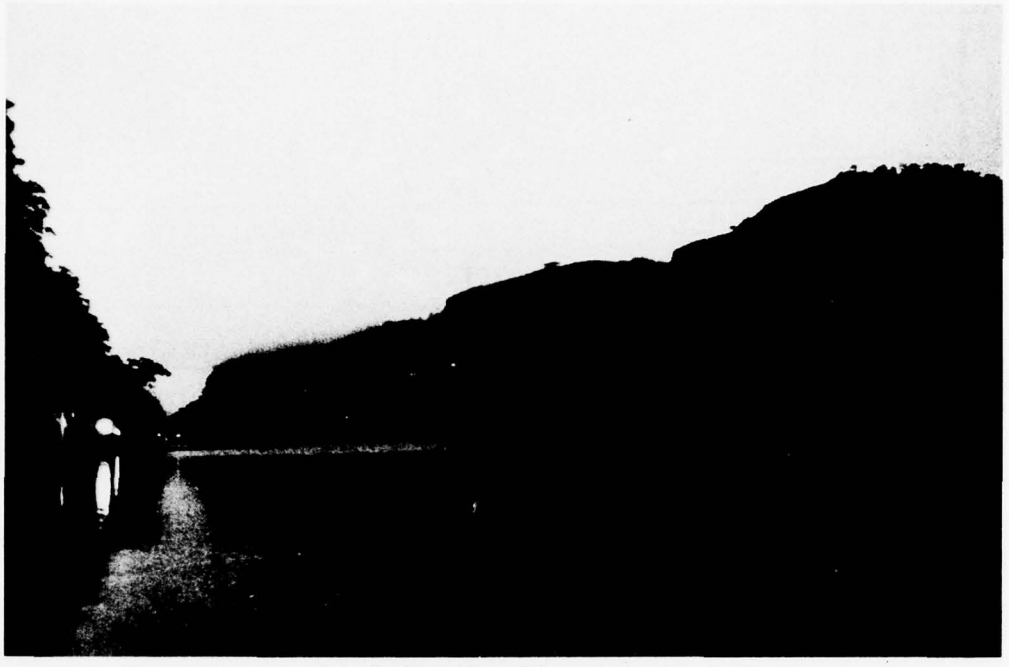

a. Section with partial coverage.

b. Section with full coverage.

FIGURE 43. Early Morning Views of Canal Showing Film Coverage.

TABLE 8. Treatment and Observations – Test Period

Date 1973	Area Treatment: Gaillard Cut (387 acres) Total lbs. TA	Gaillard Cut (387 acres) Lbs. per acre	Chagres River (225 acres) Total lbs. TA	Chagres River (225 acres) Lbs. per acre	Early Morning Observations (≈0430-0700): Chagres Bridge to Marker 1760 FC-%	Chagres Bridge to Marker 1760 Sky Cover	Chagres Bridge to Marker 1760 Vsby. (Est Ft.)	Marker 1760 to Lapita FC-%	Marker 1760 to Lapita Sky Cover	Marker 1760 to Lapita Vsby. (Est Ft.)	Lapita to Marker 1900 FC-%	Lapita to Marker 1900 Sky Cover	Lapita to Marker 1900 Vsby. (Est Ft.)	Marker 1900 to Gold Hill FC-%	Marker 1900 to Gold Hill Sky Cover	Marker 1900 to Gold Hill Vsby. (Est Ft.)	Canal shipping state (from A.M. obs.): Open to 2-way traffic	Open to 1-way traffic	Closed	Fog tended to develop: Yes	No	Remarks
Sept. 13	100	0.26	50	0.22						UNOBSERVED												
14	60	0.16	40	0.18						UNOBSERVED												
15	60	0.16	40	0.18						UNOBSERVED												
16	60	0.16	40	0.18						UNOBSERVED												
17	60	0.16	40	0.18						UNOBSERVED												
18	120	0.31	30	0.13	70	①AC	U	40	①AC	U	60	①AC	U	60	①AC	U	X				X	light rain during night, no fog
19	80	0.21	20	0.31						UNOBSERVED												
20	80	0.21	20	0.31						UNOBSERVED												
21	80	0.21	20	0.31	40	50	660	30	30	330	30	50	330	40	20	100			X	X		dense fog
22	80	0.21	20	0.31						UNOBSERVED												
23	80	0.21	20	0.31	50	①SC	U	20	①SC	U	90	①SC	U	30	+SC	U	X			X		light fog in Gold Hill slide area, Empire & banks of Chagres
24	180	0.47	20	0.31	20	200	U	20	100	U	70	100	U	30	100	U	X			X		fog lower along banks than over Canal, dense fog in Chagres
25	180	0.47	20	0.31	100	200	2640	100	100	U	100	200	U	100	200	U	X			X		excellent vsby. in Cut, dense fog in Chagres and Gatun
26	180	0.47	20	0.31	100	200	U	90	200	U	20	100	2640	40	50	1000		X		X		vsby. & film cover correlate, fog dense in Gatun
27	200	0.52	DISCONTINUE		100	①ST	U	80	200	U.R.	60	+SC	U.R.	50	+SC	U.R.	X				X	Stratus began forming but washed out in light rain
28	160	0.41								UNOBSERVED												
29	160	0.41			30	Clear	U	100	+ST	U	70	+ST	U	100	①ST ①SC	U	X			X		light patchy fog along banks
30	160	0.41			90	200	U	100+	500	U	100	700	U	100	100	2640	X			X		poorest conditions were S. of Gold Hill (untreated area)
Oct. 1	160	0.41			100	200	2640	100	+ST	U	100	300	U	100	200	5280	X			X		fog tended to thicken at Gold Hill
2	160	0.41			95	①ST ①AC	U	90	Clear	U	95	Clear	U	30	①ST ①AC	U	X			X		light fog vicinity Gamboa, weak development
3	160	0.41			70	①SC ①C1	U	100	①SC +C1	U.R.	75	①SC +C1	U	85	+SC	U	X				X	light rain, no fog
4	160	0.41			85	600	U	60	①ST	U	80	200	U	90	200	3960	X			X		weak development, stratus lower & thicker S. of Lapita
5	160	0.41			100	Clear	U	40	Clear	U	100	Clear	U	95	Clear	U	X				X	no fog
6	160	0.41			100	Clear	U	100	Clear	U	98	①SC	U	100	①SC	U	X				X	no fog

TABLE 8. (Contd.)

Date 1973	Area Treatment: Gaillard Cut (387 acres) Total lbs. TA	Gaillard Cut (387 acres) Lbs. per acre	Chagres River (225 acres) Total lbs. TA	Chagres River (225 acres) Lbs. per acre	Early Morning Observations — (0430-0700): Chagres Bridge to Marker 1760 FC-%	Sky Cover	Vsby. (Est. Ft.)	Marker 1760 to Lapita FC-%	Sky Cover	Vsby. (Est. Ft.)	Lapita to Marker 1900 FC-%	Sky Cover	Vsby. (Est. Ft.)	Marker 1900 to Gold Hill FC-%	Sky Cover	Vsby. (Est. Ft.)	Canal shipping state (from A.M. obs.) Open to 2-way traffic	Open to 1-way traffic	Closed	Fog tended to develop Yes	No	Remarks
7	160	0.41	...	...	98	Clear	U	50	150	U	80	200	U	70	Zero	1000		X		X		fog most dense vcnty Gold Hill. Patchy along banks.
8	160	0.41	...	...	90	150	U	98	200	U	98	150	U	50	150	U	X			X		Broken to overcast stratus layer.
9	160	0.41	...	...	98	150	U	80	50	1320	98	Zero	500	98	75	1000			X	X		dense fog.
10	160	0.41	...	...	98	25	2640	98	75	1000	80	150	1320	70	Zero	1000		X		X		fog most intense vicinity Gold Hill.
11	160	0.41	...	...	98	⊕SC	U	40	÷SC	U	95	⊕SC	U	60	÷SC	U	X			X		patchy fog along banks.
12	160	0.41	...	...	100	÷C1	U	75	⊕SC ⊕C1	U	95	⊕SC ⊕C1	U	55	⊕ST ⊕C1	U	X			X		dense fog on *both* banks vsby. reduced on return trip.
13	160	0.41	...	...	80	÷SC	U;R-	15	÷SC	U;R-	85	⊕SC ÷AC	U	100	⊕ST ⊕AC	U	X				X	*light rain-no fog*
14	160	0.41	...	...	100	⊕AC ÷C1	U	90	⊕SC ⊕AC	U	85	⊕SC ÷AC	U	100	⊕SC ÷AC	U	X				X	no fog.
15	160	0.41	...	...	90	⊕SC ÷C1	U	95	Zero	<500	98	⊕ST ⊕C1	U	98	⊕SC	U			X	X		late forming fog. Shallow and patchy but dense.
16	160	0.41	...	...	90	⊕SC	U	95	⊕SC	U	90	⊕SC	U	98	⊕SC	U	X				X	no fog.
17	160	0.41	...	...	10	⊕SC	U	2	÷SC	U	2	÷SC	U	2	÷SC	U	X				X	no fog.
18	160	0.41	...	...	2	÷SC	U	0	÷SC	U	0	÷SC	U;R-	0	÷SC	U;R-	X				X	light rain-no fog.
19	160	0.41	...	...	900	500	U	50	500	U	75	500	U	20	500	U	X			X		stratus layer completely across Cut.
20	160	0.41	...	...	90	Clear	U	90	⊕SC	U	90	Clear	U	80	Clear	U	X				X	stratus cap on Gold Hill, otherwise no fog.
21	160	0.41	...	...	40	⊕ST ÷C1	U;R-	30	⊕ST ⊕C1	U;R-	30	⊕ST ÷C1	U	20	⊕SC ⊕C1	U;R-	X					light rain-no fog.
22	160	0.41	...	...	90	⊕ST	U	90	⊕ST	U	90	⊕SC	U	60	⊕SC	U	X			X		light fog along banks.

LEGEND:

- U: Unrestricted
- ⊕: Scattered
- ⊕: Broken
- ÷: Overcast
- ST: Stratus
- SC: Stratocumulus
- AC: Altocumulus
- CI: Cirrus
- R-: Light Rain
- -: Thin

1. Visibility minimums for shipping were explained to NWC personnel as follows:

   <1000': Canal closed.
   1000' - 1500': Open to one-way traffic.
   >1500': Open to two-way traffic.

2. Beginning on 19 September Chagres River treated to Log Boom only (64 acres).

TABLE 9. Observations – Control Period

Date 1973	Early morning observations – (≈0430-0700)								Canal shipping state (from A.M. obs.)			Fog tended to develop		Remarks
	Chagres Bridge to Marker 1760		Marker 1760 to Lapita		Lapita to Marker 1900		Marker 1900 to Gold Hill		Open to 2-way traffic	Open to 1-way traffic	Closed	Yes	No	
	Cig (Est. ft.)	VSBY (Est. ft.)	Cig (Est. ft.)	VSBY (Est. ft.)	Cig (Est. ft.)	VSBY (Est. ft.)	Cig (Est. ft.)	VSBY (Est. ft.)						
Oct. 23	Zero	500	Zero	500	Zero	750	Zero	750			X	X		dense fog to water surface
24	500	U	500	U	500	U	1000	U	X			X		light patchy fog along banks
25	Zero	1000	Zero	500	Zero	500	Zero	500			X	X		dense fog to water surface
26	50	1000	Zero	500	Zero	1000	Zero	1000			X	X		dense fog to water surface
27	500	U	⊕ST	U	⊕SC	U	⊕SC	U	X			X		light fog along west bank
28	Zero	2000	Zero	500	Zero	300	Zero	300			X	X		dense fog to water surface
29	50	U	100	U,R-	⊕ST ⊕SC	U,R-	⊕ST ⊕SC	U,R-	X				X	light rain prevented fog
30	150	1000	200	U	⊕AC ⊕C1	U	⊕AC ⊕C1	U		X		X		vsby. reduced on return trip
31	200	2640	100	1500	Zero	800	50	1200			X	X		variable fog conditions
Nov. 1	300	U	300	U	⊕ST	U	⊕ST	U	X			X		stratus across Cut
2	Clear	U	Zero	2000	Zero	2000	Zero	2000	X			X		thin fog to water surface
3	Clear	U	⊕SC	U,R-	⊕SC	U,R-	⊕SC	U,R-	X				X	light rain-no fog
4	Clear	U	Clear	U	⊕SC	U	⊕SC	U	X			X		fog up Chagres and along banks

LEGEND:
- U - Unrestricted
- ⊕ - Scattered
- ⊕ - Broken
- ⊕ - Overcast
- ST - Stratus
- SC - Stratocumulus
- AC - Altocumulus
- C1 - Cirrus
- R- - Light Rain
- – - Thin

Supplementing the foregoing data, PCC made available instrumental visibility measurements from their Gamboa transmissometer and Lapita videograph (Figure 39). However, both of these stations proved to have shortcomings. The Gamboa transmissomter base line paralleled the Canal at approximately 50 feet up the bank and thus did not measure the visibility over the Canal proper, while the videograph lacked sensitivity and response in the lower visibility range.

RESULTS

Tables 10 and 11 present comparative Canal conditions from the instrumented stations, early morning observations, and the Marine Traffic Logs for days when fog tended to develop. Table 10, which covers the test period, begins with 25 September, the first day in which the film appeared to be sustained through the night. Table 11 covers the control period. Major discrepancies are obvious during both periods; the Marine Traffic Logs indicate too many Canal closures while measurements from the Lapita videograph indicate none. While information from the Gamboa transmissometer appears more probable there may well have been instances when it measured fog along the banks that did not extend over the Canal proper.

A comparison of conditions existing during the early morning observations for the test and control periods indicates that during the test period poor visibility caused 'closure' in only 2 of 11 days, or 45%. While the figures are inadequate for statistical purposes, there is a fair indication that evaporation suppression by the long-chain alcohol technique did provide positive results.

TABLE 10. Comparative Indicated Canal Conditions (Test Period)(0430 – 0700 LST)

Date 1973	Instrumented Stations								Early morning observations				Marine traffic log	
	Gamboa				Lapita									
	Min. vsby. (ft.)	Open to 2-way traffic	Open to 1-way traffic	Closed	Min. vsby. (ft.)	Open to 2-way traffic	Open to 1-way traffic	Closed	Min. vsby. (ft.)	Open to 2-way traffic	Open to 1-way traffic	Closed	Canal open	Canal closed
Sept. 25	1320		X		1374		X		2640	X				X
26	U	X			U	X			1000		X			X
29		MISSING DATA			U	X			U	X				X
30		MISSING DATA			1743	X			2640	X				X
Oct. 1		MISSING DATA			2112	X			2640	X				X
2	U	X			U	X			U	X			X	
4	U	X			2640	X			3960	X				X
7	2112	X			1584	X			1000		X			X
8	O			X	1584	X			2000	X				X
9	O			X	1584	X			500			X		X
10	O			X	1848	X			1000		X			X
11	U	X			U	X			U	X				X
12	O			X	1005		X		U	X				X
15	O			X	1320		X		<500			X	X	
19	U	X			U	X			U	X			X	
22	1056		X		1320		X		U	X				X
Totals		6	2	5		12	4	0		11	3	2	3	13

TABLE 11. Comparative Indicated Canal Conditions (Control Period)(0430-0700 LST)

Date 1973	Instrumented Stations								Early morning observations				Marine traffic log	
	Gamboa				Lapita									
	Min. vsby. (ft.)	Open to 2-way traffic	Open to 1-way traffic	Closed	Min. vsby (ft.)	Open to 2-way traffic	Open to 1-way traffic	Closed	Min. vsby. (ft.)	Open to 2-way traffic	Open to 1-way traffic	Closed	Canal open	Canal closed
Oct. 23		MISSING DATA			1584	X			500			X		X
24		MISSING DATA			1637	X			U	X			X	
25		MISSING DATA			1056		X		500			X		X
26	O			X	1056		X		500			X		X
27	U	X			U	X			U	X				X
28	O			X	1056		X		300			X		X
30	O			X	1056		X		1000		X			X
31	O			X	1056		X		800			X		X
Nov. 1	U	X			U	X			U	X				X
2	O			X	1056		X		2000	X				X
4	U	X			U	X			U	X			X	
Totals		3	0	5		5	6	0		5	1	5	2	9

DISCUSSION

PHASE I - AERIAL DISPENSING OF CHARGED WATER DROPLETS

Results of the 13 fog and stratus dispersal tests, while inconsistent, did produce certain positive indications that dispersal effects were induced. Physical indications of these positive effects increased with minor system modification accomplished in the field.

The principles of electrostatically enhanced coalescence are sound; however, certain engineering problems must be solved to improve the efficiency of the present system prior to future field testing. Increased quantities of spray droplets carrying higher charges are needed. Also, an improved and automated, airborne data system to record parameters pertinent to the charged spray is required.

PHASE II - CHARGED, HYGROSCOPIC BUBBLES

While the principles of charged, hygroscopic bubbles are the same as those applicable to charged droplets, bubble dispensing is more adaptable to a surface-based system. The problems of bubble production and buoyancy as well as targeting must be resolved. The use of helium to provide the required lift is far too expensive for practical application. Hot air may be the ultimate answer.

Since the airborne electrostatic charging system is in a more advanced state of design and gives promise for a more immediate and portable fog dispersal system it is recommended that further work on the surface dispensing, charged-bubble system be held in abeyance until the airborne electrostatic charging system is finalized.

PHASE III - EVAPORATION SUPPRESSION TESTING

Results of these field trials in the Panama Canal, which involved the establishment and maintenance of a monomolecular film of long-chain fatty alcohols on the Canal water surface, proved a strong correlation between fog intensity and film coverage. In areas where the film remained intact (100% cover) fog (stratus) ceilings held at 100 to 200 feet with good surface visibility, while in areas where the film became broken and patchy, ceilings lowered and visibility reduced to below that required for safe navigation. Treatment quantities of less than 0.5 lb/acre of tallow alcohol appear to be inadequate for maintaining the film intact through the nocturnal fog formative hours. It seems reasonable to conclude that with proper engineering, evaporation suppression by the long-chain alcohol technique may well solve the fog problem in the Panama Canal.

REFERENCES

1. Naval Weapons Center. *Project Foggy Cloud I*, by E. Alex Blomerth and others. China Lake, Calif., NWC, August 1970. 85 pp. (NWC TP 4929, publication UNCLASSIFIED.)

2. _____. *Project Foggy Cloud III, Phase I*, by Tommy L. Wright and others. China Lake, Calif., NWC, April 1972. 68 pp. (NWC TP 5297, publication UNCLASSIFIED.)

3. _____. *Project Foggy Cloud IV, Phase I*, by E. E. Hindman, II, and others. China Lake, Calif., NWC, August 1973. 52 pp. (NWC TP 5413, publication UNCLASSIFIED.)

4. _____. *Project Foggy Cloud IV, Phase II*, by R. B. Loveland and others. China Lake, Calif., NWC, December 1972. 42 pp. (NWC TP 5338, publication UNCLASSIFIED.)

5. _____. *Project Foggy Cloud V*, by R. S. Clark and others. China Lake, Calif., NWC, December 1973. 92 pp. (NWC TP 5542, publication UNCLASSIFIED.)

6. V. V. Smirnov and A. D. Solov'ev. "Generation and Properties of Particles With Expanded Surfaces (Liquid Bubbles)," in *Proceedings of the Institute of Experimental Meteorology*, Vol. 1, No. 33, pp. 3-23. Moscow, Trudy Institut Eksperimental' noi Meteorologii, 1972.

7. Y. S. Sedunov. "Laboratory Experiment on the Cloud Droplet Spectrum Formation and Its Modification," presented at the Third Conference on Weather Modification, Rapid City, S.D., June 1972.

8. Institute of Water Utilization, Agriculture Experiment Station, Univ. of Arizona. *Evaporation Reduction Investigations Relating to Small Reservoirs in Arid Regions*, by C. B. Cluff and S. D. Resnick. Tucson, Ariz., Univ. of Arizona, October 1964. 33 pp.

9. Commonwealth Scientific and Independent Research Organization of Australia (Ser. No. 74). *Summary of Field Trials on the Use of Cetyl Alcohol To Restrict Evaporation From Open Storages During the Season 1954-55*. 1955.

10. Bakharova and others. "Results of Tests on Methods of Modifying Steam Fog," *Trudy Ukrnigmi*, No. 77 (1969), pp. 144-51.

11. National Bureau of Standards. *A Summary of Low Visibility Conditions at the Arcata Airport*, by James E. Davis and others. Washington, D.C., NBS, U.S. Dept. of Commerce, November 1968. 40 pp. (NBS Report No. 9958, report UNCLASSIFIED.)

12. Atmospheric Research Group. *Operation Pea Soup 1959*, by T. J. Lockhart and R. J. Beesmer. Altadena, Calif., ARG, 18 December 1959. 23 pp. (ARG59 FR 58, report UNCLASSIFIED.)

13. Aeronautical Icing Research Laboratories, Bartlett, N.H. *Fog Studies at Arcata, California Under "Operation Pea Soup" 1960*, by G. P. Ettenheim, Jr., and others, for the U.S. Air Force, Bedford, Mass., March 1961. 34 pp. (Technical Note No. 570, AFCRL 261, report UNCLASSIFIED.)

14. Aeronautical Icing Research Laboratories, Arcata, Calif. *Fog Studies at Arcata, California Under "Operation Pea Soup" 1961*, by G. P. Ettenheim, Jr., for the U.S. Air Force, Bedford, Mass., June 1962. 26 pp. (Technical Note No. 571, AFCRL 62-804, report UNCLASSIFIED.)

15. R. W. Tate and E. O. Olson. "Spray Droplet Size of Pressure-Atomizing Burner Nozzles," *Amer. Soc. Heating, Refrig. Air-Cond. Eng. J.*, Vol. 4 (1962), pp. 39-42.

16. J. H. Perry and others. *Chemical Engineers' Handbook*. New York, McGraw-Hill, 1963. Pp. 5-59 to 5-62.

17. C. V. Boys. *Soap-Bubbles, Their Colors and the Forces That Mold Them*. New York, Dover Publications, Inc., 1959. 192 pp.

18. B. J. Mason. *The Physics of Clouds*. Oxford, England, Clarendon Press, 1971. P. 86.

19. S. Twomey. "The Supersaturation in Natural Clouds and the Variation of Cloud Droplet Concentration," *Geofis. Pura. Appl.*, Vol. 43 (1959), p. 243.

20. A. C. Delany and others. "Tropospheric Aerosol: The Relative Contribution of Marine and Continental Components," *J. Geophys. Res.*, Vol. 78 (1973), pp. 6249-6265.

21. C. E. Junge. "Recent Investigations in Air Chemistry," *Tellus*, Vol. 8 (1956), pp. 127-139.

22. Y. Miyake. "The Chemical Nature of the Saline Matter in the Atmosphere," *Geophys. Mag.*, Vol. 16 (1948), pp. 64-65.

23. C. E. Junge. *Air Chemistry and Radioactivity*. New York and London, Academic Press, 1963. Pp. 160-166.

Appendix A

DETAILS OF AIRBORNE FOG DISPERSAL TESTS

TEST VI-FA(1) 0440-0655 PDT - 3 September 1973

Conditions

Fog onset occurred at 1706 PDT on 2 September. Two 40-minute periods of clearing were recorded (0730 and 0955 PDT) during the 18-hour fog regime. The surface air temperature decreased from 50° to 43°F from fog onset to seeding time. Relative humidity remained at 100% during this period. During the 30 minutes prior to seeding, visibility ranged from .16 to .24 nmi and averaged .18 nmi. Prevailing wind was northeasterly and averaged 1 knot at 20 ft AGL and 1.5 knots at 50 ft AGL.

Operation

Ten passes were made over the runway at fog top (500 ft MSL) from 0523 to 0554 PDT. Only 28 gallons of water were dispensed over the runway, as the remainder of the total output (155 gallons) was dispensed while completing the racetrack patterns (Fig. 19). A positive charge of 15 kV was applied to the port spray boom, but equipment failure prevented application of a negative charge to the starboard boom. During seeding the prevailing wind at 50 ft AGL was northerly and averaged .6 knot. Changes in visibility during the test are shown in Figure A-1. Winds, which carried induced effects away from the point of measurement, are noted in Table A-1.

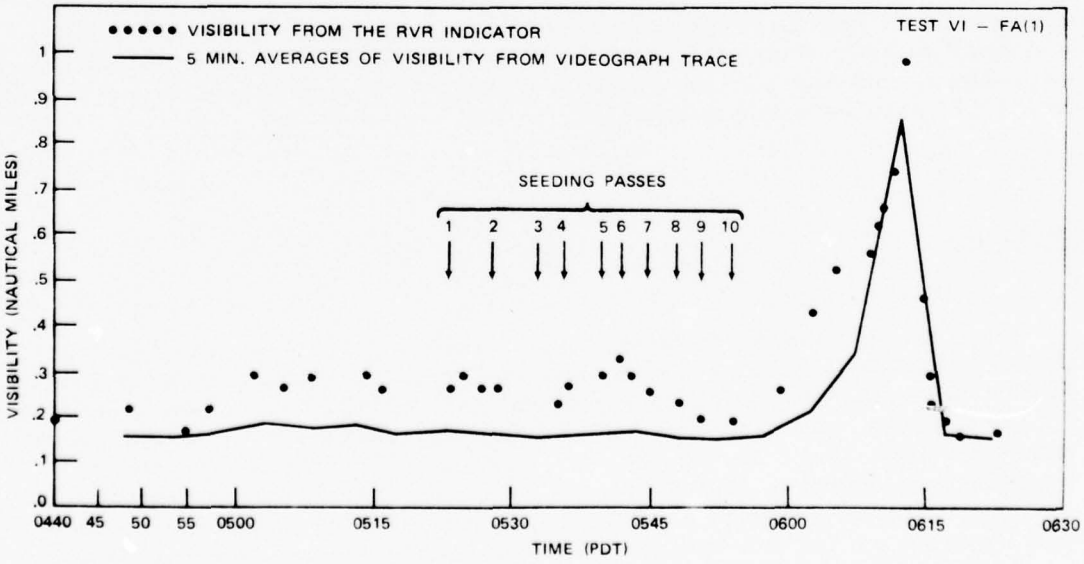

FIGURE A-1. Visibility During Test FA (1).

TABLE A-1. Wind Drift During Test FA(1).

TIME	20 Ft. AGL		50 Ft. AGL	
	Prevailing Direction	Avg. Speed	Prevailing Direction	Avg. Speed
PDT	Degrees	Knots	Degrees	Knots
0445-0500	070	1.3	065	1.7
0500-0515	040	.9	030	1.3
0515-0530	355	.1	350	.4
0530-0545	025	.9	015	.9
0545-0600	040	.1	030	.4
0600-0615	005	2.2	005	2.2
0615-0630	010	1.3	355	2.2
0630-0645	015	1.3	005	1.7

TEST VI-FA(2) 1320-1550 PDT - 4 September 1973

Conditions

A combination of ground fog, haze, smoke and fog restricted visibility from 0155 to 1157 PDT. From 1157 until 1955 PDT visibility was restricted by fog only. Visibility did remain above 1 nmi except from 1057 to 1257 PDT. Data from the laboratory aircraft were used to construct a temperature/dewpoint profile to 5,300 feet MSL just prior to seeding. Prevailing wind during the 45-minute period before seeding was southwesterly and averaged 6.8 knots at both 20 and 50 feet AGL. Since a dense fog bank, extending seaward from the northwest end of Runway 31, was selected as the seeding target, visibility measurements from the instrumentation site were not meaningful.

Operation

Ten seeding passes were made just above the 900 feet MSL fog top, from 1417 to 1447 PDT. A 45-second pass began at the northwest end of Runway 31, using an indicated airspeed (IAS) of 130 knots, and a heading of 310 degrees. Seeding rate was 5 gal/min. Charge to the spray booms was a positive 16 kV on the port and negative 15 kV on the starboard. Intermittent charging system failure occurred when the booms penetrated the fog. Prevailing wind direction and average wind speed during seeding is noted in Table A-2. Aerial photographic documentation from a handheld 35 mm camera and a downpointing T-11 camera are available.

TABLE A-2 Sustained Winds Advecting and Mixing Fog During Test FA(2).

TIME	20 Ft. AGL		50 Ft. AGL	
	Prevailing Direction	Avg. Speed	Prevailing Direction	Avg. Speed
PDT	Degrees	Knots	Degrees	Knots
1330-1345	200	6.5	190	7.0
1345-1400	195	6.5	185	6.5
1400-1415	200	7.0	150	7.4
1415-1430	185	8.3	175	8.7
1430-1445	180	7.8	170	8.3
1445-1500	185	7.0	180	7.8
1500-1515	195	7.0	185	7.4
1515-1530	210	7.4	195	7.4
1530-1545	205	8.3	195	8.7
1545-1600	195	7.8	190	8.7

TEST VI-FA(3) 1810-2045 PDT - 4 September 1973

Conditions

Fog remained in the area after Test VI-FA(2) was completed. Just prior to start of seeding, fog top was 1,800 ft MSL over the airport. South and west of the airport fog top was lower and there was a large clear area over Humboldt Bay. Data from preseed laboratory aircraft passes indicated a decreasing trend in liquid water content (LWC) from .24 to .18 g/m^3. The wind vector from surface to fog top was 170 degrees at 1,034 ft/min. Prevailing wind direction at 50 ft AGL was southeasterly and averaged 6.5 knots during the 45-minute period before seeding.

Operation

Eight seeding passes were made, just above fog top, from 1917 to 1944 PDT. A dogbone pattern was used and offset to the south to compensate for the wind vector. Under radar control the seeding aircraft moved toward the airport on successive passes in order to repeatedly seed the same fog volume. Seventy-five gallons of water were dispensed with a flow rate just under 2 gal/min. Only 10 gallons were applied to the target volume because the water was dispensed continuously from 1901 PDT. Charge to both the positive and negative booms varied from 15 to 16 kV. Data for a temperature/dewpoint profile to 5,300 ft MSL were collected by the laboratory aircraft during seeding.

TEST VI-FA(4) 0420-0610 PDT - 10 September 1973

Conditions

Fog onset occurred at 2356 PDT on 9 September and restricted visibility until 1157 PDT on 10 September. Smoke from a forest fire southeast of the airport reduced visibility after noon on 10 September. Fog top was 750 ft MSL at 0455 PDT. Average LWC of the fog increased from .17 g/m^3 at 0440 PDT to .24 g/m^3 at 0455 PDT. Surface air temperature fell from 50°F at fog onset to 47°F at start of seeding. Visibility ranged from .17 to .24 nmi and averaged .18 nmi during the 30-minute period before seeding began. Prevailing wind direction was northwesterly and averaged 3.5 knots at 20 ft AGL and 4 knots at 50 ft AGL during the same period. A vertical profile of air temperature and dewpoint temperature, from surface to 5,250 ft MSL was obtained just prior to start of seeding.

Operation

Ten seeding passes were made over Runway 31, just above fog top, from 0501 to 0542 PDT. Charged spray was dispensed continuously throughout the circuit of the racetrack pattern during the first three passes but was confined to the 1.6 mile leg (middle marker to end of runway) of the pattern for the final seven passes. Only 160 gallons of the 360 gallons dispensed were applied over the runway. A positive 12 kV charge was applied to the port spray boom and a negative 16 kV to the starboard boom. Nozzles rated at 8 gal/hr, were used providing an estimated 20 gal/min flowrate. Prevailing wind direction at 50 ft AGL was northwesterly and averaged 3.6 knots during seeding (Table A-3), so the treated volume may have drifted away from the visibility measurement site. Surface visibility was steady during the test period (Figure A-2).

TABLE A-3. Winds During Test FA(4).

TIME	20 Ft. AGL		50 Ft. AGL	
	Prevailing Direction	Avg. Speed	Prevailing Direction	Avg. Speed
PDT	Degrees	Knots	Degrees	Knots
0430-0445	320	3.5	305	4.3
0445-0500	310	3.0	300	3.9
0500-0515	315	3.5	305	3.9
0515-0530	325	3.0	310	3.5
0530-0545	325	3.0	310	3.5
0545-0600	325	2.2	315	2.1
0600-0615	325	1.3	325	2.2

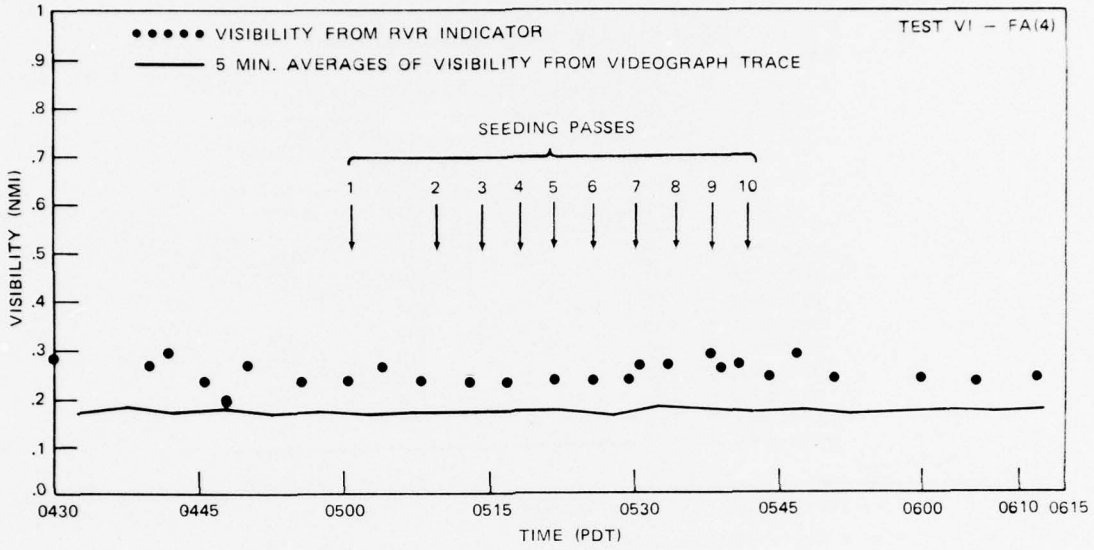

FIGURE A-2. Visibility During Test FA (4).

TEST VI-FA(5) 0610-0805 - 10 September 1973

Conditions

Fog top, which was 600 ft MSL thirty minutes before seeding began, lowered to 500 ft MSL by the time seeding started. Average LWC was .19 g/m^3 thirty minutes before seeding. Visibility ranged from .17 to .26 nmi and averaged .18 nmi from 0605 to 0635 PDT. Prevailing wind direction was northwesterly and averaged 2 knots at 50 ft AGL during the same period.

Operation

Ten seeding passes were made over Runway 31, just above fog top, from 0635 to 0706 PDT. One hundred sixty gallons of charged water were dispensed over the 1.6 nmi seeding leg of the racetrack pattern. Charge to the port boom was a positive 12 kV and the negative charge to the starboard boom varied from 7-9 kV. Prevailing wind direction at 50 ft AGL was northwesterly and averaged only 1.5 knots during the seeding period (Table A-4). Photographic documentation in the main text (Fig. 23) shows that the fog was cleared over the runway. Visibility measured at the instrument site was outside of the cleared swath and served to document the low visibility in the untreated portion of the fog (Figure A-3).

TABLE A-4. Low Winds During Test FA(5).

TIME	20 Ft. AGL		50 Ft. AGL	
	Prevailing Direction	Avg. Speed	Prevailing Direction	Avg. Speed
PDT	Degrees	Knots	Degrees	Knots
0600-0615	325	1.3	325	2.2
0615-0630	025	1.3	355	1.7
0630-0645	335	1.3	355	1.3
0645-0700	310	1.3	295	1.7
0700-0715	325	.9	310	1.3
0715-0730	310	.9	295	1.3
0730-0745	010	.4	350	.4
0745-0800	065	.1	030	.2

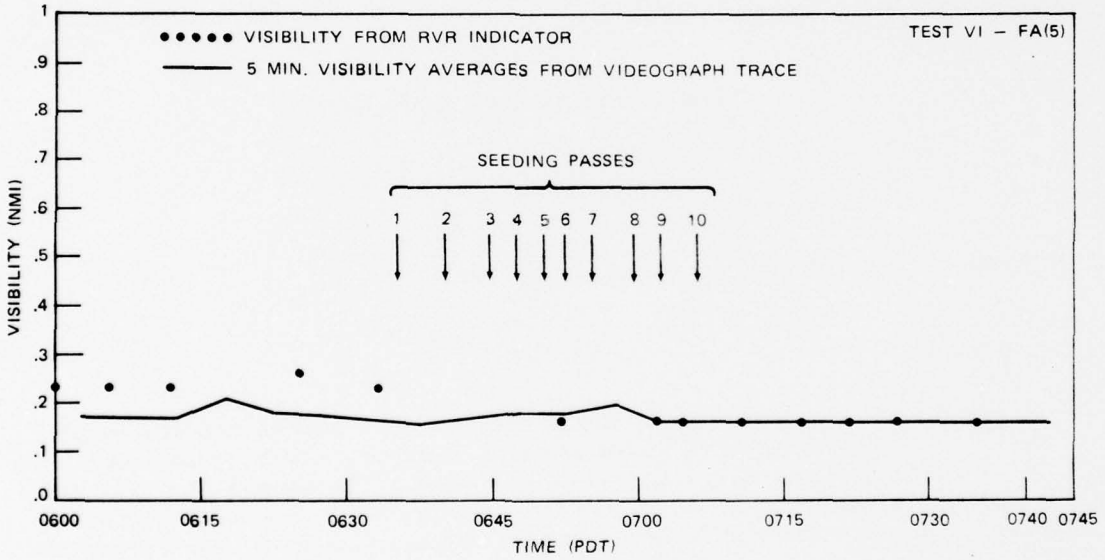

FIGURE A-3. Visibility in Unaffected Area, During Test FA (5).

TEST VI-FA(6) 0540-0705 PDT - 11 September 1973

Conditions

A stratus overcast prevailed from 0158 PDT on 11 September to 0435 PDT on 13 September. Tests VI-FA(6) through (9) were conducted during this period. Stratus base was never less than 300 ft AGL throughout the period. Just before the start of Test (6) stratus top was 1,900 ft MSL. Data from the laboratory aircraft, which obtained a vertical profile of temperature and dewpoint, at 0610 PDT, tends to confirm the height of stratus

top (Figure A-4). Average LWC decreased prior to seeding: from 1.04 g/m^3 at 0557 PDT to .69 g/m^3 at 0610 PDT. The wind vector for the layer from surface to stratus top was 152 degrees at 540 ft/min. Prevailing wind direction, at 50 ft AGL, was northeasterly and averaged 2.5 knots during the 45-minute period before seeding began.

Operation

Ten seeding passes were made, just above stratus top, from 0613 to 0643 PDT. The dogbone pattern was offset to permit repeated treatment of the same volume as it drifted toward the airport. After Test FA(5) the nozzles were cleaned, resulting in more than a doubling of the flow rate; therefore 320 gallons of charged water were dispensed over the 1.6 nmi seed leg of the pattern. Positive charge to the port boom was 13 kV and negative charge to the starboard boom was 16 kV. A light drizzle began at the airport shortly after seeding began. It is possible that the treatment triggered the precipitation from the thick stratus which was possibly conditionally unstable colloidally.

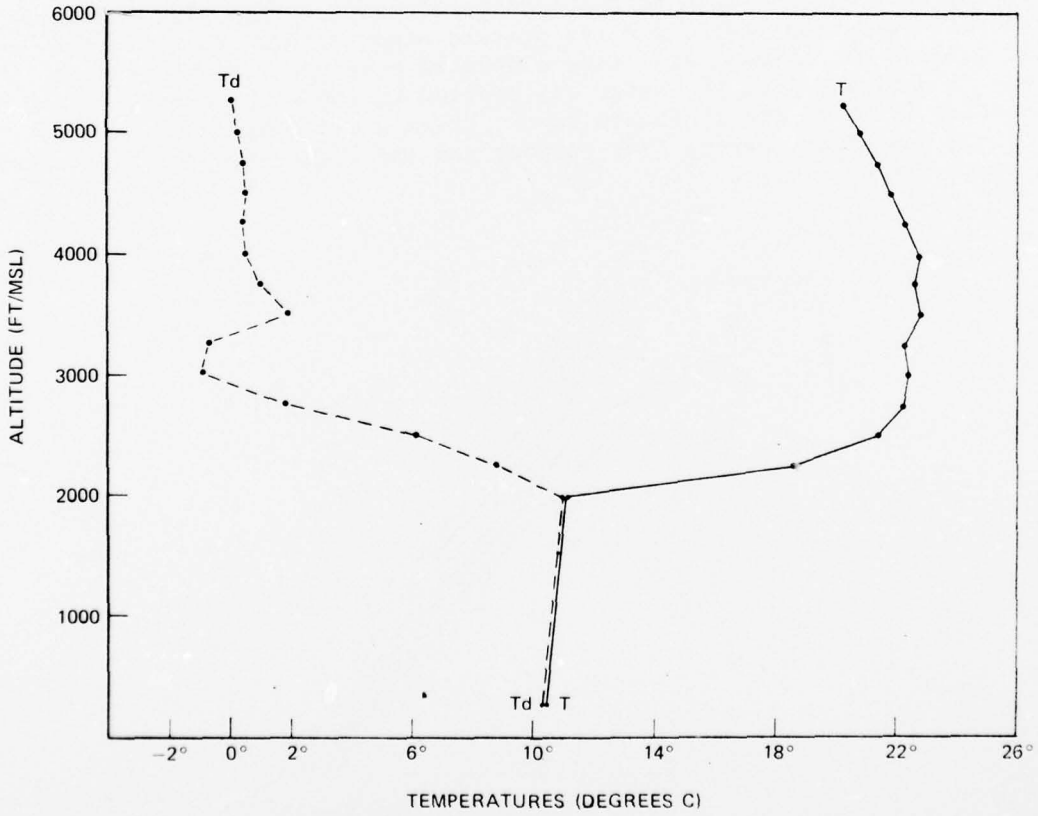

FIGURE A-4. Temperature/Dewpoint Profile Taken Just Before Seeding Time on Test FA (6).

TEST VI-FA(7) 0705-0855 PDT - 11 September 1973

Conditions

Test FA(6) may have affected the conditions existing prior to the start of this test. Stratus top, which had lowered to 1700 ft MSL during Test FA(6), was again 1,900 ft MSL when seeding began on this test. Average LWC was .48 g/m^3 at 0701 PDT. Light drizzle, which began at 0615 PDT, continued throughout the test period. The preseed wind vector, of the layer from surface to stratus top, was 150 degrees at 512 ft/min. Prevailing wind at 50 ft AGL was northeasterly at 1.5 knots during the 45-minute period before seeding.

Operation

Eight seeding passes were made at stratus top from 0731 to 0751 PDT. Figure A-5 is an accurate reproduction of a part of the radar plot showing the pattern flown by the seeding aircraft. This plot indicates accurate targeting based upon the preseed wind vector. Approximately 240 gallons of charged water were dispensed over the 1.6 nmi seeding leg. A positive 12-13kV charge was applied to the port spray boom and a negative 16 kV to the starboard boom. Drizzle was continuous before, during, and after seeding. The stratus was apparently too thick to clear a swath through it.

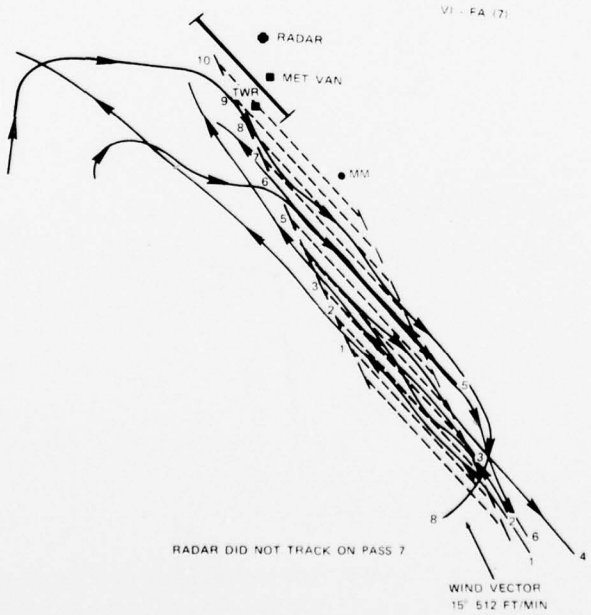

FIGURE A-5. Seeder Aircraft Pattern Flown During Test FA (7).

TEST VI-FA(8) 0520-0650 PDT - 12 September 1973

Conditions

The 1,200 ft thick stratus deck seeded during this test had been in the area 28 hours. Just before seeding began, bases were at 600 ft MSL and tops at 1,800 ft MSL. Average LWC content data showed an increasing trend, from .6 to .69 g/m^3, prior to seeding. The preseed wind vector of the layer from surface to stratus top was 341 degrees at 284 ft/min. Prevailing wind, at 50 ft AGL, was northwesterly and averaged 1.5 knots during the 45-minute period prior to seeding. Figure A-6, a temperature/dewpoint profile taken at 0559 PDT, shows the nearby isothermal stratus layer.

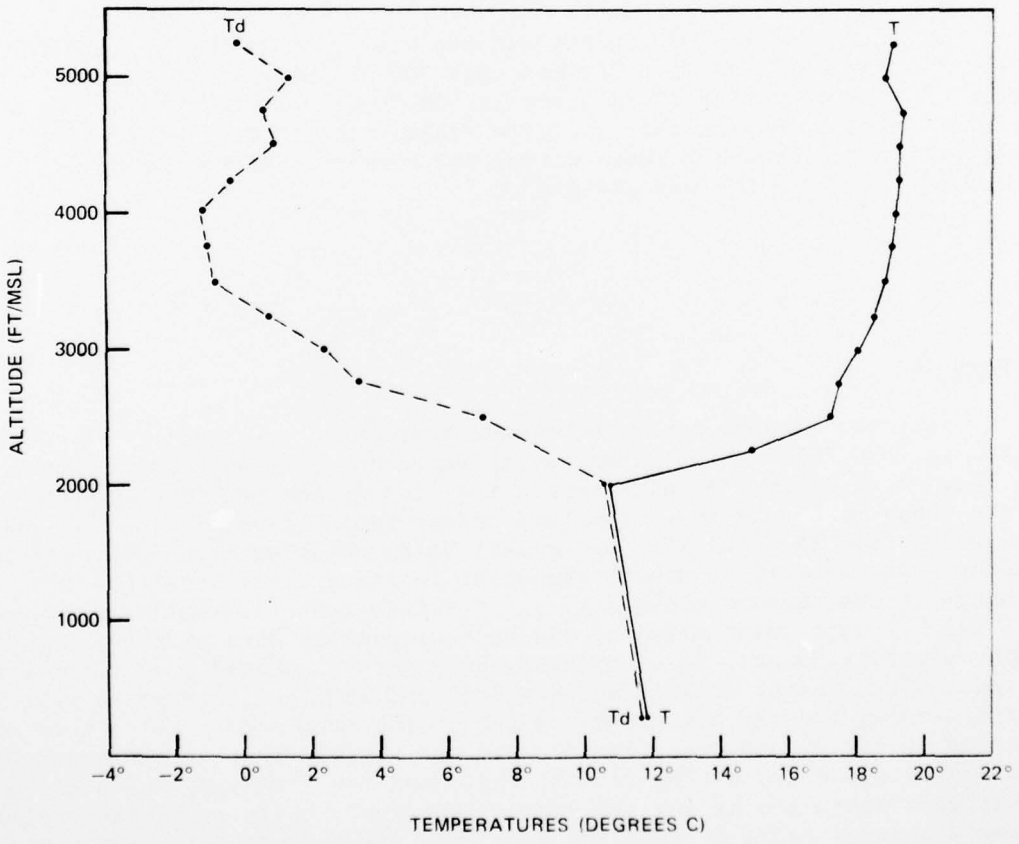

FIGURE A-6. Temperature/Dewpoint Profile Taken Just Before Seeding Time on Test FA (8).

Operation

Ten seeding passes were made above the stratus top from 0608 to 0635 PDT. As in Test FA(7), the offset dogbone pattern was used. Approximately 320 gallons of charged water were dispensed over the 1.6 nmi seeding leg. Only 6 to 10 kV positive charge could be applied to the port boom, but a negative 13 to 14 kV was applied to the starboard boom. Arcing of the charging system made it necessary to fly approximately 100 ft above the stratus top causing evaporation of much of the spray in the warm, dry air of the inversion.

TEST VI-FA(9) 1340-1635 PDT - 12 September 1973

Conditions

Stratus base was 500 ft MSL and top was 1,500 ft MSL at 1400 PDT. when seeding began at 1452 PDT base was 700 ft MSL and top was 1,200 ft MSL. A wind vector of 296 degrees at 928 ft/min was used to set up the offset dogbone seeding pattern. Prevailing wind at 50 ft AGL was westerly and averaged 7 knots during the 45-minute period prior to seeding. Average LWC was .24 g/m^3.

Operation

Thirteen seeding passes were made just above the stratus top, from 1452 to 1533 PDT. A ten-minute delay encountered between passes 5 and 6 because of commercial air traffic resulted in the modified dogbone pattern shown in Figure A-7. Positive charge ranged from 17 to 19 kV and negative from 15 to 21 kV. After Test FA(8) the discharge points on the spray booms were filed smooth resulting in the greater magnitude of charge to the booms without arcing. For this test the smaller nozzles (1 gal/hr) were reinstalled providing a dispensing rate of about 5 gal/min. Approximately 50 gallons of charged water were dispensed over the 1.6 nmi seeding leg. Light drizzle between 1505 and 1605 PDT correlated well with seeding and may have been induced by the treatment. Holes were observed in the seeded swath and the sun was visible through the swath. The solar radiation trace (Figure A-8) indicated two peaks, during seeding, that were unequaled at any other time that day. Solar radiation varied over a greater range between the time from first seed pass until 5 minutes after last seed pass than during the three hour periods before or after seeding.

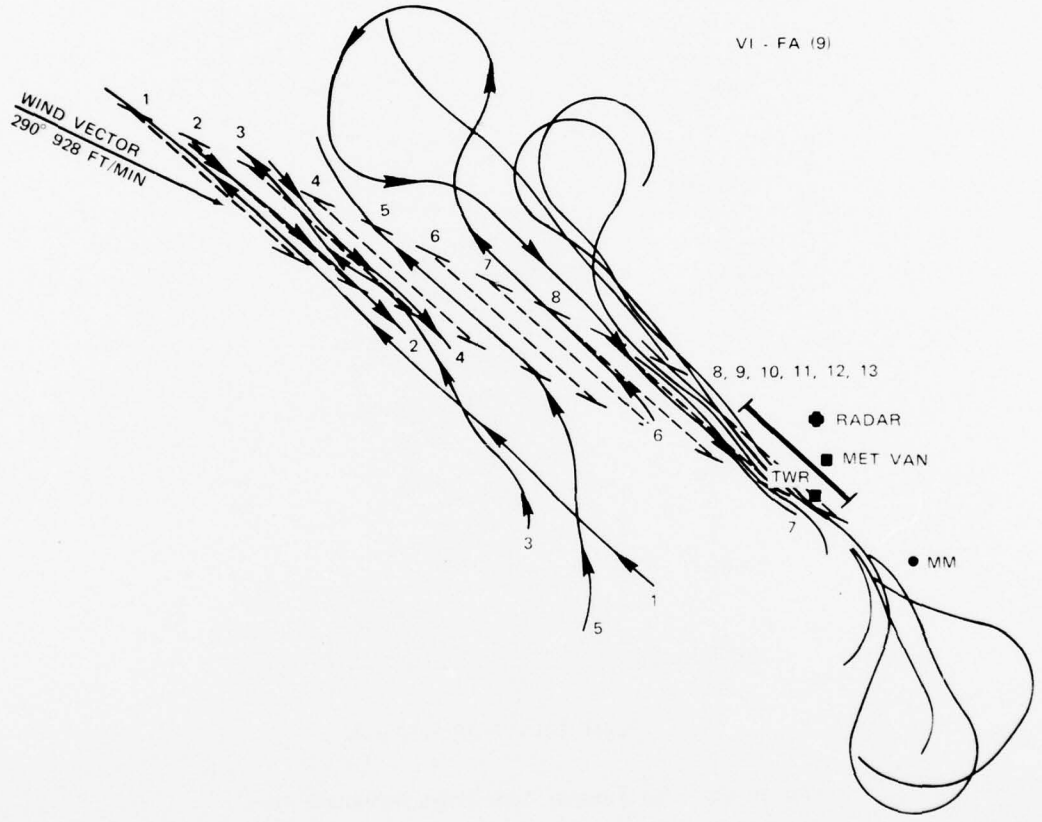

FIGURE A-7. Modified Dogbone Pattern Flown by Seeder Aircraft During Test FA (9).

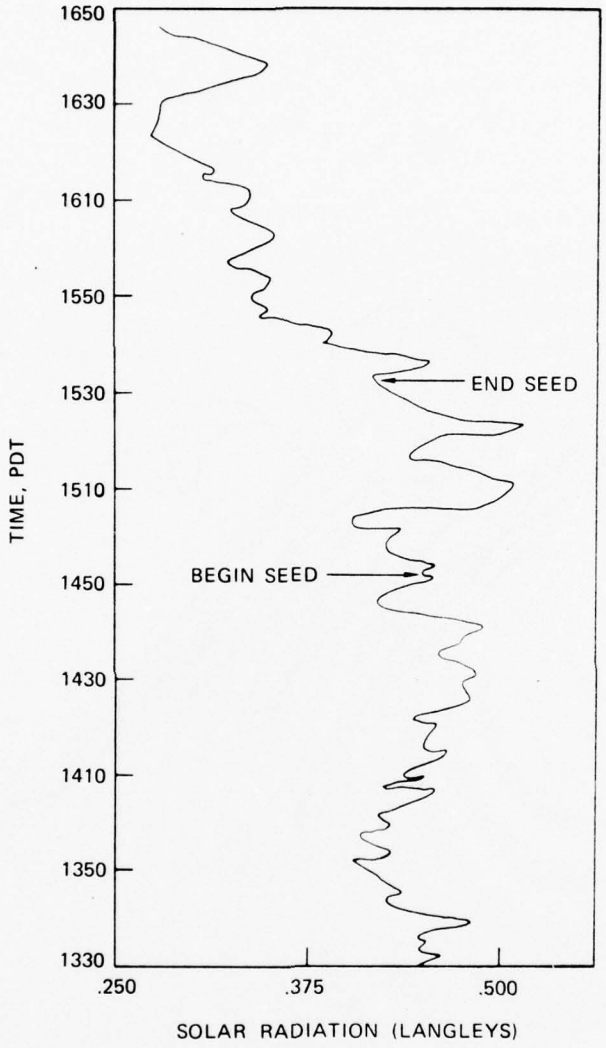

FIGURE A-8. Solar Radiation Trace Before, During, and After Test FA (9).

TEST VI-FA(10) 0540-0715 PDT - 15 September 1973

Conditions

Fog onset occurred at 1600 PDT on 14 September and restricted visibility until 1630 PDT on 15 September. Just prior to seeding, fog top was 1,400 ft MSL and average LWC was .19 g/m^3. From midnight until start of seeding, surface air temperature was 51 to 52°F and relative humidity

was steady at 100%. A wind vector through the fog layer taken at 0612 PDT was calm. Prevailing wind at 50 ft AGL was southwesterly and averaged .9 knot during the 30-minute period before seeding. Visibility ranged from .18 to .36 nmi and averaged .24 nmi during the same period. Light drizzle began falling at 0617 PDT.

Operation

Ten seeding passes were made at fog top (1,400 to 1,200 ft MSL) over the runway from 0625 to 0651 PDT. Charge to the spray booms ranged from 18 to 21 kV. A total of 40 gallons of water were dispensed over the 1.6 nmi seeding leg using the dogbone pattern (Figure A-9). A wind vector of the fog layer taken at 0701 PDT confirmed the persistence of calm air. Average LWC increased to .23 g/m^3 by 0655 PDT. Visibility increased substantially after Pass 5 and continued to increase for 20 minutes after seeding ended (Figure A-10).

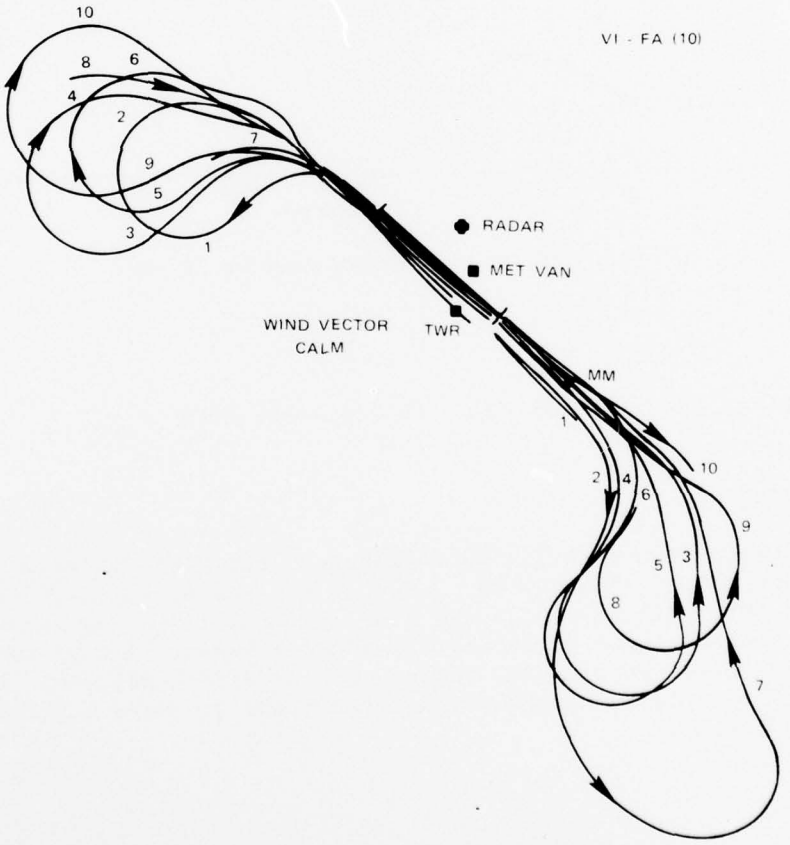

FIGURE A-9. Seeder Aircraft Pattern Flown During Test FA (10).

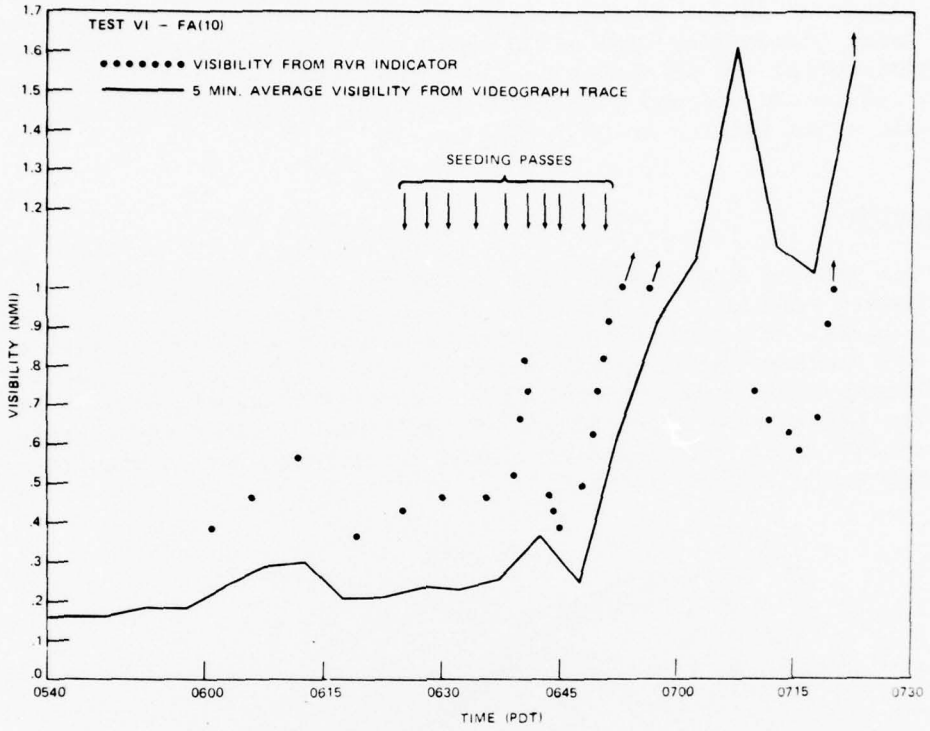

FIGURE A-10. Visibility During Test FA (10).

TEST VI-FA(11) 0715-0905 PDT - 15 September 1973

Conditions

Effects from Test FA(10) influenced conditions existing just before this test began. Fog top was 1,200 ft MSL and average LWC was .21 g/m^3 at 0718 PDT. Visibility ranged from .36 to 2.1 nmi and averaged 1.1 nmi during the 30-minute period before seeding began. A wind vector of the fog layer taken at 0701 PDT indicated a no-wind condition. Prevailing wind at 50 ft AGL was east-southeasterly and averaged 1.5 knots from 0645 to 0730 PDT.

Operation

Seeding began at 0720 PDT, but was interrupted for commercial air traffic after the fourth pass at 0729 PDT. Treatment resumed at 0740 PDT and 10 more passes were made by 0805 PDT. Passes were made just above

fog top and directly over the runway using the dogbone pattern. Fifty-five gallons of charged water were dispensed over the 1.6 nmi seeding leg. Charge to the spray booms ranged from 19 to 21 kV. Prevailing wind at 20 and 50 ft AGL was southeasterly and averaged 2.5 knots during the seeding period (Table A-5). The wind vector of the fog layer, taken at 0813 PDT, was 147 degrees at 370 ft/min. Therefore, any effect of the treatment was carried away from the instrument observation site. Figure A-11 shows that visibility decreased after the fourth pass. Average LWC increased to .34 g/m^3 by 0811 PDT.

TABLE A-5. Increasing Wind Speeds During Test FA(11).

TIME	20 Ft. AGL		50 Ft. AGL	
	Prevailing Direction	Avg. Speed	Prevailing Direction	Avg. Speed
PDT	Degrees	Knots	Degrees	Knots
0645-0700	170	.9	150	1.3
0700-0715	110	.1	100	.4
0715-0730	105	2.2*	095	2.6
0730-0745	110	2.2	105	2.4
0745-0800	*135*	*2.2*	*130*	2.8
0800-0815	195	1.7	190	2.4
0815-0830	210	2.4	210	2.8
0830-0845	220	2.4	220	2.6
0845-0900	200	1.3	195	2.2

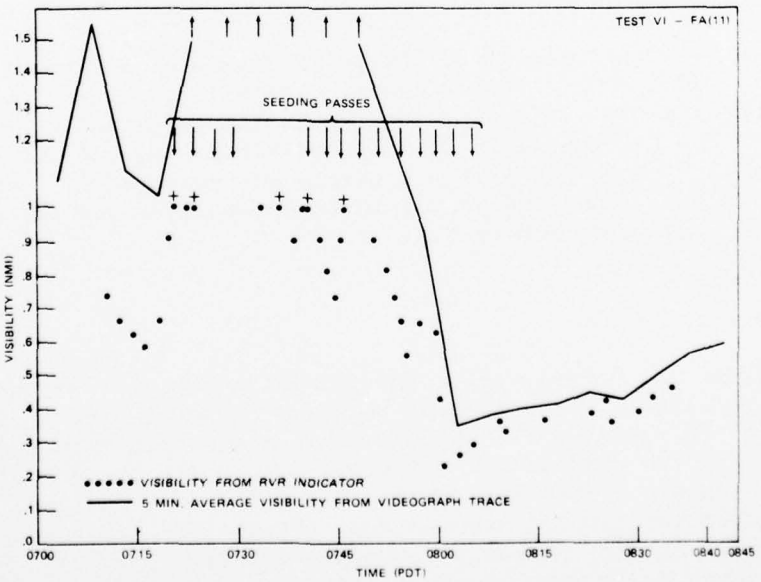

FIGURE A-11. Visibility During Test FA (11).

TEST VI-FA(12) 0900-1100 PDT - 25 September 1973

Conditions

Fog onset occurred at 0330 PDT on 25 September. Visibility was greater than 1 nmi until 0650 PDT and then was 1 nmi or less until 1100 PDT, by which time a natural breakup was well under way. Seeding was delayed because of problems with the dispensing system. By the time seeding could begin the fog over the airport had begun dissipating so a fog bank over the ocean and west of the airport was selected as the target. Fog top was irregular and varied from 600 to 810 ft MSL.

Operation

Ten seeding passes were made from 0945 to 1021 PDT using a racetrack pattern. The 1.6 nmi seeding leg of the pattern was positioned several miles offshore and parallel to the coastline. Seeding altitude ranged from 800 to 400 ft MSL, resulting in the dispensing of charged water in the fog part of the time. Charge to the spray booms ranged from 18 to 20 kV. Dissipating fog conditions made this test inconclusive.

TEST VI-FA(13) 0620-0815 PDT - 29 September 1973

Conditions

Fog onset occurred at 1400 PDT on 28 September and restricted visibility until 1300 PDT on 30 September. Visibility ranged from .27 to .52 nmi and averaged .35 nmi during the 30-minute period before seeding. At 0640 PDT fog top was 1,050 ft MSL and average LWC was .25 g/m^3. Prevailing wind at 50 ft AGL was easterly and averaged 1.3 knots from 0620 to 0650 PDT. The wind vector for the fog layer was taken at 0640 PDT and was 090 degrees at 258 ft/min.

Operations

A solution of 75% glycerine and 25% water was the charged seeding agent for this test. Nine seeding passes were made, just above fog top, parallel to the runway. The dogbone pattern was offset to the east to compensate for the wind vector (Figure A-12). With the 8 gal/hr nozzles reinstalled in the dispensing system, 200 gallons of charged solution were delivered over the 1.6 nmi seeding leg. Visibility increased slightly just after two seeding passes were completed (Figure A-13). Effects were not as apparent as in most of the tests using charged water as the seeding agent.

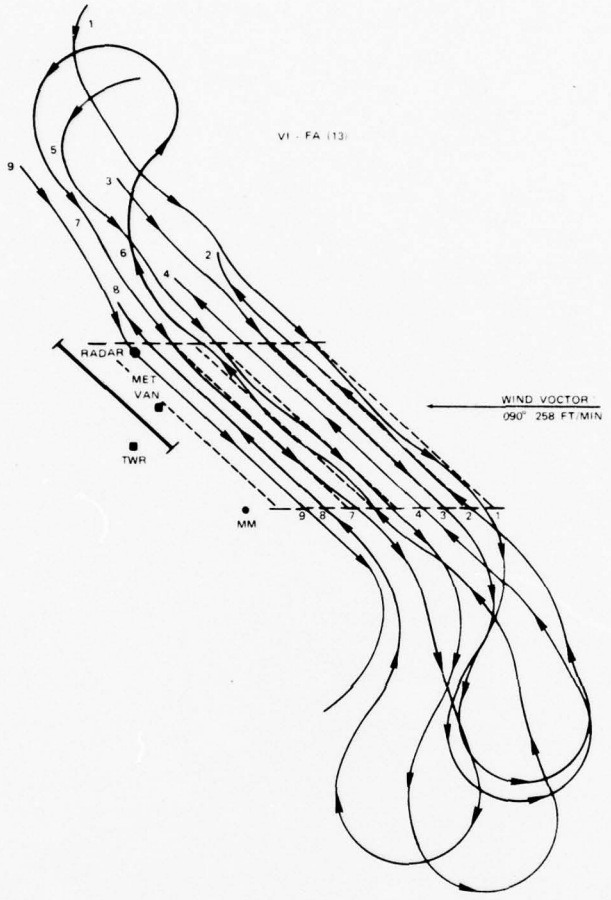

FIGURE A-12. Seeder Aircraft Pattern Flown During Test FA (13).

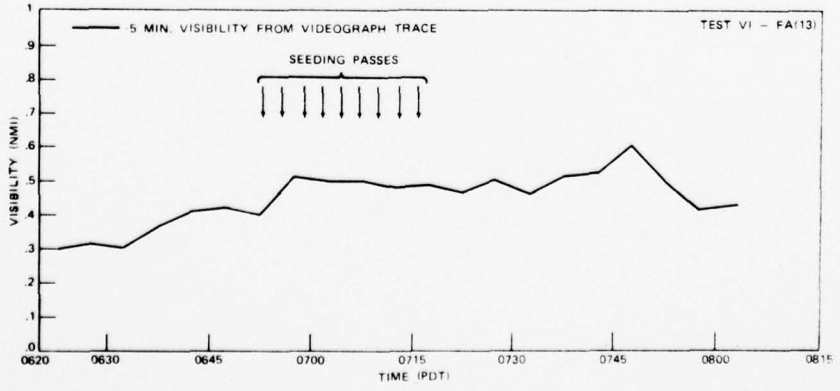

FIGURE A-13. Visibility During Test FA (13).

Appendix B

CLOUD CONDENSATION NUCLEI AT THE ARCATA-EUREKA AIRPORT

INTRODUCTION

Cloud condensation nuclei and the chemical composition of aerosols in the vicinity of the Arcata-Eureka airport were measured during September 1973. The work was carried out in connection with a program of warm fog clearing experiments conducted by the Naval Weapons Center to evaluate the possible effects of nuclei concentration on the formation and stability of fog and to see what effect this might have on the success or failure of attempts to clear the fog. Nuclei in the Arcata area arise from the sea, from forest fires, from a number of industrial operations such as sawdust burning and lumbering, and from wind-blown dust and similar sources.

The cloud condensation nuclei (CCN) were counted at a supersaturation with respect to liquid water of 0.23%, using a MEE Industries CCN counter, Model No. 310. This value (0.23%) was chosen on the basis of work by Mason,[18] that indicates a close correlation between concentrations of cloud droplets and of CCN that can be activated at supersaturations of a few tenths of one percent. The instrument was operated continuously from 11 September to 19 September. During this period, the fog and stratus regime transitioned into that of winter storms, permitting observations during relatively stable air and during periods of instability.

A four-stage, rotating drum, cascade impactor, capable of segregating particles by size (Lundgren Impactor, Model 4220), was used to capture samples of the atmospheric aerosol. The impactor was operated from 0645 PDT on 15 September to 0245 PDT on 16 September 1973. Both instruments were operated at a remote location away from the airport.

MEASUREMENTS OF CCN BY THE MEE COUNTER

In Figures B-1 through B-6, CCN are plotted versus time. Wind direction greater than 90° are indicated by the symbol .

The CCN counter was put in continuous operation at 2000 PDT on September 11, using a supersaturation of 0.23 (Figure B-1). At 2030 PDT a check was made of nuclei counts at lower and higher supersaturations. About 160, 400, and 1,800 nuclei/cc were observed at supersaturations of 0.1, 0.23 and 3.1 percent, respectively. Counts at the lower supersaturation are approximately half way between those for

---

[18] B. J. Mason. *The Physics of Clouds*. Oxford, England, Clarendon Press, 1971. P. 86.

PRECEDING PAGE BLANK-NOT FILMED

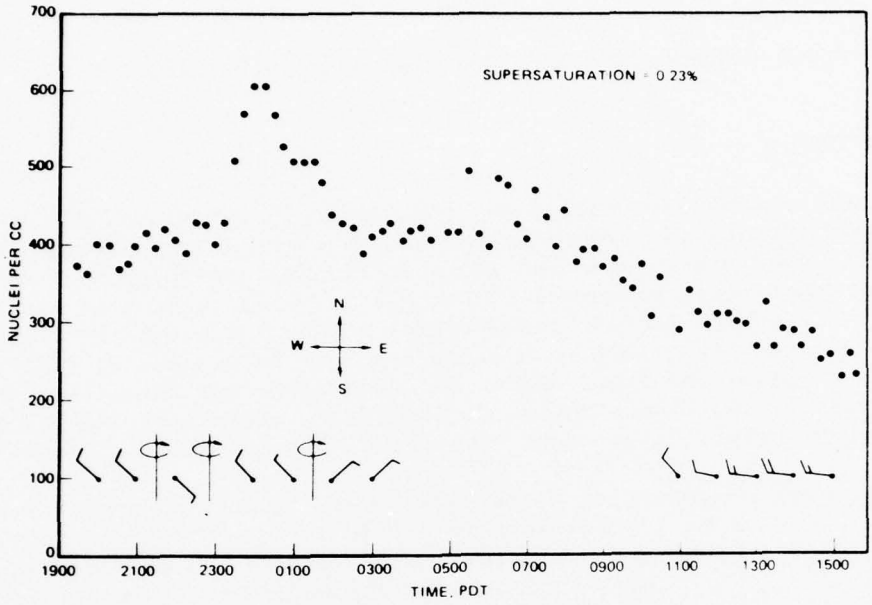

FIGURE B-1. Cloud Condensation Nucleus Counts September 11th to 12th, 1973.

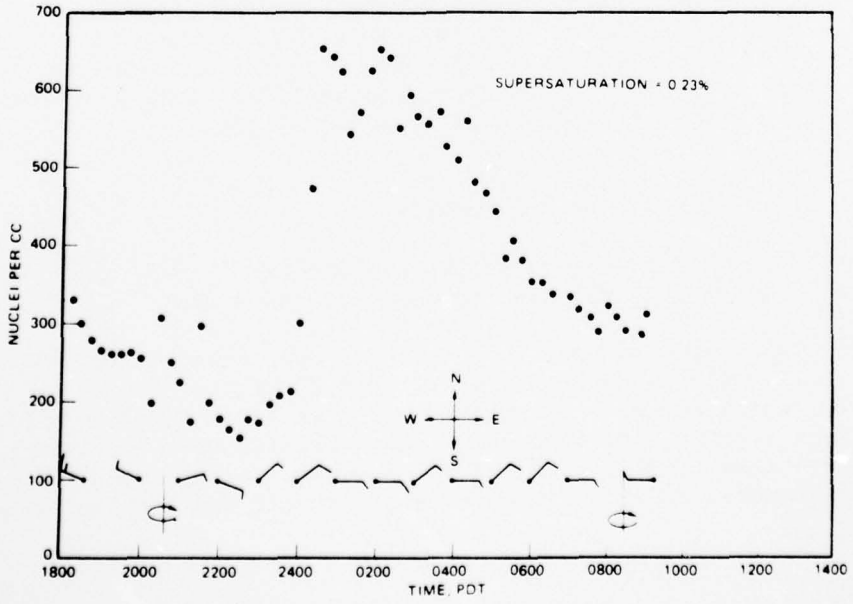

FIGURE B-2. Cloud Condensation Nucleus Counts September 13th to 14th, 1973.

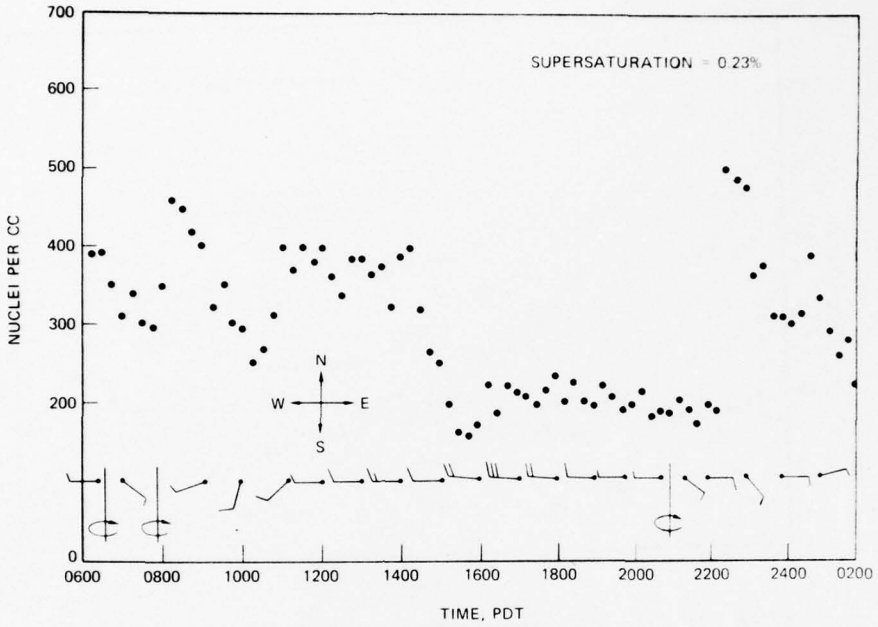

FIGURE B-3. Cloud Condensation Nucleus Counts Beginning 0600 September 15, 1973.

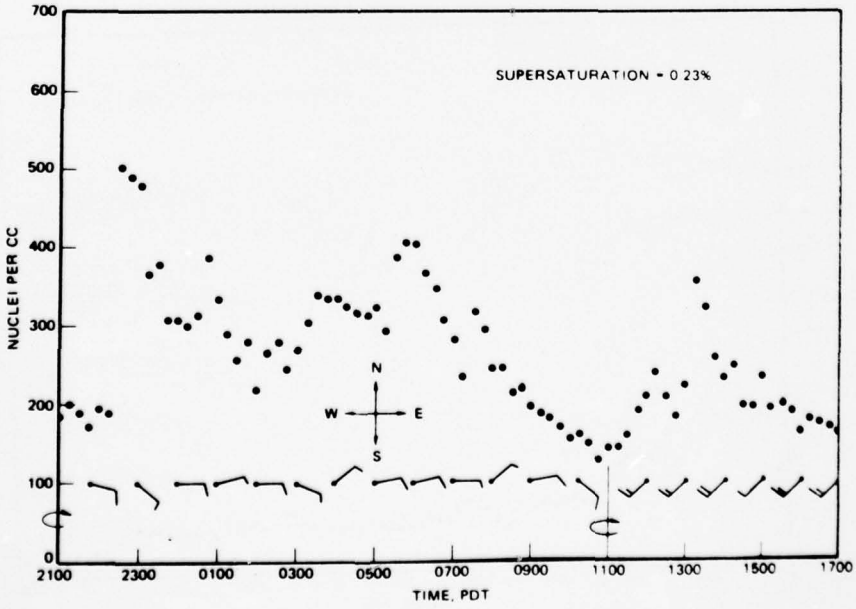

FIGURE B-4. Cloud Condensation Nucleus Counts September 15th to 16th, 1973.

AD-A040 980 NAVAL WEAPONS CENTER CHINA LAKE CALIF F/G 4/2
PROJECT FOGGY CLOUD VI: DESIGN AND EVALUATION OF WARM-FOG DISPE--ETC(U)
MAY 77 R F REINKING, R S CLARK, W G FINNEGAN

UNCLASSIFIED NWC-TP-5824 NL

2 OF 2
AD A040980

END

DATE FILMED
7-77

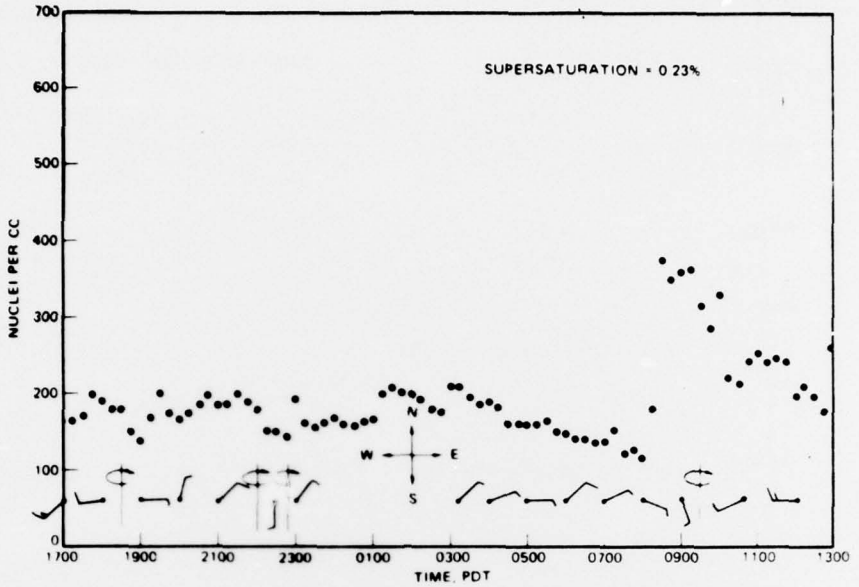

FIGURE B-5. Cloud Condensation Nucleus Counts September 16th to 17th, 1973.

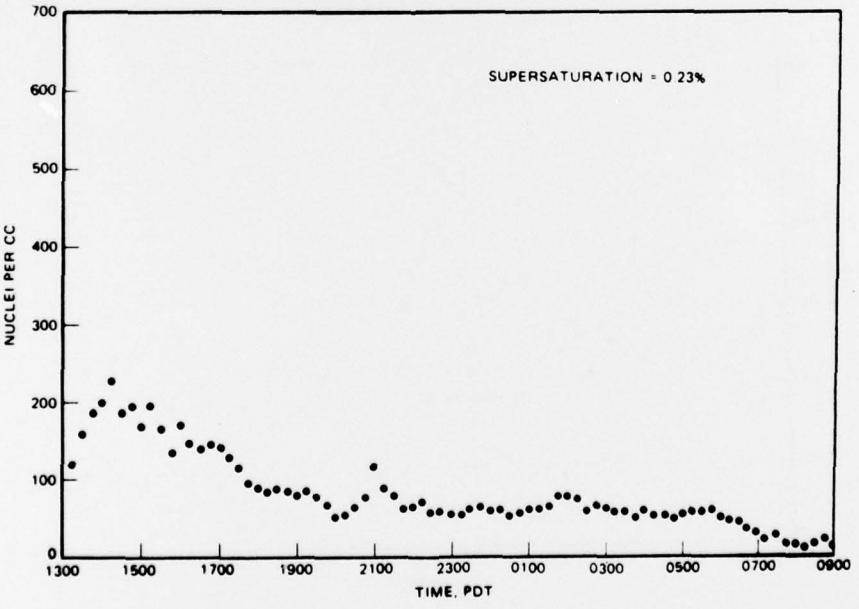

FIGURE B-6. Cloud Condensation Nucleus Counts September 17th to 18th, 1973.

maritime and continental air as found by Twomey[19] while counts at the high supersaturation are about the same as those found by Twomey for continental air. One would think that with a northwest wind (off the ocean), counts would be more in line with those found by Twomey for maritime air. Apparently, smoke from forest fires to the south had circulated around to the north, over the ocean, and mixed with the marine air.

At about 2130 PDT, the northwest wind shifted to a light southeasterly flow until about 2300 PDT, whereupon it switched back to the northwest at 5 to 10 knots. Near midnight, the CCN count abruptly increased from about 400 to 600 per cc. Apparently, smoke from the Arcata area had circulated out to sea and had come into our site with the northwest wind. The CCN count dropped rapidly as the northwesterly flow set in, and leveled off to around 400 per cc at about 0300 PDT on September 12.

Winds became light and variable, mostly varying between northeast and northwest, from 0300 to 1000 PDT. Stratus, with bases at 600 ft MSL and tops at 1,800 ft MSL, were treated from above with electrically-charged water droplets between 0600 and 0700 PDT with no apparent success. During this period of treatment, CCN counts varied from about 400 to 500/cc at ground level. As the day progressed, the counts slowly decreased, and the westerly wind increased after 1100 PDT. At about 1450 PDT, another stratus dissipation test with electrically-charged water droplets was conducted and the sun broke through the stratus momentarily after treatment. The CCN count during this treatment was only 250/cc at ground level. Recorder malfunction at about 1600 PDT temporarily halted data collection; however, counts had decreased to 200/cc. Stratus remained throughout the afternoon and evening.

Cloud condensation nuclei were not recorded continuously until after 1800 PDT on September 13 (see Figure B-2). Previously, the sky had cleared of stratus at about 1230 PDT, and between 1315 and 1330 PDT, periodic readings were taken and CCN counts averaged about 200/cc. Cloud condensation nuclei counts, Figure B-2, were about 300/cc at 1800 PDT and slowly decreased to below 200/cc until about 2400 PDT, whereupon they suddenly increased to about 650/cc at 0030 PDT, September 14. This increase was probably due to the change in air flow from westerly to easterly at about 2040 PDT. This CCN count was the highest observed during the entire period of monitoring. Possibly it was due to smoke from Arcata, held under an inversion layer. A strong inversion existed at the time; the temperature at 20 feet was 5°F colder than the temperature at 50 feet from 2045 PDT September 13 to 0815 PDT September 14. The air aloft was dry; at the 50 ft level the difference between the temperature and the dew point ranged from 3 to 5°F, while at the 20 ft-level the difference ranged from 2 to 4°. No fog formed. The CCN

---

[19]S. Twomey. "The Supersaturation in Natural Clouds and the Variation of Cloud Droplet Concentration," *Geofis. Pura. Appl.*, Vol. 43 (1959), p. 243.

count fell steadily after 0200 PDT to about 300/cc at 0900 PDT, at which time recorder failure again precluded data collection.

Continuous monitoring of CCN began again on September 15 at 0600 PDT, when the CCN count was 400/cc (Figure B-3). A seeding test was conducted from 0625 to 0650 PDT and the CCN count decreased from 390 to 310/cc. As recorded by the visiblity measuring device (Videograph, Model B), a sharp increase from 0.25 to 1.6 miles in visibility occurred from 0647 to 0707 PDT. Maximum visibility of 3.25 miles occurred at 0728 PDT, at which time the CCN count reached a minimum of about 300/cc. At 0720 PDT, another seeding test was initiated which lasted until 0805 PDT. However, visibility decreased from 2 to 0.35 miles during the period 0745 to 0810 PDT. During the same time period, the CCN increased from 295 to 460/cc. The wind had shifted from light westerly to light southeasterly at 0640 PDT and then back to westsouthwesterly at about 0755 PDT. Apparently, a parcel of CCN-contaminated air had come into the test area with the southeasterly wind and this possibly contributed to the failure of the second test.

The CCN count dropped from 460 to 250/cc during the period 0815 to 1015 PDT with an onshore wind from the westsouthwest, and at 1000 PDT, the wind shifted to a southwesterly direction, whereupon the CCN increased from 250 to 400cc. Fog conditions remained with a 300-ft ceiling and one-mile visibility, or less until 1230 PDT. The CCN remained fairly constant at about 360 to 400/cc until 1400 PDT when the stratus cleared. The wind had increased to 15 knots from the west by 1400 PDT. The CCN count dropped to a low of 155/cc at 1545 PDT and averaged about 200/cc from 1600 to 2215 PDT. A wind shift from westerly to southeasterly occurred at 2100 PDT, and later, the CCN increased sharply to 500/cc at 2230 PDT.

Fog with a ceiling of 300 ft, and one mile or less visibility formed at 2115 PDT and persisted until 0430 PDT on September 16. The CCN counts fell from a high of 500/cc at 2230 PDT to a low of 220/cc at 0200 PDT (Figure B-4) on September 16. A small increase to 340 nuclei/cc occurred shortly after 0300 PDT and then increased to 410 nuclei/cc shortly before 0600 PDT. The wind remained light from a generally easterly direction from 2100 PDT September 15 to 1100 PDT September 16.

From 0600 to 1045 PDT on September 16, CCN gradually decreased to 130/cc. After 0900 PDT, the stratus dissipated and the weather became clear and sunny. A gradual wind shift to a southwesterly direction began prior to 1100 PDT. The CCN count increased after 1100 PDT to a maximum of 360/cc at 1315 PDT. This peak in CCN count corresponded to an abrupt decrease in visibility from 10 to 0.5 miles. After 1315 PDT, CCN decreased to about 160/cc at 1700 PDT and varied from 150 to 200/cc until 0500 PDT on September 17 (Figure B-5). Winds during this period were light and variable, mostly easterly to northeasterly.

On the morning of September 17, a strong temperature inversion existed from 0300 to 0800 PDT (i.e., the 20-ft level was from 2 to 6°F colder than the 50-ft level. Cloud condensation nuclei count had decreased to about 120/cc at 0800 PDT. After 0800 PDT the wind switched from northeasterly to a southerly direction, and the CCN count abruptly increased to 375/cc. Much smoke or haze had been noted previously to the southeast of the test area. At 0810 PDT, with a clear sky at the observing site, fog tended to come up to the other side of the air strip from the ocean and dissipate. The wind switched to the west at 0925 PDT. It may be asked whether the fog was unstable due to the low number of CCN which had drifted to sea during the night and morning hours, or whether it dissipated due to other meteorological conditions.

After 0900 PDT, the CCN decreased, with some variations at 1300 PDT which may have been due to aircraft traffic, to below 100/cc after 1730 PDT (Figure B-6). Prefrontal fog came in from the west at 1445 PDT and lasted until 1505 PDT, after which increasing cloudiness occurred. Rain fell for less than an hour after 1856 PDT. Unfortunately, no wind records exist after 1300 PDT because of malfunction of the recording equipment. The CCN count generally varied from 50 to 80/cc throughout the evening and morning hours until 0600 PDT on September 18. Precipitation began at 0530 PDT as drizzle, developed into rain by 0700 PDT and ended at about 0730 PDT. Cloud condensation nuceli counts after 0700 PDT decreased to between 0 and 30/cc during the precipitation period. Relative humidity became so high that the dry and wet bulb temperatures of an electronic psychrometer (MEE Industries, Inc., Model No. 501) were the same; yet ground fog did not form. It is possible that supersaturated conditions existed for a time, but lack of CCN prevented formation of fog.

Low CCN counts (0-30 nuclei/cc) existed during rain, throughout September 18th and 19th. In fact, at a supersaturation of 3%, only 25 to 60/cc were found during these two days. Apparently, the precipitation had scavenged much of the CCN from the atmosphere.

MEASUREMENT OF TRACE ELEMENTS

The Lundgren impactor was set at an airflow rate (4 cfm) so that aerosol particles as small as 0.15 μm radius were captured. The various size ranges of particles, captured on paraffin coated Mylar film on the revolving drums, are shown in Table B-1. The films were sent to the University of California at Davis, where trace elements were determined by cyclotron activation analysis. A summary of the analysis of various elements is shown (Table B-1) for five consecutive time periods, expressed as nanograms of the element per cubic meter of air.

In Table B-2, the mole ratios, Na/K, Na/Si, Cl/Na and S/Cl, are shown for the various time intervals. All the captured particles above 0.15 μm are included in these ratios. For comparison, the mole ratios

TABLE B-1. Trace Element Analysis of Aerosol Collected by the Lundgren Impactor on September 15th to 16th.

Amounts of the elements are shown in units of nanograms per cubic meter of air.

Time, PDT	Particle Radius >5 μm	1.5 to 5 μm	0.5 to 1.5 μm	0.15 to 0.5 μm
Sodium				
0645-1045	171	245	273	77
1045-1445	229	436	552	232
1445-1845	91	570	548	159
1845-2245	330	665	323	120
2245-0245	51	86	*	90
Magnesium				
0645-1045	134	35	95	96
1045-1445	92	125	150	28
1445-1845	68	133	118	44
1845-2245	62	88	77	58
2245-0245	19	*	120	*
Chlorine				
0645-1045	869	602	437	165
1045-1445	741	1113	*	*
1445-1845	452	1821	767	*
1845-2245	1236	1848	554	*
2245-0245	*	*	*	*
Potassium				
0645-1045	43	59	31	59
1045-1445	40	93	96	106
1445-1845	10	60	56	*
1845-2245	43	67	*	24
2245-0245	24	13	*	52
Calcium				
0645-1045	63	44	40	*
1045-1445	141	207	147	36
1445-1845	36	93	66	*
1845-2245	83	91	27	15
2245-0245	*	*	39	17
Iron				
0645-1045	60	63	28	40
1045-1445	57	107	61	14
1445-1845	17	73	29	20
1845-2245	62	78	37	21
2245-0245	69	51	33	18
Sulfur				
0645-1045	*	*	185	286
1045-1445	68	221	975	1788
1445-1845	*	110	183	785
1845-2245	97	119	93	655
2245-0245	34	24	111	685
Silicon				
0645-1045	96	67	41	46
1045-1445	106	159	124	*
1445-1845	63	82	85	35
1845-2245	106	149	45	42
2245-0245	136	112	111	52

Only a trace of manganese and bromine (i.e., 12 and 24 nanograms per cubic meter of air, respectively) were found at 2245 to 0245 PDT with radii of 1.5 to 5 μm and 0.15 to 0.5 μm, respectively.

*Not detectable

for the Eastern Pacific and Scott's Bluff, Arizona, as found near sea level by Delany and others,[20] are also shown in Table B-2.

TABLE B-2. Mole Ratios of Important Elements for Particle Radii Larger than 0.15 μm.

Location, Material, or Time, PDT	Na/K	Na/Si	Cl/Na	S/Cl
0645-1045	6.8	3.7	1.8	0.2
1045-1445	7.4	4.5	0.8	1.9
1445-1845	18.6	6.3	1.4	0.4
1845-2245	18.3	5.1	1.6	0.3
2245-0245	4.5	0.7	0	---
Eastern Pacific*	23.8	0.7	1.0	---
Scotts Bluff*	0.7	0.04	0.6	---
Seawater†	47.4	---	1.2	0.055
Continental Soil†	0.85	0.02	0.013	---
Sedimentary Rock (clays and shales)	0.5	0.04	0.013	---

*Mole ratios found by Delany *et al.* (1973) near sea level.
†Mole ratios as shown by Delany *et al.* (1973) and Junge (1963).

Junge,[21] found that the S/Cl ratio is higher for the air of coastal areas than for sea water. This fact is true for the air at Arcata (Table B-2). If this ratio exceeds a value of about 0.5, man-made aerosols are usually thought to be present. Table B-1 also shows that the S/Cl mole ratio at Arcata decreased with increasing particle size, an observation also made by Junge.

The Na/K ratio is a very good indicator of the origin of the aerosol. Delany and others[20] found that over a continental site this ratio was nearly the same as in the continental soil, and in sedimentary rock, while a high Na/K ratio which approached that of sea water was found in the marine air over the ocean (Table B-2). As indicated by Delany and others, the Na/Si ratio shows many of the features of the Na/K ratio, but it does not identify the marine air as well as the Na/K ratio. Our ratios indicate smaller amounts of silicon than found by Delany and others over the ocean.

---

[20]A.C. Delany and others. "Tropospheric Aerosol: The Relative Contribution of Marine and Continental Components, *J. Geophys. Res.*, Vol. 78 (1973), pp. 6249-6265.

[21]C. E. Junge. "Recent Investigations in Air Chemistry," *Tellus*, Vol. 8 (1956), pp. 127-139.

The Cl/Na ratio as discussed by Delany and others can vary below and above the same ratio for sea water. In fact, Miyak, who analyzed fog precipitation in Japan, found that Cl/Na ratios show chlorine depletion in sea fogs and chlorine enrichment in high-altitude mountain fogs[22]. The ratios were 1.18 and 3.25, respectively. Also, the Cl/Na ratios given by Delany and others at altitudes above 5 km over continental areas show an excess of chlorine when compared to the same ratio for sea water.

Table B-3 shows chlorine- and sulfur-containing particle concentrations. These concentrations were calculated assuming the smallest particle in each size range and assuming the dry forms of sodium chloride and ammonium sulfate. In reality, sodium chloride and ammonium sulfate may exist as solution droplets at sufficient humidities. For example, a solution droplet of sodium chloride at 95% relative humidity is about two times larger in radius than when it is at low relative humidities.

TABLE B-3. Particle Concentrations (Based on the Smallest Particle Radius in Each Range) of Chlorine and Sulfur Assumed as Dry Sodium Chloride and Ammonium Sulfate.

Values given are number of particles per cubic centimeter.

Time, PDT	Particle Radius				
	5μm	1.5 μm	0.5 μm	0.15 μm	⩾0.15 μm
			Sodium Chloride		
0645-1045	0.0013	0.034	0.67	9.3	10.2
1045-1445	0.0011	0.063	*	*	0.06
1445-1845	0.0007	0.103	1.18	*	1.28
1845-2245	0.0019	0.104	0.85	*	0.96
2245-0245	*	*	*	*	*
			Ammonium Sulfate		
0645-1045	*	*	0.86	49.3	50
1045-1445	0.0003	0.038	4.5	308	313
1445-1845	*	0.019	0.85	135	136
1845-2245	0.0005	0.020	0.43	113	113
2245-0245	0.0002	0.004	0.52	118	119

*Not detectable

Therefore, the particle concentrations in Table B-3 may be low, since the relative humidity averaged over 75% during the period for which the data were taken. The number of solution droplets per cc were probably 20 to 200% larger than the number of dry particles. The assumption that most of the chlorine is in the form of sodium chloride is fairly realistic. Table B-1 shows that the amount of sodium is usually smaller than the amount of chlorine needed for stoichiometric balance for the case of sodium chloride; thus the chlorine may be associated with some magnesium, potassium and calcium whose equivalent weight relationship to chlorine

[22]Y. Miyake. "The Chemical Nature of the Saline Matter in the Atmosphere," *Geophys. Mag.*, Vol. 16 (1948), pp. 64-65.

is similar to that of sodium to chlorine. The assumption that the sulfur is in the form of ammonium sulfate is somewhat artificial because sulfur exists in several chemical forms. In reality, the sulfur-containing particle concentration could be lower than those shown in Table B-3. For example, in the most extreme case, the concentration could be a factor of four smaller than the concentrations in Table B-3 if all the sulfur existed in the elemental form.

For the period 0645 to 1045 PDT on September 15, the Na/K ratio (Table B-2) indicates a mixture of continental and marine air on the basis of values given by Delany and others.[20] However, the observed Na/Si ratio is much higher than the value for marine air found by Delany and others, although they indicate that this ratio is not as good as the Na/K ratio for identifying the marine layer. Based on the above mentioned observations of the Cl/Na ratio, by Miyake[22] and Delany and others, some of the air during the period 0645 to 1045 PDT may have originated from higher continental elevations. The S/Cl ratio was small, indicating that man-made nuclei were not present in any significant number. From Table B-3, the total number of NH_4SO_4 and NaCl particles was near 60/cc (or more, depending on the relative humidity as discussed above). This concentration is far from the CCN average of 325/cc found with the MEE counter. Apparently, this difference is due to particles having radii between 0.10 and 0.15 μm, which were not captured by the last stage of the impactor, and to particles containing elements that were not detected such as nitrogen in the form of nitrates. The particle concentration of 10/cc (possibly up to about 20/cc depending on the relative humidity) for sodium chloride was the largest found for any of the time periods. The total number of sea-salt particles is too small to be of any major importance for the formation of cloud or fog droplets since the concentration of all chloride particles larger than 0.1 μm is of the order of 1 to 10/cc (Table B-3 and Junge[23]).

During the period of 1045 to 1445 PDT, the CCN count as read from the MEE counter seemed to hold steady at near 400 per cc after increasing from a low of 250 per cc as discussed in the previous section. The increase followed a wind shift, to southwesterly (Fig. B3), at about 1000 PDT, although by about 1200 PDT the wind shifted to westerly. As noted from the S/Cl ratio of Table B-2, the airflow from the southwest apparently brought a parcel of air containing sulfur-rich CCN into the area. The source could have been the pulp mills located near Eureka. Fog conditions remained at 300-ft ceilings with one-mile or less visibility until 1230 PDT. Also, as shown in Table B-3, the total sulfur (assumed as NH_4SO_4) particle concentration was 313 per cc (and possibly larger as discussed above) for those particles over 0.15 μm. The number of chloride particles was found to be negligible during this period. Also, the Cl/Na ratio showed the air to be richer in sodium than is normal, possibly in the form of sodium sulfate or sodium sulfite. The

[23] C. E. Junge. *Air Chemistry and Radioactivity*. New York and London, Academic Press, 1963. Pp. 160-166.

Na/K and Na/Si ratios, as in the previous time period, were indicative of mixed continental and marine aerosols.

During the two periods, 1445 to 1845, and 1845 to 2245 PDT, the wind was from the west and the ratios of Table B-2 indicate more of a marine influence. The S/Cl ratio substantially lowered indicating a lessening of the influence of man-made aerosols. In Table B-3, the sodium chloride particle concentration was about 1/cc, but the sulfur, (assumed as ammonium sulfate) particle concentration was about 100/cc and possibly larger, depending on the relative humidity, for the two periods, over which the MEE counter showed 200 CCN/cc. Fog formed at 2115 PDT, during the low CCN count of 200/cc, but an hour later the count shot up to 500/cc. This high CCN count occurred over such a small time interval compared to the 4-hour period that it is hard to determine how much effect it had on the S/Cl ratio.

In the last time period, i.e., 2245 to 0245 PDT, there appeared to be no unnaturally high sulfur content in the air higher than the previous two periods (Tables B-1 and B-3). The CCN count decreased steadily from 500 to 250/cc during this period. The wind was from the east during much of the period although initially it had switched rapidly around to the southeast from the west. The air during this period must have had more of a continental influence than the air of any of the previous time periods as indicated by the ratios of Table B-2.

SUMMARY

Although monitoring with the MEE counter was conducted over a short period, the CCN counts varied widely, depending on meteorological conditions, especially wind direction. It was noted that CCN, during normal diurnal flow in a fog-producing regime, increased sharply sometime between 2200 and 2400 PDT in the cases cited in Figures B-1, B-2, B-3, and B-4. Some increases were noted, also, between 0500 and 0800 PDT as shown in Figures B-1, B-3, B-4, and B-5. Based on only two days (Figures B-1 and B-3), there are indications that existing fog dispersal methods are quite effective when CCN are below 300/cc as measured at a supersaturation of 0.23%, while for counts over 400/cc they are ineffective.

Based on the data taken with the Lundgren impactor, the chemical character of the atmospheric aerosol can vary greatly at Arcata. Three types of aerosol regimes were found. One type occurred with an easterly flow in the early morning hours. The air was found to contain a mixture of continental and marine aerosols with a low amount of sulfur-rich particulate matter. Another regime was encountered with a southwesterly wind that occurred, in this case, during the forenoon hours. The air contained a mixture of continental and marine aerosols, but with a high sulfur content which was indicative of man-made sources. The third type of regime is that primarily composed of marine aerosol of low sulfur content. This regime occurred in the afternoon when the wind was blowing relatively strongly from the west.

Sulfur in the assumed form of ammonium sulfate existed in relatively large numbers of particles between 0.15 to 0.5 μm. The number of sodium chloride-containing particles was negligibly small in the 0.15 μm and larger size ranges. This observation was noted for all samples taken and agrees with others (Junge[23]) that the number of sodium chloride particles is too small to be of any significant importance in the formation of fog.

INITIAL DISTRIBUTION

1 Director of Navy Laboratories (MAT-03L)
9 Naval Air Systems Command
  AIR-30212 (2)
  AIR-370 (1)
  AIR-520 (1)
  AIR-532 (1)
  AIR-540 (2)
  AIR-954 (2)
3 Chief of Naval Operations
  OP-09 (1)
  OP-097 (1)
  OP-098 (1)
2 Chief of Naval Material
  MAT-03 (1)
  MAT-03PB (1)
4 Naval Sea Systems Command
  SEA-03 (1)
  SEA-04H (1)
  SEA-09G32 (2)
2 Naval Weather Service Command
  Code 70 (1)
1 Chief of Information
1 Chief of Naval Research, Arlington (ONR-460)
1 Secretary of the Navy
3 Commandant of the Marine Corps
  Code AAJ (2)
  Code RD-1, Dr. A. Slafkosky (1)
1 Marine Corps Development and Education Command, Quantico (C-E Division)
1 Commander in Chief, Alaska
1 Commander in Chief, Atlantic
1 Commander in Chief, European
1 Commander in Chief, Pacific
1 Commander in Chief, Southern
1 Commander in Chief, Atlantic Fleet
1 Commander in Chief, Pacific Fleet
1 Commander in Chief, Naval Forces, Europe
1 Allied Forces, Southern Europe
1 Amphibious Force, Pacific Fleet
2 Amphibious Groups (one each)
  1, 2

1 Second Fleet
1 Third Fleet
1 Sixth Fleet
1 Seventh Fleet
1 Fleet Numerical Weather Central, Naval Postgraduate School, Monterey
4 Fleet Weather Central (one each)
Guam, Norfolk, Pearl Harbor, Rota
2 Fleet Weather Facilities (1 each)
Suitland, Keflavik
1 Naval Academy, Annapolis
1 Naval Air Force, Atlantic Fleet
1 Naval Air Force, Pacific Fleet
1 Naval Air Test Center (CT-176), Patuxent River
3 Naval Environmental Prediction Research Facility, Monterey
Commanding Officer (1)
P. M. Tag (1)
Technical Library (1)
1 Naval Intelligence Support Center
1 Naval Postgraduate School, Monterey
1 Naval Research Laboratory
1 Naval Surface Force, Atlantic Fleet
2 Naval Surface Weapons Center, White Oak
KEB-2F, FENN (1)
Technical Library (1)
1 Naval Ocean Systems Center, San Diego (Code 133)
1 Naval War College, Newport
41 Naval Weather Service Environmental Service Detachments (one each)
Adak, Agana, Andrews, Asheville, Atsugi, Barbers Point, Bermuda, Brunswick, Cecil Field, Chase Field, China Lake, Corpus Christi, Cubi Point, Dallas, Ellyson Field, Fallon, Glenview, Guantanamo Bay, Imperial Beach, Kenitra, Key West, Kingsville, Lakehurst, Lemoore, Mayport, Memphis, Meridian, Midway Island, Miramar, Moffett Field, New Orleans, Oceana, Patuxent River, Roosevelt Roads, San Clemente, Saufley Field, Sigonella, South Weymouth, Whidbey Island, Whiting Field, Willow Grove
5 Naval Weather Services Facilities (1 each)
Alameda, Jacksonville, Pensacola, San Diego, Glenview
1 Operational Test and Evaluation Force
1 Operational Test and Evaluation Force, Pacific
2 Pacific Missile Test Center, Point Mugu
Code 3250, Geophysics Officer (1)
2 Sea Frontiers (1 each)
Eastern, Western
1 Training Command, Atlantic Fleet
1 Training Command, Pacific Fleet
3 Office Chief of Research and Development
Dr. Leo Alpert (1)
Code CRDES (2)
2 Office Assistant Chief of Staff for Intelligence (ACSI-DD)

1 Office Assistant Secretary of the Army (Assistant for Research)
1 Army Combat Development Command, Fort Leavenworth (Combat Arms Group)
1 Army Combat Development Command, Fort Sill (Field Artillery Agency)
3 Army Electronics Command, Fort Monmouth (AMSEL)
  BL-AM (2)
  BL-FM-P (1)
1 Army Materiel Development and Readiness Command (AMCRD-H)
1 Army Test & Evaluation Command, Aberdeen Proving Ground (NBC Directorate)
1 Army Arctic Test Center, Fort Greely
2 Army Ballistics Research Laboratories, Aberdeen Proving Ground (AMXBR-BL)
1 Army Cold Regions Research & Engineering Laboratory, Hanover (Code RP, Dr. Yin Chao Yen)
2 Aberdeen Proving Ground (Technical Library)
2 Army Security Agency, Arlington
  IACDA-P (L) (1)
  IACDA-P (T) (1)
2 Army Tropic Test Center, Fort Clayton (STETC-AD-TL)
3 Engineering Division, Projects Branch, Panama Canal Company, Balboa Heights
4 White Sands Missile Range
  STEWS-AD-L (3)
  Alex Blomerth (1)
1 Strategic Air Command, Offut Air Force Base
1 Strike Command, MacDill Air Force Base
1 Air Force Cambridge Research Laboratories, Laurence C. Hanscom Field (Dr. Robert Cunningham)
1 Air Force Civil Engineering Center, Tyndall Air Force Base (AFCEC/DE/21, Robert H. Marly)
3 Air Weather Service, Scott Air Force Base (DNP)
1 Armament Development & Test Center, Eglin Air Force Base (DLOSL)
1 Environmental Technical Applications Center, Scott Air Force Base (CB)
4 Secretary of Defense
1 Director of Defense Research & Engineering (Technical Library)
1 Deputy Director of Defense Research & Engineering
4 Deputy Director for Operations (OJCS, Environmental Services)
1 Armed Forces Staff College, Norfolk
1 Arms Control and Disarmament Agency
12 Defense Documentation Center
1 Industrial College of the Armed Forces, Fort Lesley J. McNair
1 Energy R&D Administration (Division of Biomedical & Environmental Research, Director)
1 Bureau of Reclamation (Dr. A. Kahan)
1 Central Intelligence Agency
1 Department of Commerce (Assistant Secretary for Science & Technology)
1 Department of Interior (Jim Kerr)
1 Department of State (Dr. Robert Weber)

1 Federal Aviation Administration (Director, Systems Research and Development Service)
2 Library of Congress (Exchange and Gift Division)
1 National Academy of Sciences, National Research Council
1 National Aeronautics & Space Administration (Code RP)
2 George C. Marshall Space Flight Center (S&E-AERO)
  Code ES41 (1)
  Code ES43, D. Camp (1)
2 National Center for Atmospheric Research, Boulder, CO
  Dr. W. O. Roberts (1)
  Library, Acquisitions-Receipts (1)
2 National Oceanic & Atmospheric Administration, Boulder, CO
  Atmospheric Physics & Chemistry Laboratory (1)
  Program Manager for Weather Modification RX-9 (1)
1 National Oceanic & Atmospheric Administration, Rockville, MD (National Oceangraphic Data Center-D722)
1 National Oceanic & Atmospheric Administration, Silver Spring, MD (Technical Processes Branch-D823)
2 National Science Foundation
  Currie S. Downie (1)
  Edwin X Berry (1)
1 National Security Agency, Fort George Meade (TDL)
1 National War College
1 Weather Bureau (Weather Modification Service)
1 American Meteorological Society, Meteorological & Geoastrophysical Abstracts

NWC 3173 (6/77) 425